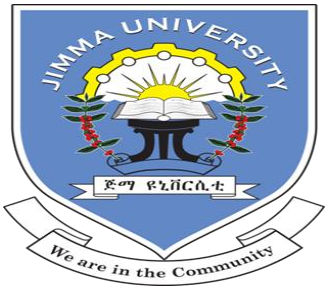

JIMMA UNIVERSITY

SCHOOL OF GRADUATE STUDIES

JIMMA INSTITUTE OF TECHNOLOGY

FACULTY OF CIVIL AND ENVIRONMENTAL ENGINEERING

HYDROLOGY AND HYDRAULIC ENGINEERING CHAIR

MASTERS OF SCIENCE PROGRAM IN HYDRALIC ENGINEERING

IMPACT OF LAND USE LAND COVER CHANGE ON SURFACE RUNOFF: THE CASE OF AMBO TOWN, ETHIOPIA

BY :ADISU FIKIRE CHALCHISA

A THESIS SUBMITTED TO THE SCHOOL OF GRADUATE STUDIES OF JIMMA UNIVERSITY IN PARTIAL FULFILLMENT OF THE REQUIREMENT FOR THE DEGREE OF MASTERS OF SCIENCE IN HYDRAULIC ENGINEERING

FEBURARY, 2020

JIMMA, ETHIOPIA

JIMMA UNIVERSITY

SCHOOL OF GRADUATE STUDIES

JIMMA INSTITUTE OF TECHNOLOGY

FACULTY OF CIVIL AND ENVIRONMENTAL ENGINEERING

HYDROLOGY AND HYDRAULIC ENGINEERING CHAIR

MASTERS OF SCIENCE PROGRAM IN HYDRALIC ENGINEERING

IMPACT OF LAND USE LAND COVER CHANGE ON SURFACE RUNOFF: THE CASE OF AMBO TOWN, ETHIOPIA

BY : ADISU FIKIRE CHALCHISA

A THESIS SUBMITTED TO THE SCHOOL OF GRADUATE STUDIES OF JIMMA UNIVERSITY IN PARTIAL FULFILLMENT OF THE REQUIREMENT FOR THE DEGREE OF MASTERS OF SCIENCE IN HYDRAULIC ENGINEERING

MAIN ADVISOR: Dr.Ing TAMENE ADUGNA (PhD)

CO-ADVISOR:WALABUMA OLI (MSc.)

FEBURARY, 2020

JIMMA, ETHIOPIA

DECLARATION

This thesis is my original work and has not been presented for a degree at any other University.

ADISU FIKIRE CHALCHISA	----------	----------
Candidate	Signature	Date

This thesis has been submitted for examination with my approval as a university Supervisor.

TAMENE ADUGNA (PhD.)	----------	----------
Advisor	Signature	Date

WALABUMA OLI (MSc.)	----------	----------
Co-Advisor	Signature	Date

APPROVAL SHEET

We certify that, the Thesis entitled “Impact of land use land cover change on surface runoff; The case of Ambo town on Huluka river watershed, Abay river basin, Ethiopia” is the work of Adisu Fikire Chalchisa. We hereby recommend for the acceptance by a School of Graduate Studies of Jimma University in partial fulfillment of the requirement for the Degree of Masters of Science in Hydraulic Engineering.

Dr.-Ing TAMENE ADUGNA	----------	----------
Main Advisor	Signature	Date
WALABUMA OLI (MSc.)	----------	----------
Co-Advisor	Signature	Date

As the member of Board of Examiners of MSc. Thesis Open Defense Examination, we certify that we read, evaluated the Thesis prepared by Adisu Fikire Chalchisa and examined the candidate. We recommended that the Thesis could be accepted as fulfilling the Thesis requirement for the Degree of Masters of Science in Hydraulic Engineering.

Wana Geyisa (MSc.)	----------	----------
Chairman	Signature	Date
Dr. Kassa Tadele	----------	----------
External Examiner	Signature	Date
Chala Hailu (MSc.)	----------	----------
Inernal Examiner	Signature	Date

ABSTRACT

The Impact of Land use Land cover change over the world currently develops direct and indirect impacts on surface runoff. Expansion of Ambo town urban areas causes the reduction of Huluka river watershed potential which is the main source of water supply and other miscellaneous use for the residents of Ambo town. Because of increasing of urbanization, floods are the main causes to affect the property, buildings, and infrastructures in case of Ethiopia. The main objective of this study was Impact of Land use Land cover change on surface runoff in the case of Ambo town on Huluka river watershed. Satellite image downloaded for 1997, 2005 and 2011 of the watershed area was taken based on the quality of data and the available resolution. Excel statistical software was used for filling missing value of precipitation data and data consistency was checked up using double mass curve. The surface runoff generated from the watershed was estimated based on the rainfall intensity and major characteristics of the watershed area which are the major factors for designing urban storm water drainage facilities and structures. Arc Geographical Information System and Geographical Information System extension tools were used to extract hydrological characteristics of the watershed; Hydrologic Engineering Center Hydrologic Modeling System to simulate rainfall - runoff process and Hydrologic Engineering Center River Analysis System for flood inundation assessement. The daily rainfall and stream flow data was used for Hydrologic Engineering Center Hydrologic Modeling System calibration and validation. To evaluate the accuracy of the model, calibration and validation was conducted. Nash Sutcliff efficiency during calibration and validation was 0.744 and 0.72 respectively where as coefficient of determination during these two processes was 0.8556 and 0.8122 respectively. The hydrological and hydraulic modeling are accomplished by dividing the watershed in to different sub-basin. Hydrological modeling depending on land use/land cover of the peak discharge was generated 1997, 2005 and 2011 at the outlet was 36.5, 47.56 and 61.04 m^3/s respectively. The peak discharge simulated by frequency storm method for 10, 25, 50 and 100 return periods was 38.2, 47.2, 54.2 and 61.4m^3/s. The result found from Hydrologic Engineering Center Hydrologic Modeling System frequency storm method used for flood inundation map generation. Flood inundation maps produced using Arc Geographical Information System to visualize flood depth and extent for each return period. Accordingly, maximum flood depth of 17.7632, 17.8779, 17.9548 and 18.0347m for 10, 25,50, and 100 year return periods respectively was found with flood extent of 97.58, 100.56, 103.34 and 105.54 ha for 10, 25, 50 and 100 year return periods at the middle of the final reach of the study area.

Keywords: *DEM, Flood modeling; HEC-HMS/RAS; HEC- GeoHMS/RAS; Urbanization*

ACKNOWLEDGEMENTS

First of all, honor to almighty God who made it possible, to begin and finished this thesis successfully.

My appreciation also goes to my advisor Tamene Adugna (PhD.) and co-advisor Walabuma Oli (MSc.) giving general constructive comment and suggestion to implement this thesis.

I like also to say Ethiopian Road Authority to give this enjoyable chance with cooperative to Jimma University.

Moreover, I wish to express my deepest gratitude my family and all of my friends for providing financial supporting and strength motivation to success in my study. In addition, all friends and professional collogues thanks your collaboration and motivation.

Finally, my deepest gratitude and humble thanks go my immediate parents for their never ending support, encouragement and motivation.

CONTENTS

LIST OF FIGURES

LIST OF TABLE

ACRONYMS / AND ABBREVIATION

CN	Curve Number
DEM	Digital Elevation Model
DFID	Department for International Development
DTM	Digital Terrain Model
ERA	Ethiopian Road Authority
FAO	Food and Agricultural Organization
GDEM	Global Digital Elevation Model
GHG	Green House Gases
GIS	Geographical Information System
HEC-HMS	Hydrologic Engineering Center Hydrologic Modeling System
HEC-GeoHMS	Hydrologic Engineering Center Geospatial Hydrologic Modeling System
HEC-RAS	Hydrologic Engineering Center River Analysis System
HEC-GeoRAS	Hydrologic Engineering Center Geospatial River Analysis System
HSG	Hydrological Soil Groups
IDFC	Intensity Duration Frequency Curve
IPCC	Intergovernmental Panel on Climate Change
LULC	Land Use/Land Cover
NRCS	Natural Resources Conservation Service
NSE	Nash-Sutcliffe efficiency
RMS	Root Mean Square
RS	Remote Sensing
R^2	Coefficient Determination
TIN	Triangulated Irregular Network
SCS	Soil Conservation Service
USA	United State of America
USDA	United States Department of Agriculture
UTM	Universal Transverse Mercator
USGS	United States Geological Survey
USACE	United State Army Corps of Engineers

1. INTRODUCTION

1.1 Background

Nowadays there is a great need to detect spatial patterns of land use/land cover (LULC) change at local, regional and global scales. Understanding LULC change is a fundamental importance for environmental monitoring, urban planning and governmental decision making around the world. One particular consequence of LULC change is its considerable impacts on hydrological processes by affecting the nature of surface runoff and water quality, hence further impact on ecosystems, biotic systems, and even on human health (Chunhao, 2011).

Land-use and land-cover changes may have four major direct impacts on the hydrological cycle and water quality: they can cause floods, droughts, changes in river and groundwater regimes and they can affect water quality (McColl *et al.*, 2017). Globally floods are most devastating natural disasters affecting human life than any other natural disasters. In 2010 alone, 178 million people were affected by floods and the total financial losses in the exceptional years such as 1998 and 2010 exceeded $40 billion (Shabir, 2013). It is also reported that one sixth of the global population (one billion people); the majority of them among the world's being low income earners live in the potential path of a 1 in 100 year flood according to Department for International Development (DFID). Ethiopia is facing the same global challenges of climate change effects such as droughts and floods (Kotir, 2011).

The country experiences two types of floods: flash floods and river floods. Flash floods are the ones formed from excess rains falling on upstream watersheds and gush downstream with massive concentration, speed and force. Often, they are sudden and appear unnoticed. Therefore, damage caused by such kind of floods becomes pronounced and devastating when they pass across or along human settlements and infrastructures. For example, in the recent incident, that the Dire Dawa City experienced is typical of flash flood. On the other hand, much of the flood disasters in Ethiopia are attributed to rivers that overflow or burst their banks and inundate downstream plain lands. The flood that has been happened in Southern Omo Zone and Awash River is a typical manifestation of river floods (Gashaw & Dagnachew , 2011).

On the other hand, population growth is increasing; runoff of rainwater's is expected to increase due to the decrease of the permeability of the urban environment. For the last one

hundred seventeen years it has been noticed that there is an intensive conversion of rural land to urban development like buildings, transportation networks and facilities (airports and highways), recreation areas, reservoirs and other man made structures (Gant*et al*., 2011). Roads and bridges are destroyed, overtopped and washed away. Therefore, to reduce the impact of flood, during design of roads, bridges and culverts estimation of flood magnitudes using the appropriate parameters is very essential.

Generally, Ethiopia is one part of the developing country. Among that, Ambo town is one of the currently expanding and developing towns, as a result, rural residents are migrating to the town and are causing rapid urbanization.

1.2 Statement of the problem

Generally, floods are the causes of major destruction of property, buildings and infrastructures in Ethiopia and this problem is getting worse and worse in urban areas due to high rate of urbanization in the country (Jha, 2011). This has led to deforestation, use of high quality corrugated roofs and paved surfaces or asphalts and its effect are high with the higher raindrop intensity on the city and also town. Urbanization has different stages and various effects can be noticed through those stages. At early, removal of vegetation and trees may decrease evapotranspiration and interception, which increase stream sedimentation (Davis, 2005). When construction of streets or roads, bridges, houses and culverts begins, infiltration will decrease and stream flow will increase. In addition to this when the development of residential and commercial buildings has been completed imperviousness increase consequently; the time needed for runoff will reduce; concentration will be peak with higher discharges and occur sooner after rainfall starts in basins. The volume of runoff and flood damage potential will greatly increase (Ching, 2014). As a result, the rainfall– runoff process in an urban area tends to be quite different from that in natural conditions (Barbero-Sierra, 2013).

The impacts of high rate of growth of Ambo town particularly in the study area reflected through street flooding and over topping as well as bridge, road, culvert materials are washed way. On the other hand, many river flood plains in the town have not yet been delineated considering the land use change and most of small tributary rivers in the town are ungauged. It is obvious, hydrological alterations and channel disturbances along streams

because of changes in inputs like; slope, vegetation cover, geology, stream geomorphology and hydrologic processes from year to year. Therefore, its need to see carefully hydrologic responses to urbanization to improve the understanding of stream response to land use change for rivers found in towns. This study objectives to show the effects of urbanization on the amount surface runoff generated at Huluka River watershed in the case of Ambo town.

1.3 Objective of the study

This study has the following general and specific objectives.

1.3.1 General objective

The General objective of this study was the Impact of Land use Land cover change on the surface runoff in the case of Ambo town on Huluka river watershed.

1.3.2 Specific objectives

This study has the following specific objectives:

1. To evaluate performance of HEC-HMS to simulate rainfall-runoff on Huluka river watershed
2. To assess the Land use Land cover change on surface runoff in the case of Ambo town
3. To develop flood inundation map of the study area.

1.4 Research questions

1. How to evaluate performance of HEC-HMS to simulate rainfall-runoff for Huluka river watershed?
2. How to assess the Land use Land cover change on surface runoff?
3. What seems flood inundation area of Huluka river watershed?

1.5 Significance of the study

This study can give full information concerning the characteristics of the study area watershed, peak discharge magnitude and its frequency, assessessment of Land use Land cover change on surface runoff, indication of the floodplain depth and its extent, for those who will go to take action for effects of urbanization on surface runoff measures and decision making.

And also it can be used as a reference for researchers who intended to carry out a further investigation up on (rainfall-runoff modeling, LULC change effects on surface runoff, flood

frequency analysis and flood inundation mapping) of the watershed using more advanced tools.

1.6 Scope of the study

The study was geographically limited to Huluka river watershed, which is the sub basin of Abbay river basin. In general, the study were Impact of Land use Land cover change on surface runoff the case of Ambo town on Huluka River watershed. The assessessment of Land use Land cover change on surface runoff was conducted based on the required types of method for the estimation of peak discharges, assessment of LULC change on surface runoff in the case of Ambo town and the floodplain mapping that indicates the surface runoff profile for Huluka river watershed (i.e. ArcGIS,HEC- HMS, HEC-RAS) and also the required GIS extensions (i.e,HEC-GeoHMS and HEC-GeoRAS) was conducted within the core steps to fit the required specific objectives of the study area.

2. LITERATURE REVIEW

2.1 Urbanization

2.1.1 Urbanization from world perspective

Urbanization is a process whereby populations move from rural to urban area, enabling cities and towns to grow. It can also be termed as the progressive increase of the number of people living in towns and cities (Kirkby, 2018). It is highly influenced by the notion that cities and towns have achieved better economic, political, and social mileages compared to the rural areas. Urbanization is a population shift from rural to urban areas, "the gradual increase in the proportion of people living in urban areas", and the ways in which each society adapts to the change Urbanization is not merely a modern phenomenon, but a rapid and historic transformation of human social roots on a global scale, whereby predominantly rural culture is being rapidly replaced by predominantly urban culture (Kabangure, 2016). Urbanization is simply defined as the shift from rural to an urban society, which is triggered by social, economic, and political developments (Pawan, 2016)

Urbanization typically replaces permeable vegetated land surface with imperious surface area and significantly changes the hydrologic fluxes of a drainage basin. It decreases infiltration, base flow, and lag times while increasing flood volume, peak flow, and water depth etc. Since urbanization develops so rapidly nowadays, flood problems in cities are becoming steadily worse. In developed regions, the flood risk problem is much more serious due to the highly developed economy, dense population, and high degree of urbanization. Many researches on simulating and assessing the hydrological response to urbanization on the watersheds scales have been carried out (Zhou *et al*., 2013). Pointed out that urbanization would increase the runoff volume and peak flow while decreasing the stream flow variability in a Mediterranean climate watershed. Urban flood control is facing enormous challenges, because of the accelerated process of urbanization. In order to deal with the problem, the urban flood control pattern has been evolved from single city flood control to urban agglomerations flood control (Guohua, 2018)

Urbanization presents considerable challenges for urban planners and decision makers. It is of great interest to accurately document the pattern and extent of urban expansion and to evaluate its impacts on surface runoff and water quality. Urban sprawl has been conventionally investigated based on surveying and site-specific mapping. However, those processes are too expensive and time consuming to be applied in large areas with frequent updates. Taking advantage of geographic information system (GIS) and remote sensing (RS) techniques, LULC change can be mapped in a more accurate and timely manner. RS/GIS–based land use mapping provides an efficient way of documenting LULC change over a long period, which allows for a rapid assessment of effects on surface runoff and water quality (Li, 2009).

Urbanization levels reflect the degree of economic development of a region, but it also changes water cycle in many aspects. It modifies hydrological process by affecting runoff generation and concentration which has been research focus currently (Schaeffer *et al*., 2012).

In the 1950s the world population was mostly rural and more than two thirds of people lived in rural settlements, since then world urbanization increased rapidly. In the year 2014, just over half of the world population resided within urban centers. This trend is expected to increase over the next 35 years to the extent that, by 2050, two thirds of the world's population will reside in urban areas (Zhang, 2016). Urban areas have many linkages with climate change and its centers are drivers of global warming because they concentrate industries, transportation, households and many of the emitters of greenhouse gases (GHG) and affected by climate change (Hoornweg, 2011).

The IPCC Working Group II in their Report-5 (AR5), 2013, on cities has confirmed that the world's main urban agglomerations are condensed in relation to variations in observed and projected temperature. This predicted temperature change for the year 2025 verify that the vast majorities of the world's population living in the biggest urban agglomerations will be exposed to minimum 2^{o}C rise in temperature compared to pre-industrial period level. This means that mean temperature rise in some cities could be over 4 ^{o}C (Arsiso, 2017).

2.1.2 Urbanization in Ethiopia

Ethiopia has a population of approximately 87.95 million people and ranking as the third most populous country in Africa (Tausch , 2019). The national population growth rate for the period 1994 to 2007 was 2.5 %; the urban and the rural rates being 3.8 and 2.3 % respectively. However as compared to Asian and other African cities, the annual urbanization growth rate in Ethiopia is slower than the other mentioned. According to population projections made by the Ethiopian Central Statistics Agency (CSA, 2013), the estimated 2012 urban population is about 17.5 million and expected to increase to close to 42.3 million at annual growth rate of 3.8 %, while the level of urbanization is expected to reach 31 % by 2037 (Arsiso, 2017).

Urbanization is occurring at a very high pace in Ethiopia. Ambo town is one of the administrative and political seats of the country and attracts the highest number of migrants from other parts of the zones and countries. This increasing population in the town leads to land use change in many dimensions and also forces the town to expand outward putting pressure on the rural land and natural recourses surrounding the town. The expansion of the town increase impervious surface throughout its plan due to the development of asphalt road and other infrastructure which is very sensitive in reducing ground water recharge that in turn affect the surrounding stream flow found in this town like that of Huluka river watershed which is one source of water supply for the town. Impervious surfaces reduce infiltration, generally resulting in increased surface runoff and reduced base flow.

The severity of the impacts of climate change depends upon the state of the urban environment. In particular, urban environments have their own microclimate, air quality and hydrological regimes. An increasing temperatures and/or decreasing precipitation will have a double impact, increased Evapotranspiration and lowered recharge rates reduce the total water available in the hydrological system while also increasing the total end-user demand. Supply declines while demand increases. The global trend of urbanization and the growing population of towns require increasing volumes of water to be extracted and transported (Wang, 2016).

Securing sufficient supplies of fresh water for growing towns is primary concern and may be seriously hindered by the spatial and temporal variability of water demand and supply (Buytaert, 2012). Incorporating this information into the planning of water supply systems for the Ambo towns can ensure adequate future levels of drinking water. Currently many models

are developed to solve these problems. Especially models like HEC-HMS, HEC-RAS and GIS tools have been tested and widely used globally in flood modeling for several years (Hungr *et al*., 1987).

Estimation of flood magnitudes using the appropriate parameters is very essential.In addition to this, models are readily available and the result of the models was calibrated well during design and decision making for both local and national level. In this study, geographic information system (GIS) software and GIS extension tools were used in combination with hydrologic and hydraulic modeling software's to estimate the generated flood and its effect on Huluka River watershed (Jantz *et al*., 2004).

2.2 Hydrological Processing and Components

The land surface, the underground and the atmosphere are the three principal elements involved in that continuous water exchange through vertical and horizontal mass fluxes which istermed hydrological cycle (Monteith, 2013). Precipitation and runoff are only the visible components of this process. Other components such as evaporation, infiltration, transpiration, percolation, ground water recharge and discharge are other important mechanisms of this cycle (Kim, 2011). The water exchange between land surface and atmosphere is based on the continuous evaporation of water from the Earth, the temporary storage of water in the form of water vapor in the atmosphere and the return of water to the land surface through several forms of precipitation such as rain, snow, sleet or hail (Berner & Robert, 2012).

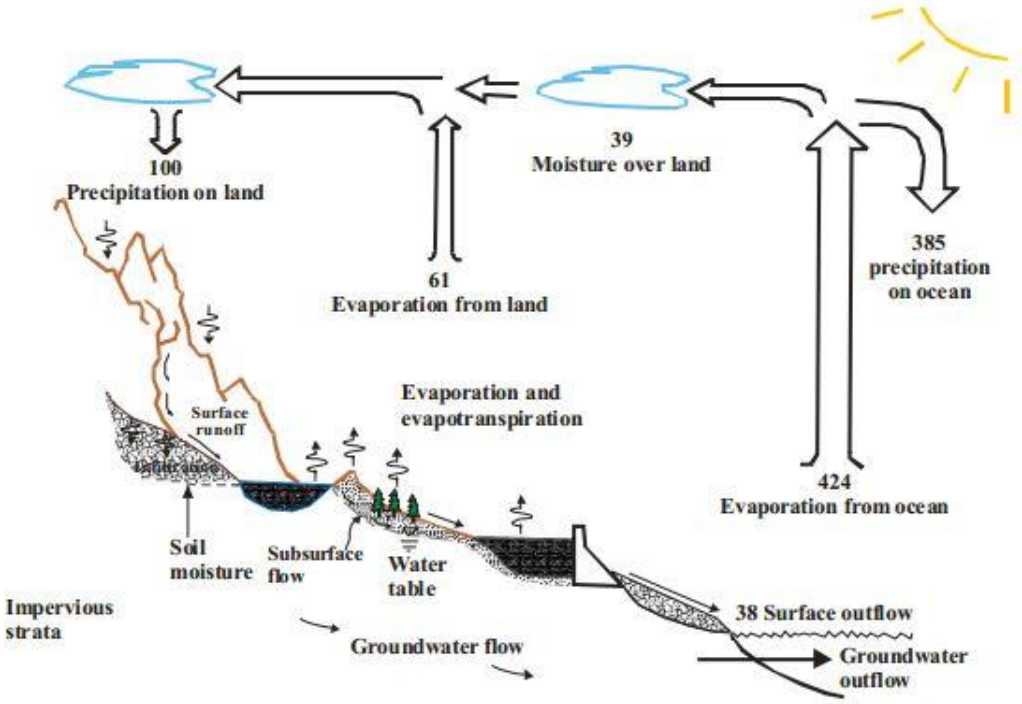

Figure 2.1 Urban Hydrologic cycle representation

Source; (Berner & Robert, 2012)

Precipitation that reaches the land surface is partially intercepted by vegetation. The amount of water intercepted by a plant, termed interception, largely depends on plant form. Water held on the leaf surface can trickle down reaching the ground or evaporate (Manning, 2016). Another part of water falls directly on the ground. Here water can evaporate with a rate that depends on wind speed, solar radiation, heat and humidity in the air, or enter into the soil, or flow down the land surface as runoff. The amount of water that penetrates into the surface of soil through the infiltration process is related to soil properties such as texture, structure, moisture content and in particular to soil permeability and porosity. Conditions at the soil‘s surface also influence infiltration. For example, a compacted soil surface or frozen soil conditions reduce the infiltration rate (Lastoria, 2008).

Vegetation canopy protects the soil surface from compaction by heavy raindrops, slows down water that flows over the soil surface, and plant roots help to create openings in the soil. Infiltration rate is also related to the intensity and duration of precipitation. Generally, the rate at which water enters the soil from the surface is a function of water-input rate (snow melt and

rain fall) and soil infiltration capacity (the maximum rate at which soil will accept incoming water) (Bilotta *et al.*, 2007).

2.2.1 Run off Modeling

Flood modeling is the processes of transformation of rainfall into a flood hydrograph and to the translation of that hydrograph throughout a watershed or any other hydrologic system (hydraulics). In this manner, the flooding processes, which consist of upstream watershed hydrological processes and river floodplain hydraulic processes and approximated either physically or mathematically (through the use mathematical equations) where the relationships between system state, input and output are represented (Mark *et al*., 2004).

Recent advances in computer technology have provided a means to rapidly process large arrays of spectral data for remote sensing and to combine these data with other geographical information, such as topography (including slope classes and aspect), vegetation types, soil types and geology. The most important contribution made from the processing of spatial data is the assessment of hydrological based indices estimated from digital terrain analysis with digital elevation models. Assumptions regarding the effects of topography and related features, such as slope, aspect and indices of soil wetness, on hydrologic processes can be evaluatedusing digital elevation data (Guarino *et al*., 2002).

The topography now can be used directly in more physically realistic structures for hydrologic modeling, such as in predicting hill slope flow paths using digital terrain models. The topography is a dominant control on how the energy is distributed, particularly in complex terrain (Peters, 1994). According to Ethiopian Road Authority drainage design manual 2013, for hydrologic analyses, the following factors shall be evaluated and included: drainage basin characteristics including : size, shape, slope, land use, geology, soil type and surface infiltration; stream channel geometry; flood plain characteristics and precipitation amounts (Ramirez, 2000).

2.2.2 Soil conservation service Curve Number (SCS-CN) Method

One of empirical methods that is widely and global used by hydrologists, water project planners and water engineering, is the curve numbers method that has been suggested and supported by the department of agriculture natural resources conservation service of USA.

Some applications of GIS are mapping curve number (CN) of catchment by using the digital data analysis, vegetation cover, land using and hydrologic soil groups (AbouzarNasiri and Hamid Alipur, 2014). This method is a versatile and widely used approach for quick runoff estimation and also relatively easy to use with minimum data and give adequate results (Panigrahya., 2008)

The SCS Runoff Curve Number (CN) method developed by Natural Resources Conservation Service (NRCS) used for estimating direct runoff from storm rain fall described by equation 2.1;

$$Q = \frac{(P-Ia)2}{(P-Ia)+S}$$----------2.1

Where; Q= Runoff (m^3/s), P= Rainfall (mm), Ia= initial abstraction (mm), S= maximum potential retention after runoff (mm)

Initial abstraction (Ia) is all losses before runoff begins. It includes water retained in surface depressions, water intercepted by vegetation, evaporation, and infiltration. Ia is highly variable but generally is correlated with soil and cover parameters. Through studies of many small agricultural watersheds, Ia was found to be approximated by the following empirical equation:

Ia =0.2S----------2.2

By removing Ia as an independent parameter, this approximation allows use of a combination of S and P to produce a unique runoff amount. By substituting the equation of initial abstraction in to equation of runoff.

$$Q = \frac{(P-0.2S)2}{(P+0.8S)}$$ ----------2.3

S is related to the soil and cover conditions of the watershed through the CN.

CN has a range of 0 to 100, and S is related to CN by:

$$S = \frac{25400}{CN} - 254$$---------- 2. 4

The major factors that determine CN are the hydrologic soil group (HSG), cover type, treatment, hydrologic condition, antecedent runoff condition, and impervious areas. On the other hand, infiltration rates of soils vary widely and are affected by subsurface permeability

as well as surface intake rates. Soils are classified into four HSG's (A, B, C, and D) according to their minimum infiltration rate (Ramakrishnan *et al*., 2009)

According to the USDA Natural Resources Conservation Service of National Engineering Hand book the four hydrologic soil groups (HSGs) are described as: Group A: soils in this group have low runoff potential when thoroughly wet. Water is transmitted freely through the soil. Group A soils typically have less than 10 percent clay and more than 90 percent sand or gravel and have gravel or sand textures. Some soils having loamy sand, sandy loam or silt loam textures may be placed in this group if they are well aggregated, of low bulk density, or contain greater than 35 percent rock fragments.

Group B: soils in this group have moderately low runoff potential when thoroughly wet. Water transmission through the soil is unimpeded (Boorman *et al*., 1995). Group B soils typically have between 10 percent and 20 percent clay and 50 percent to 90 percent sand and have loamy sand or sandy loam textures. Some soils having loam, silt loam, silt, or sandy clay loam textures may be placed in this group if they are well aggregated, of low bulk density, or contain greater than 35 percent rock fragments. Group C: soils in this group have moderately high runoff potential when thoroughly wet. Water transmission through the soil is somewhat restricted (Cosby *et al*., 1984). Group C: soils typically have between 20 percent and 40 percent clay and less than 50 percent sand and have loam, silt loam, sandy clay loam, clay loam, and silt clay loam textures. Some soils having clay, silt clay, or sandy clay textures may be placed in this group if they are well aggregated, of low bulk density, or contain greater than 35 percent rock fragments. Group D: soils in this group have high runoff potential when thoroughly wet. Water movement through the soil is restricted or very restricted (Beven, 2013).

Group D: soils typically have greater than 40 percent clay, less than 50 percent sand, and have clayey textures. In some areas, they also have high shrink-swell potential. All soils with a depth to a water impermeable layer less than 50 centimeters and all soils with a water table within 60 centimeters of the surface are in this group (Olson, 2012)

2.2.3 Hydrological Soil Group of Ethiopian

With regard to Hydrological Soil Group (HSG) of Ethiopia most of the hydrological studies in the country used the FAO soil database. Based on FOA, HSG classification in Ethiopia has

HSG-A dominates with 48.2% areal coverage followed by HSG-B (30%) and HSG-C with a real coverage of 21.6% and the remaining area is covered by HSG –D which is very small (p. Berhanu *et al.*, 2012).

2.3 Impervious surface area

Having information on land-use and land-cover is essential for selection, planning and implantation of land-use and can be used to meet the increasing demands for basic human needs and welfare. This information also assists in monitoring the dynamic of land-use resulting out the changing demands of increasing population. Impervious surfaces have been identified as an indicator of the impacts of urbanization on water resources. Some of the affected characteristics of a watershed include hydrological impacts (the amount of runoff and peak discharge rates, and base flow are altered), physical impacts (stream morphology and temperature are changed), water quality impacts (nutrient and pollutant loads increase), and biological impacts (stream biodiversity decreases) (Gulliver, 2015).

2.4 Geographical Information System (GIS) and Runoff Models

Geographic information system (GIS) technology was developed by Environmental Systems Research Institute, Inc. (Esri) established in 1969 (Maguire, 2008). The uses of geographic information systems (GIS) to facilitate the estimation of runoff from watershed have gained increasing attention in recent years. This is mainly due to the fact that rainfall runoff models include both spatial and geomorphologic variation (Han, 2010).

Run off modeling needs integration of GIS and remote sensing (RS) and has two processes: (1) hydrological parameter determination using GIS, and (2) hydrological modeling within GIS. Hydrological parameter determination using GIS entails preparing land cover, soil, and precipitation data that go into the SCS model, while hydrological modeling within GIS automates the SCS modeling process using generic GIS functions. Remote sensing is used for obtaining land cover data each year and for obtaining information about the nature, rate, and location of land use and land cover changes (McDonald, 2010)

2.5 GIS extension tools

The hydrologic Engineering Centers Geospatial Hydrologic Modeling Extension, HEC-GeoHMS, is a public domain extension to ESRI's ArcGIS software and the spatial analyst extension. It is hydrology toolkit for engineers and hydrologists. The user can visualize

information, document watershed characteristics, perform spatial analysis, and delineate sub basins and streams, construct inputs hydrologic models, and assist with report preparation. Therefore use of HEC-GeoHMS can easily and efficiently create hydrologic inputs that can be used directly for HEC-HMS (James H., 2013)

HEC-GeoRAS also an ArcGIS extension specifically designed to process geospatial data for use with the hydrologic Engineering Center's River Analysis System (HEC-RAS). This tool used to create an HEC-RAS import file containing geometric attribute data from an existing digital terrain model (DTM) and complementary data sets. Water surface profile results may also be processed to visualize inundation depths and boundaries. A result created by HEC-RAS can be processed and used an input for Arc GIS (Mathew J., 2012)

2.6 HEC-HMS Model

HEC-HMS /Hydrologic Engineering Center Hydrologic Modeling System is designed to simulate the precipitation-runoff process and developed by the Hydrologic Engineering Center under the U.S. Army Corps of Engineers. The first version of HEC-HMS developed in 1968 as HEC-1 and through a lot of efforts now version 4.2.1 is released which is used in this study. For flood simulation HEC-HMS model has three major parts these are infiltration loss simulation, converting excess rainfall to runoff and channel flow routing. Infiltration loss simulation of HEC-HMS uses initial and constant rate, SCS CN, Gridded SCS CN, green and ampt, deficit and constant rate, soil moisture accounting (SMA) and gridded SMA. Converting excess rainfall to runoff model or modeling runoff into Hydrograph of HEC-HMS model uses seven methods theses are: user-specified unit hydrograph (UH), Clark's UH, Synder's UN, SCS UH, ModClark, kinematic wave and S-graph. The third part is modeling one dimensional open channel flow routing and HEC-HMS model uses standard methods such as Kinematic wave, lag time, modified puls, Muskingum, Muskingum cunge standard section; Muskingum cunge eight point section (Sharffenberg, 2016).

The HEC-HMS simulates the precipitation-runoff processes of watershed systems. HMS uses deterministic mathematical modeling to compute various components of the hydrologic cycle (Kaffas, 2014).

These are evapotranspiration, precipitation, infiltration and runoff. Evapotranspiration is the sum of evaporation and plant transpiration from the Earth's surface to the atmosphere.

precipitation is the water being released from the clouds as rain. Infiltration is the portion of precipitation which after hitting the Earth's surface, seeps through the soil layer. runoff is precipitation that reaches the Earth's surface but does not infiltrate the soil (Good, 2015).

HMS is applicable in a wide range of geographic areas for solving the widest possible range of problems including large river basin water supply and flood hydrology, and small urban or natural watershed runoff. Hydrographs produced by HMS are used directly or in conjunction with other software for studies of water availability, urban drainage, flow forecasting, future urbanization impact, reservoir spillway design, flood damage reduction, floodplain regulation, and systems operation (Gumindoga, 2017).

2.7 HEC-RAS Model

HEC-RAS/River Analysis System is developed by U.S. Army Corps of Engineers Hydrologic Engineering Center (HEC). This software allows for us to perform one dimensional steady and unsteady flow river hydraulics calculation. The first version of HEC-RAS (version 1.0) was released in July of 1995. Since that time there have been several major releases including version: 1.1; 1.2; 2.0; 2.1; 2.2; 3.0; 3.1; 4.0,4.1,5.0.1 and now version 5.0.7 which is used for this study and released in March 2019. The HEC-RAS model can handle a full network of natural and constructed channels. In this section the model has two very important river analysis components these are steady and unsteady flow.

The steady flow component is used for calculating water surface profiles for steady gradually varied flow as well as capable of modeling subcritical, supercritical and mixed flow regime water surface profiles. The basic computational procedure is based on the one dimensional energy equation and the effect of various obstructions such as bridges, culverts dam, weirs, and other structures can be considered in flood plain computations. It is also, capable for assessing the change in water surface profile due to channel modifications, and levees. On the other hand, HEC-RAS modeling system is capable of simulating one-dimensional unsteady flow through a full network of open channels. Unsteady flow component was developed primarily for subcritical flow regime calculations. However, with release of version 3.1, the model can perform mixed flow regime (subcritical, supercritical, hydraulic jumps, and drawdowns) calculation. Then hydraulic calculations for cross-sections, bridges, culverts, and

other hydraulic structures that were developed for the steady flow component were incorporated into the unsteady flow component (Gary W., 2016)

HEC-RAS is a one dimensional model, intended for hydraulic analysis of river channels. The model is comprised of a graphical user interface, separate hydraulic analysis components, data storage and management capabilities, graphics and reporting facilities (Hasani, 2013).

The HEC-RAS system includes four river analysis components. They include the steady flow water surface profile computations, unsteady flow simulation, sediment transport computations and water quality analysis. In addition to these components, the model contains several hydraulic design features that can be invoked once the basic water surface profiles are computed. HEC-RAS applications include flood plain management studies, bridge and culvert analysis and design, and channel modification studies (ShahiriParsa, 2016)

3. MATERIALS AND METHODS

3.1 Location

Ambo town is one of the developing towns in West Shoa zone of Oromia region in Ethiopia. It is located at a distance of 114 km to the West of Addis Ababa, capital city of Ethiopia. It is endowed with rivers, one of which separates the town into two major parts known as Huluka River which starts from Dendi Lake near Wonchi town, 39 km from Ambo town, and flows from the southern part of Ambo towards the northern part of the town. In rural areas, these river waters are used for drinking, sanitation, livestock and agricultural purposes. Sewage from residential areas near these rivers is allowed to enter directly and dense weeds have occupied the sides of rivers, thus affecting the flow and photosynthesis process. Huluka River watershed has a watershed area of 206.05 km^2 and located in Abay River basin. It is located between latitude of $8^0$45'34.74"N to $9^0$00'00"N, longitude of $37^0$30'00''E to $39^0$00'00''E .

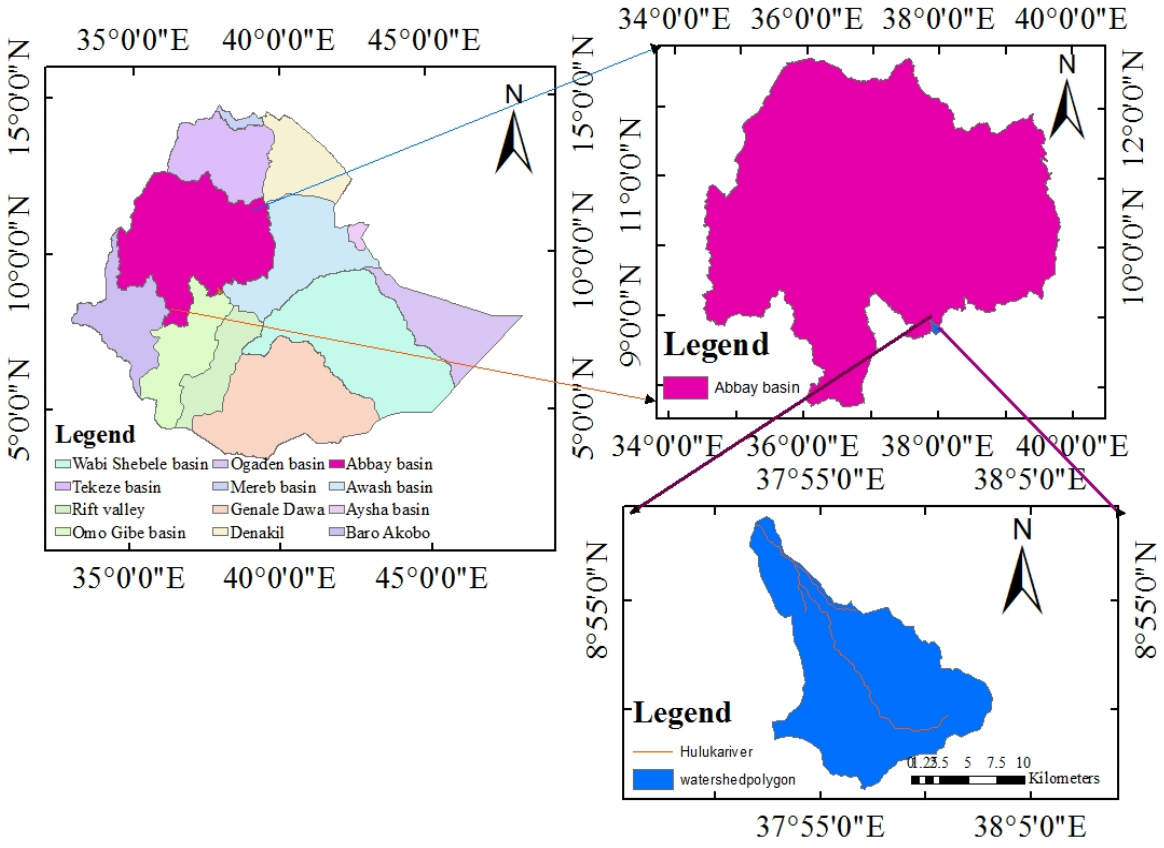

Figure 3.1 Description of study area

3.2 Climate

Despite its proximity to the equator, Ambo enjoys a mild, Afro-Alpine temperate and warm temperate climate. The lowest and highest annual average temperature are between 13°C and 27°C. April and May are the driest months. The main rainy season occurs between mid-June and mid-September, which is responsible for 70% of the annual average rainfall of 1,100 mm. It is characterized by intense rainfall of short duration. During the dry season the days are pleasantly warm and the nights are cool. During the rainy season both days and nights are cool.

3.3 Topography

The topography of a watershed like elevation, slope and aspect has an important contribution for the amount of surface runoff generated from it. According to the extracted elevation of the study area from DEM of Ethiopian river basin, the watershed is located along elevation range varies from 2112 meters to 3344 meters above sea level.

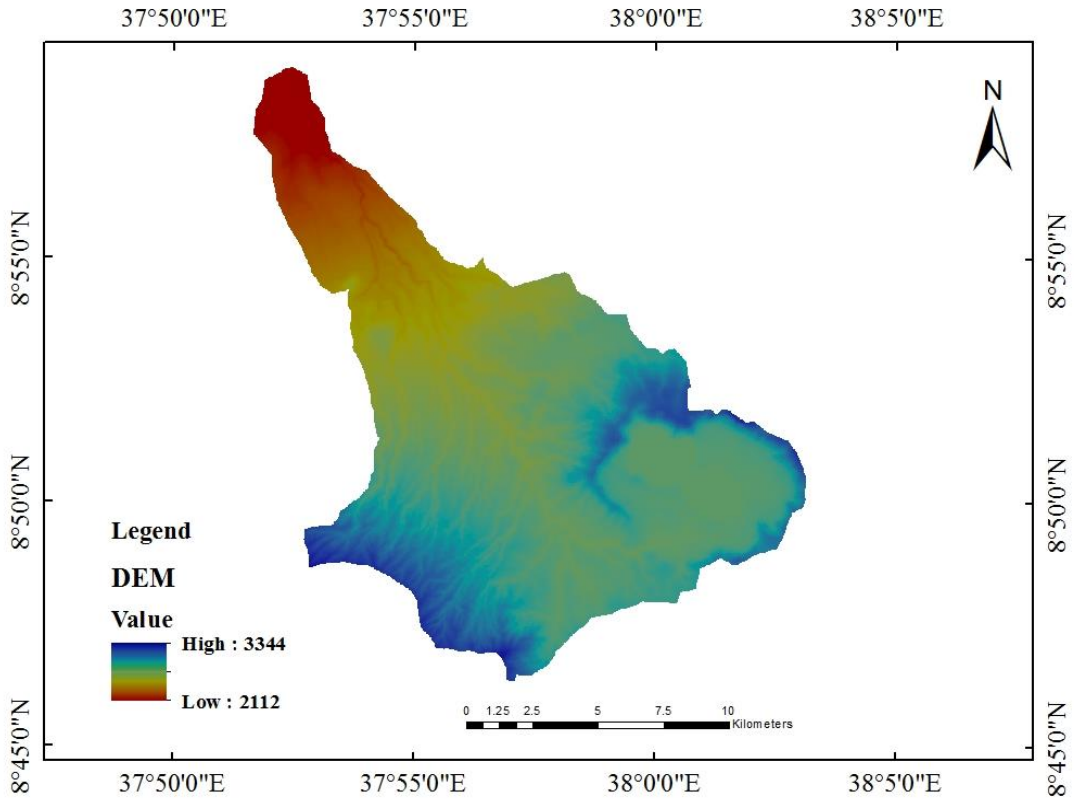

Figure 3.2 Extracted DEM of Huluka river watershed

3.4 Soil type of the study area

The soil development in the study area is mostly due to the physical disintegration and chemical decomposition of volcanic rocks. The weathering products are either remains in places and form residual soils or transported and deposited in the areas of Ambo town (Mihiretie, 2017). The soil data used for this study is obtained from Ethiopian Ministry of Water, Irrigation and Energy in vector form. Based on this data the study area has a total of six soil types and its percentage of surface area coverage are shown in (table 3.1), and (figure 3.3).

Table 3.1 Soil types and its surface coverage

S.no	Soil type	Area coverage in km^2	Surface area coverage in percentage(%)
1	Haplic Luvisols	101	49.02
2	Haplic Alisols	4	1.94
3	Haplic Nitisols	27.05	13.13
4	Chromic Luvisols	9	4.67
5	Calcic Vertisols	51	24.35
6	EutricVertisols	14	6.79
	Totals	206.05	100

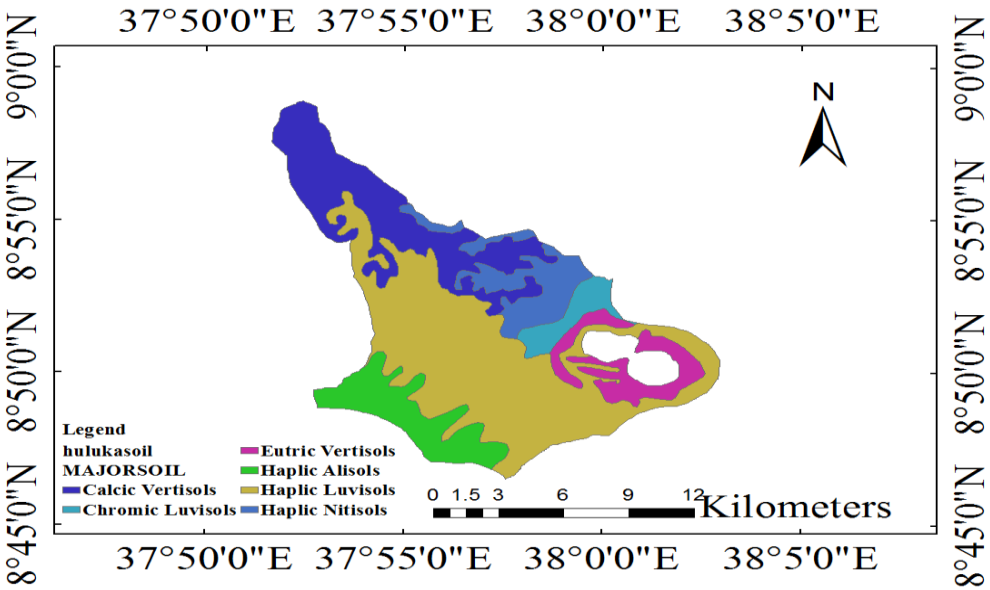

Figure 3.3 Soil type of the study area

3.5 Land Use/Land Cover (LULC)

The LULC types of Huluka river watershed classified (figure 3.4). Based on this study, the land use of the study area is changing from time to time. Since Ambo is found at the center of the watershed large portion of the agriculture land was converted in to residential. Depending up the LULC change the study watershed was classified in to four classification shown in figure 3.4

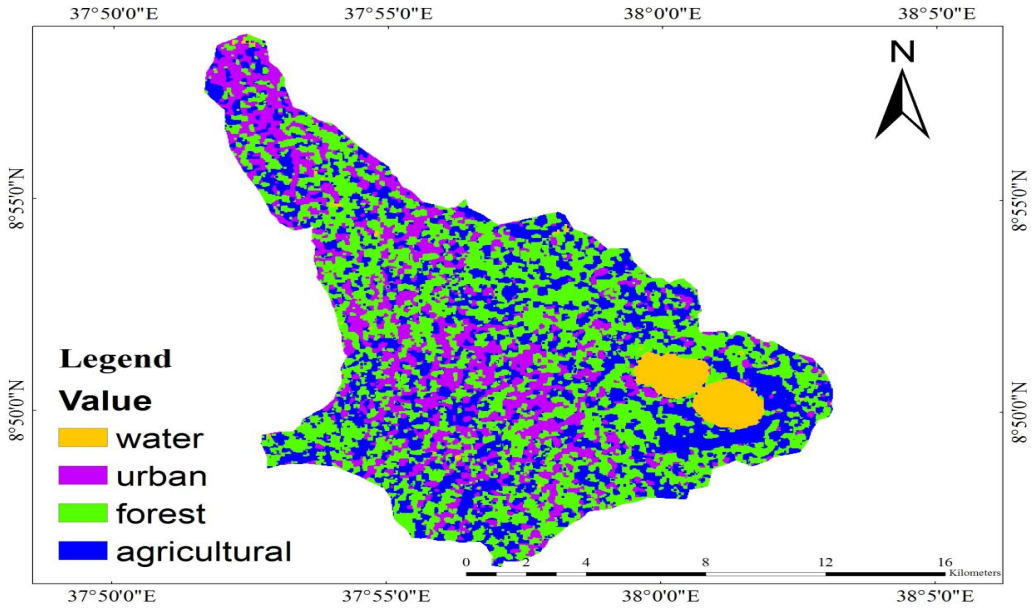

Figure 3.4 Land use types of Huluka river watershed

3.6 Materials Used (Tools)

The materials used for this particular study includes some important Softwares and its function (table 3.2).

Table 3.2 Materials used and its function

S/no	Type of materials	Its function
1	Arc-GIS 10.2	For delineation of streams to be used as an input for HEC-GeoHMS and they are terrain preprocessing
2	Microsoft excel spread sheet	for transposing daily data's from horizontal to vertical and to prepare the data for scater plot
3	HEC-GeoHMS 10.2	For CNGrid generation input data for HEC-HMS and also used to delinate study area for prepare input hydrologic HEC-HMS software
4	HEC-GeoRAS 10.2	to prepare the geometric data for import in to HEC-RAS, to generate GIS data from exported HEC-RAS
5	HEC-RAS 5.0.7	Water surface elevation visualization of stream flow, which shows of flood depth and extent
6	EASYFIT	To know best fit flood Probability distribution
7	RAINBOW	Homogeneity and stationary test
8	XLSTAT	for filling of missing data
9	USGS	for image download

3.7 Study Design

The conceptual work flow under taken throughout the study was given as in the figure 3.5.

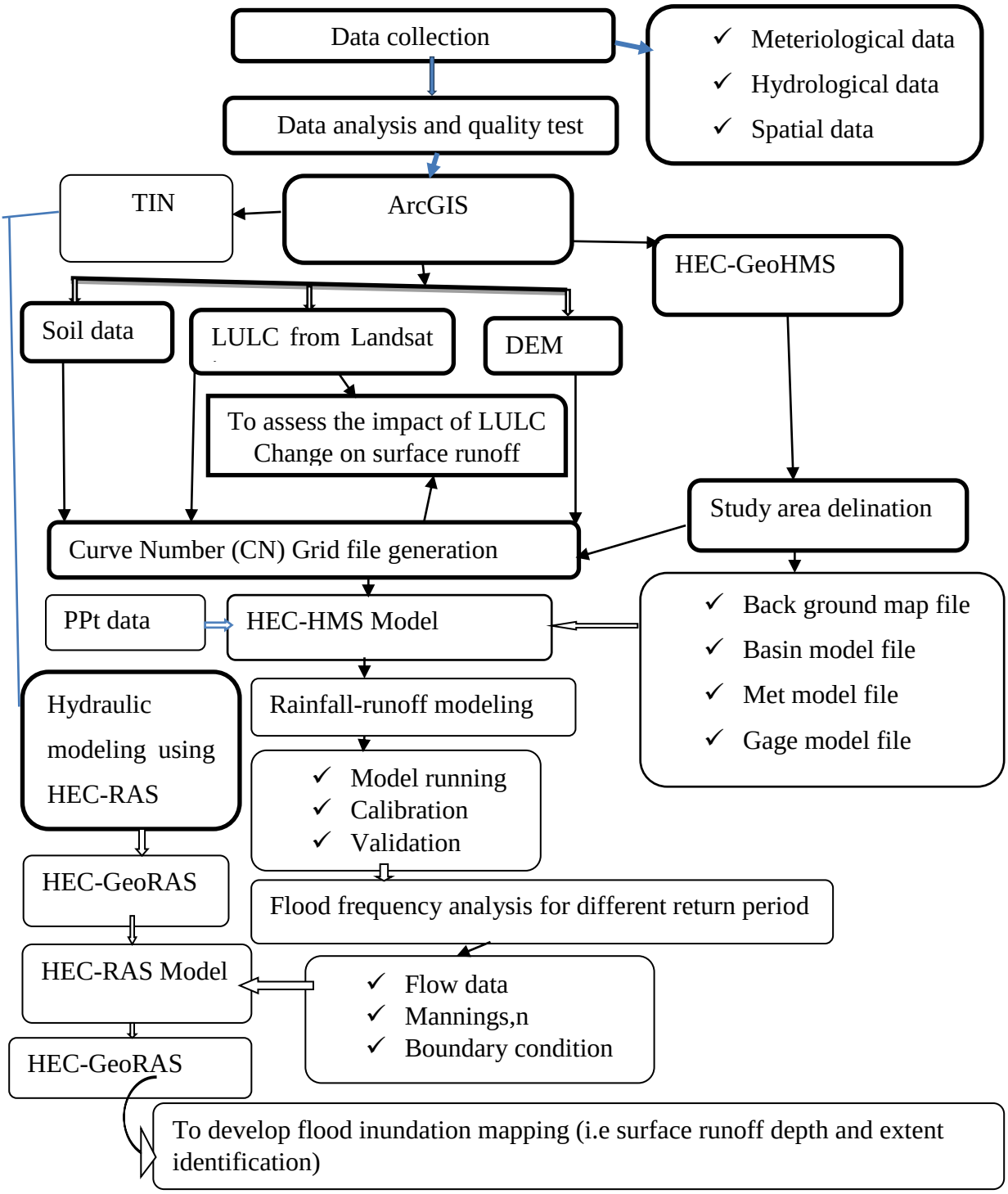

Figure 3.5 General schematic representation of work flow diagram for the study area

3.7.1 Data collection and evaluation

Secondary data was collected from the responsible organization. The data was collected annual, year and monthly report from the responsible organization (table 3.3).

Table 3.3 Type of data and its source

S.no	Type of data	Source	Period
1	DEM (30*30m)	GIS Department of MoWIE	-
2	Soil map	MoWIE	2011
3	LULC	Ethiopian Geospatial Information Agency	2011
4	Rainfall	NMAE	1987-2016
5	Stream flow	MoWIE	1997-2011

Table 3.4 Rainfall data and its geographical location

Stations names	Latitudes(in degrees)	Longitudes(in degrees)
Ambo	8.98	37.84
Guder	8.96	39.76
Dire Enchine	8.84	37.67
Waliso	8.55	37.98

Table 3.5 Stream gage data and its geographical location

Stream flow	Site	Latitudes(in degrees)	Longitudes(in degrees)
Huluka	Nr.Ambo	8.97	37.88

3.7.2 Filling missing data

The accuracy of the result was based on the quality of available data. Thus, before using collected data for analysis it has to be mandatory to check missing data, inconsistency and accuracy (Benchimol, 2015). The period of missing data has to be filled by different methods. For this study missing value was filled using linear Regression methods by XLSTAT 2018 software. XLSTAT is using for filling of missing rainfall and stream data (Taube, 2019).

XLSTAT is the richest tool for the data analysis and the statistical treatment with MS Excel. It can execute preparing, describing, visualizing, analyzing and modeling data, correlation tests, parametric and non-parametric tests, testing for outliers, homogeneity and trends. For quantitative data, XLSTAT allow to: Remove observations with missing values, use a mean imputation method, use a nearest neighbor approach and algorithm (Lloyd, 2019). This study uses a nearest neighbor approach to fill missing data.

3.7.3 Consistent check

Besides filling missing data, inconsistency problem should be checked, while data due to instrument malfunction, the records may be fail for continuity. Double mass curve is used for checking for data consistency. The plot line should be straight and the R-squared value is found between, 0.6 - 1 (Datoo, 2019). As seen (figure 3.6) the R-squared is found about 0.99 which is close to 1. So, the data is a consistent, it can be used for analysis.

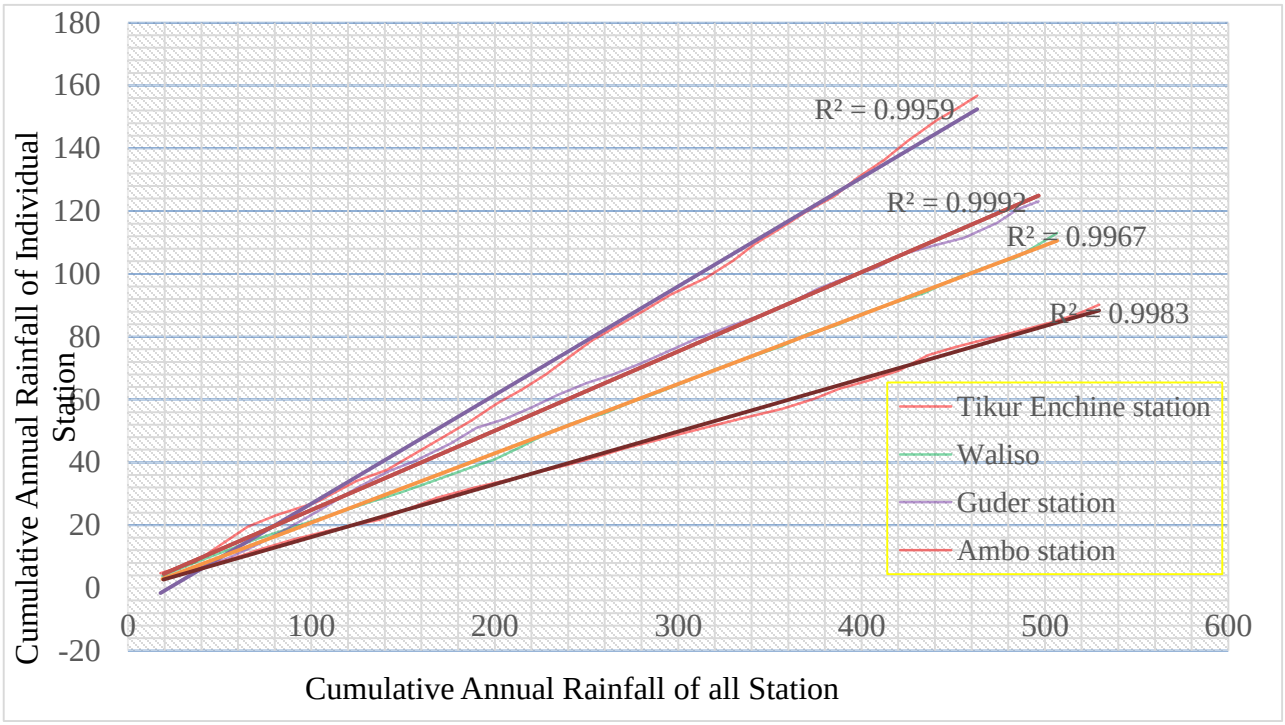

Figure 3.6 Double mass curve

3.7.4 Homogeneity and stationarity test

The homogeneity and stationarity tests were analyzed using RAINBOW software. If the observed data falls below 90% significance level the data was well homogeneous and stationary (Raes, 2006). During homogeneity and stationarity tests, the probability values below (90%, 95% and 99%) shows well homogeneous and stationary (Jameson, 2019). In this study, the p-values for the stations, ambo, guder, dire enchine and waliso rainfall data test were below 90% significance level. Therefore the data's were well homogeneous and stationary.

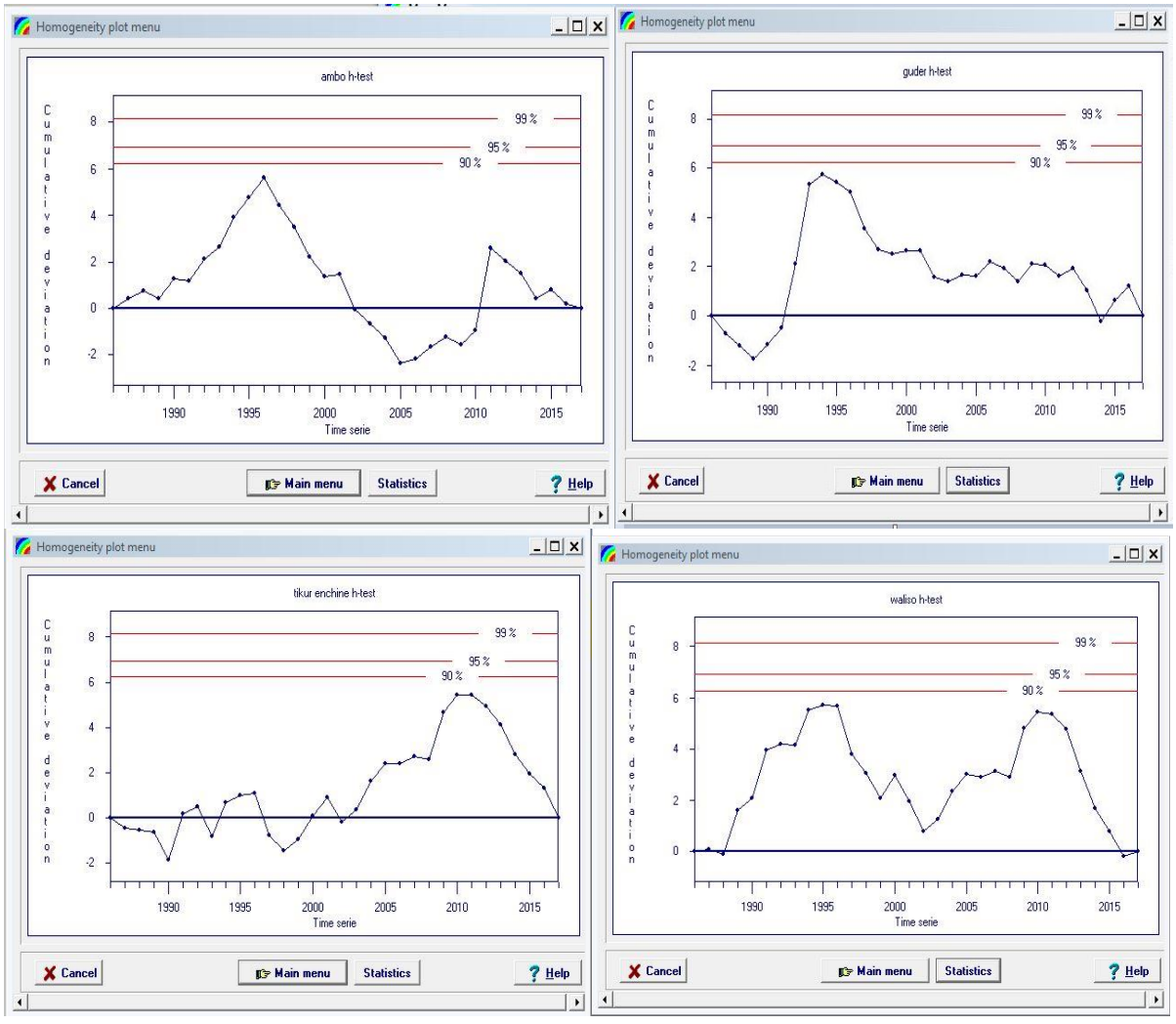

Figure 3.7 Homogeneity test

3.7.5 Digital Elevation Model Data Processing

Delineation of a watershed area using traditional method like processing topographic maps consumes much time and its accuracy is very low. But, now a time this traditional method has been replaced by automatic extraction from a Digital Elevation Model (DEM) due to the release of different type of high resolution satellites to space at different time and the production of high quality data (Nega, 2016). DEM data is used to describe topographic characteristics such as contour, slope, elevation difference, aspect and hillshade. DEM is the main dataset used for development of the basin model components and geometrical data in the HEC-HMS and HEC -RAS models respectively.

The DEM in the form of GCS_WGS_1984 raster format is changed in to the Universal Transverse Mercator (UTM) projection raster form by considering zone of the study area which Andinda, UTM Zone 37N by using Arc GIS 10.2 software package. The projected DEM clipped by using shape file of the study area. Fill sinks: If cells are available with higher elevation surrounding a cell, the water is surrounded in that cell and can not flow. Therefore this functions used to modify the elevation value to eliminate these problems by creating a depression less or hydro logically corrected DEM based on the input row DEM.

Flow directions: It is generated from the fill sinks grid and indicates the direction of the steepest descent to a neighbor cell and defined for each grid cell. the number in the legend represents directions; 1 = east, 2 = south east, 4 = south, 8 =south west, 16 = west, 32 = north west, 64 = north, 128 = north east that were listed on Appendex-A. Flow accumulation: Generated from the flow direction grid and defines the number of upstream cells draining into any given cell in the grid. Stream definition: the cells that form the stream network are defined based on a threshold number of cells that drain into a given cell.

Stream segmentation: created by splitting the streams as defined in the stream definition grid at any junction. Catchment grid delineation: For every stream segment defined by the stream segmentation grid, the corresponding watershed is delineated and stored in a grid file. Catchment polygon processing: This polygon generated from the catchment grid to delineate the boundaries of each sub basin. Drainage line processing: Generated from stream segmentation grid are transformed into a vector stream layer by this function. Adjoint catchment processing: the upstream sub basins are aggregated at any stream confluence.

Before continue to the next step of hydrological modeling, data sets in the map document should be prepared and ready by the necessary data formats. Those datasets are inputs for HEC- GeoHMS for HEC-HMS basin model generation. Raster forms are :Projected DEM (considered as raw DEM), Fil (sink filled DEM), Fdr (flow direction grid), Fac (flow accumulation grid), Str (stream network grid), StrLnk (stream link grid), Cat (catchment grid), WshSlopePct (slope grid in %). Vector forms are: Catchment, Drainage Line, AdjointCatchment.

3.8 Model set up

For rainfall runoff modeling, HEC-HMS requires Back ground map file of the study area, Basin model file, Gage file, Met file, Curve number grid, created impervious area and all these can be generated by HEC-Geo HMS.

3.8.1 HEC-Geo HMS

By using HEC-Geo HMS eight data sets can be derived from DEM that collectively describe the drainage patterns of the watershed. This includes basin slope, river slope, river length, longest flow path, basin lag time, curve number grid, created impervious area and time of concentration.

HEC-Geo HMS operates on the DEM to derive sub-basin delineation and to prepare a number of hydrologic inputs. HEC-HMS accepts the hydrologic input files as a starting boundary condition for hydrologic modeling system. HEC-Geo HMS consists of different menus that provide different functions specially, during preprocessing in Arc GIS work environment. These menu are: preprocessing, project setup, basin processing, basin characteristics, basin parameters, HMS and utility (figure 3.8).

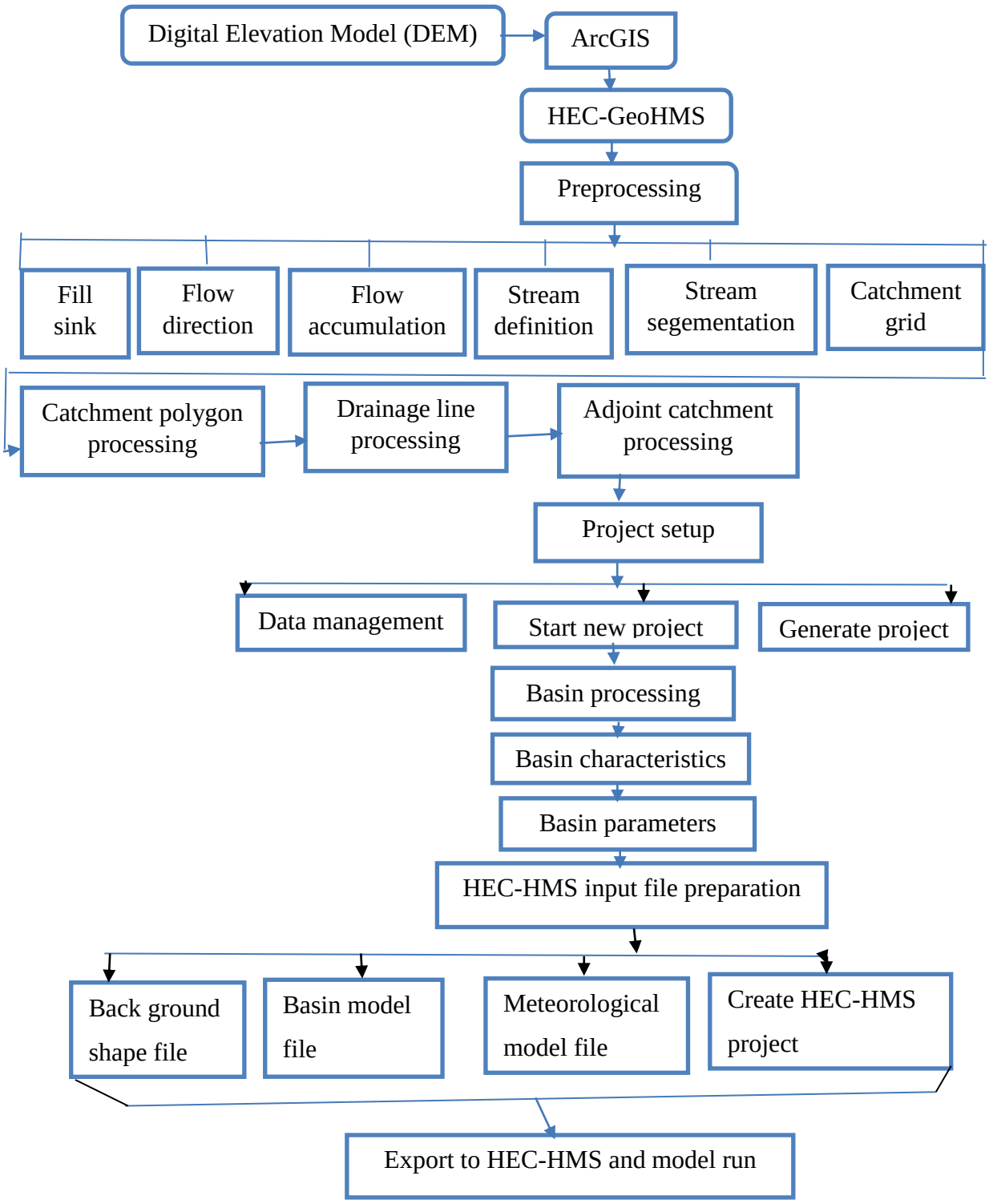

Figure 3.8 Summary of the model setup

3.8.2 Curve Number (CN) Grid Input Preparation

The runoff curve number is generated from the study area's LULC classified and hydrologic soil groups. Watershed land cover has a great importance in estimating the basin's curve number with the identification of soil textures and its permeability. Thus, according to the classification of Soil Conservation Service (SCS) method soil types of the watershed are grouped for each of the Huluka river watershed already created (figure 3.3). This method has been widely applied to estimate storm runoff depth for every cover within a watershed based on runoff curve numbers (CN). Having a curve number grid gives the utility of extracting curve number for any area in the watershed without performing any calculations. The main input data of curve number generation are clipped DEM, Land use land cover classified and soil data.

3.8.3 Preparing land use data for CN grid

Landsat Data Processing

Determination of Runoff Curve Number (CN) requires land use classification and the potential of deriving land use maps from satellite images is one of the main objective of this study due to the expansion of urbanization currently increased in Ambo town. Land use from large areas can be detected easily in a short time with low cost compared to the traditional methods.

The landsat data used is downloaded from the official website of United States Geological Survey (USGS). The landsat data of the watershed for 1997, 2005 and 2011 with a resolution of 30*30m is selected and used. The selection is based on the available daily rainfall, quality of image and resolution available.

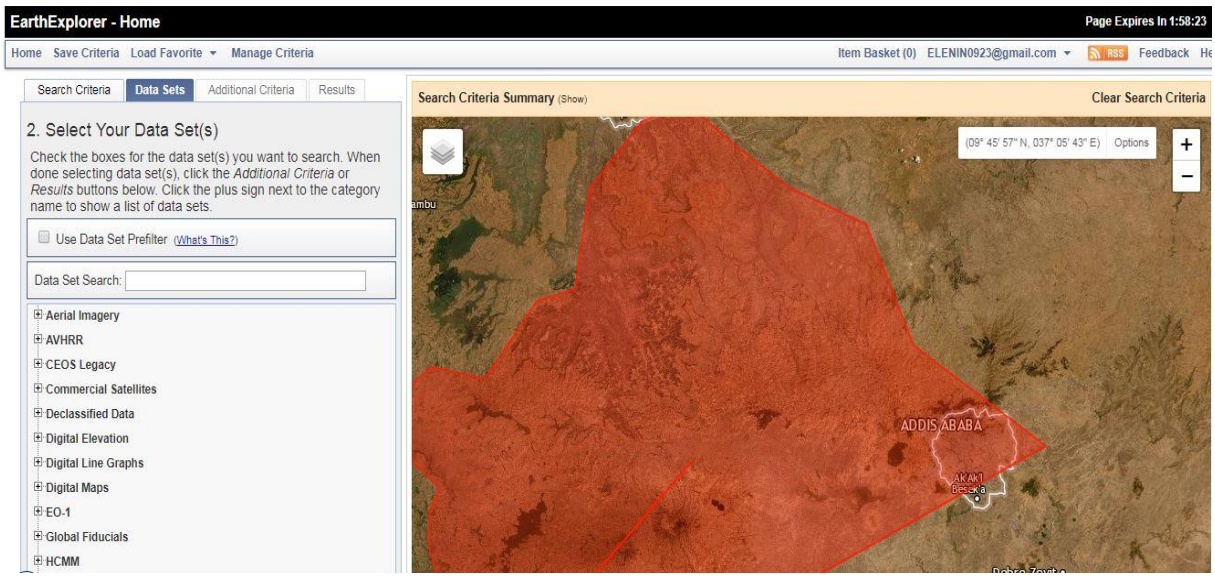

Figure 3.9 Landsat7data downloaded from official website of US Geological Survey (USGS)

As shown from figure 3.9, to downloading the landsat data first KML shape file with a maximum of 30 points of the watershed is prepared and uploaded to the above site. The landsat data downloaded from the landsat archive in the form of Geotiff with different bands. Before utilizing the data the following activities are done using Arc GIS 10.2 software package. Frist all the available bands of satellite image are combined by using composite bands function. The next step was combined landsat data in the form of GCS_WGS_1984 raster format is changed in to the Universal Transverse Mercator (UTM) projection raster form by considering zone of the study area which Adindan, UTM Zone 37N by using Arc GIS 10.2 software package. The third step was projected landsat data is clipped by using the shape file of Huluka river watershed prepared.

The fourth step were Individual bands composite in a Red, Green and Blue (RGB) combination in order to visualize the data in color. There are many different combinations that can be made but in this study case 3, 2, 1 RGB combination is selected**.** The selected color composite is as close to true color. At this stage the landsat data is ready for land use classification. The land use classification was performing using a unsupervised classification method using create signature and maximum likelihood classification functions of ArcGIS. Land use/cover class is carried out by assigning a grid code for each class. Accordingly, four types of land use were identified in the study area, namely Water body, Urban area, Forest

area and Agricultural land. The classified LULC for selected different years were indicated on Appendex-J. The classified land use raster maps were vectorized and converted to land use shape file maps using raster to polygon function. At this stage the land use data can merge with soil data for curve number generation and extraction of area coverage for each class is possible.

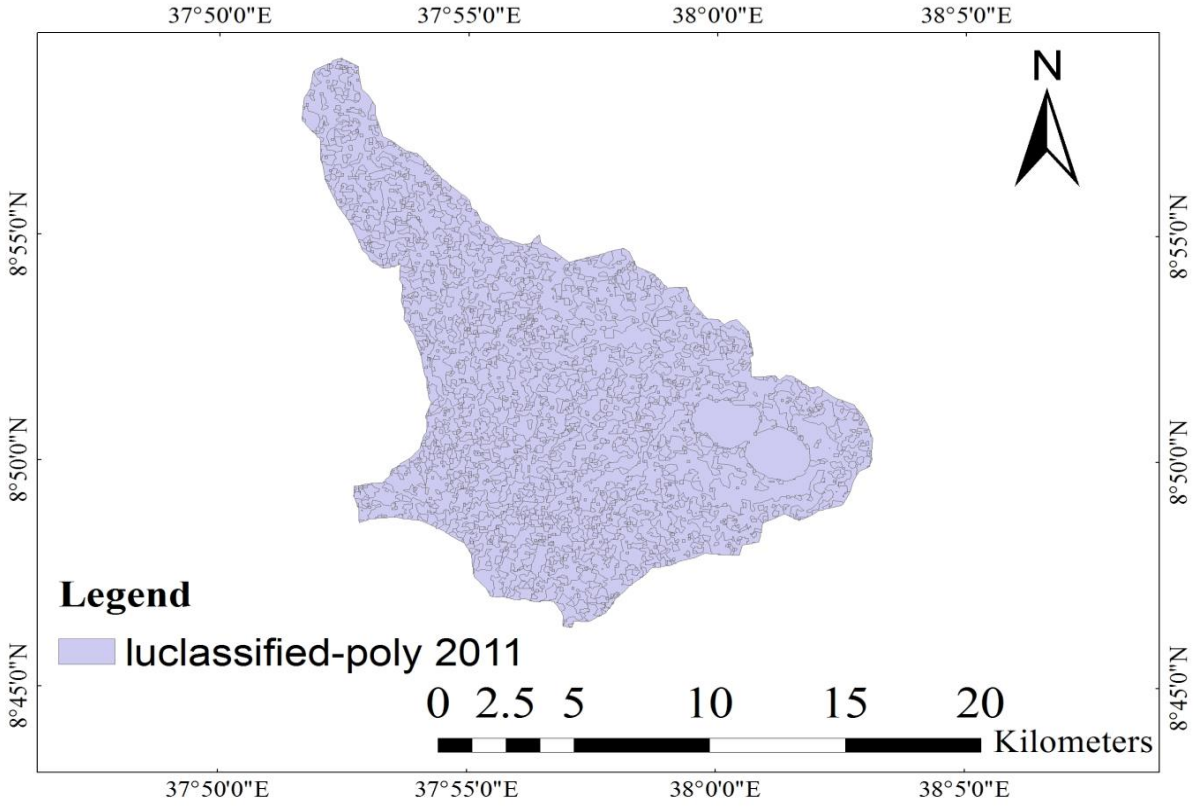

Figure 3.10 Processed land uses as shape file

3.8.4 Preparing Soil Data for CN Grid

Accordingly the soil map of the study area found as shape file and all of these soil types found in the area categorized on three Hydrological Soil Groups (HSG), namely B, C and D. Hydrological Soil Groups types (table 3.6).

Table 3.6 Soil types and its Hydrological soil group types of the study area

Soil types	Hydrological Soil Group (HSGs) types
Haplic Luvisols	D
Calcic Vertisols	D
Haplic Nitisols	B
Chromic Luvisols	B
Haplic Alisols	C
Eutric Vertisols	D

3.8.5 Merging of Soil and Land Use Data

Both the land use class and soil class of the study area are prepared in shape file format which are very important data's for curve number (CN) generation. But, to utilize this data for CN generation the two shape files are merged by using union function of ArcGIS 10.2 software package. The union function uses the both land use and soil feature classes as input. The output of merged features contains attributes values from both inputs.

3.8.6 Creating CN Look-up Table

Curve number look up table is the most fundamental input table for CN grid generation and created by using create table function of Arc GIS 10.2 and assigned Hydrological Soil Group (HSG) for each land use type (table 3.7).

Table 3.7 Created CN look up table

LUvalue	Description	A	B	C	D
1	Water body	100	100	100	100
2	Agricultura area	68	78	86	89
3	Forest area	30	60	73	79
4	Urban area	61	75	85	88

The columns represented by A, B, C and D stores curve numbers for each of corresponding soil groups for each land use category and the values are determined by using SCS TR55 (1986) which is indicated in Appendex-L. The CN values range from 100 (for water bodies)

to approximately 30 for permeable soils with high infiltration rates. Accordingly the minimum and maximum CN values of the study area are 60 and 100 respectively. Now all the necessary inputs for hydrological modeling are prepared and ready based on the required standard.

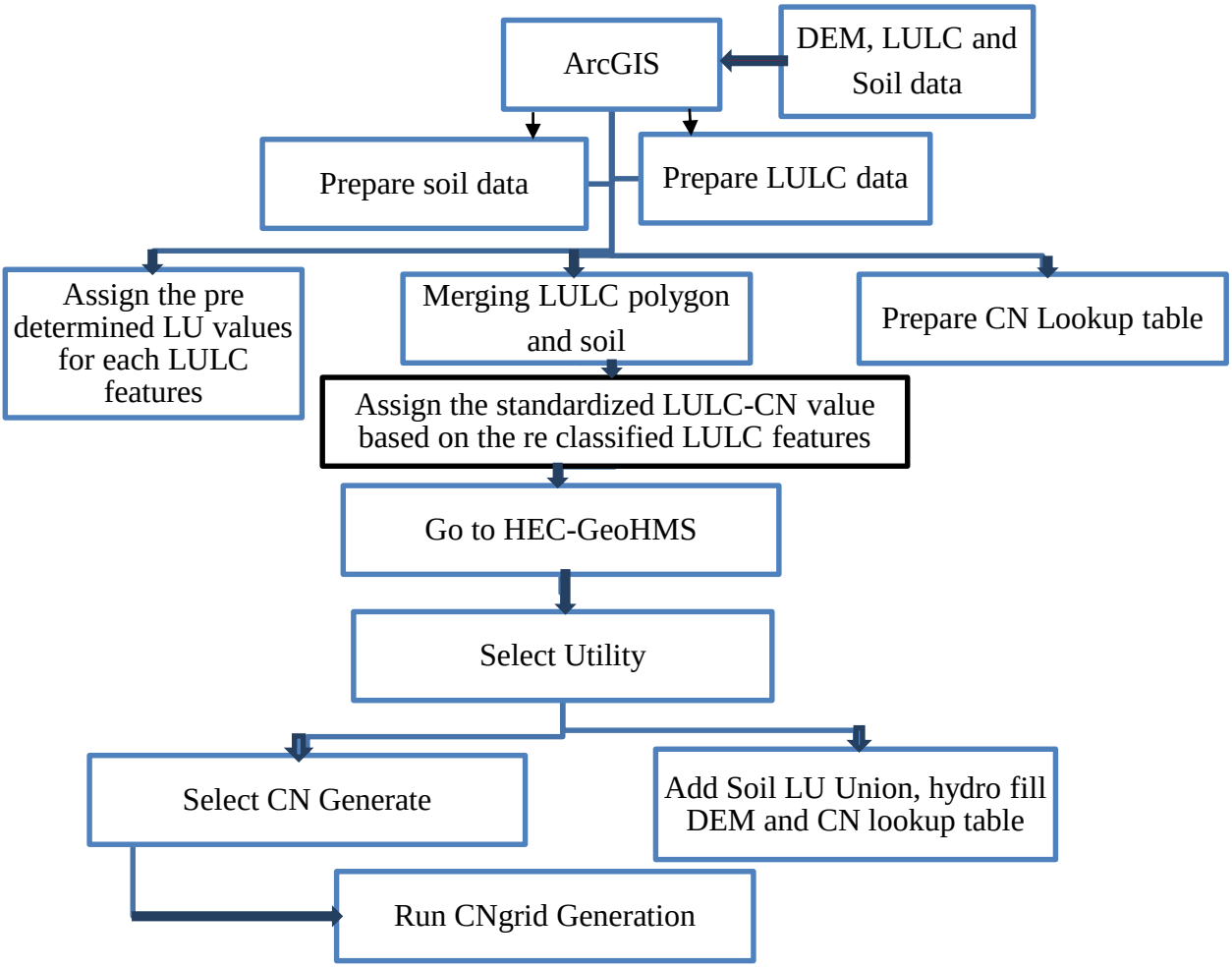

Figure 3.11 Schematic representation of CNgrid generation procedures

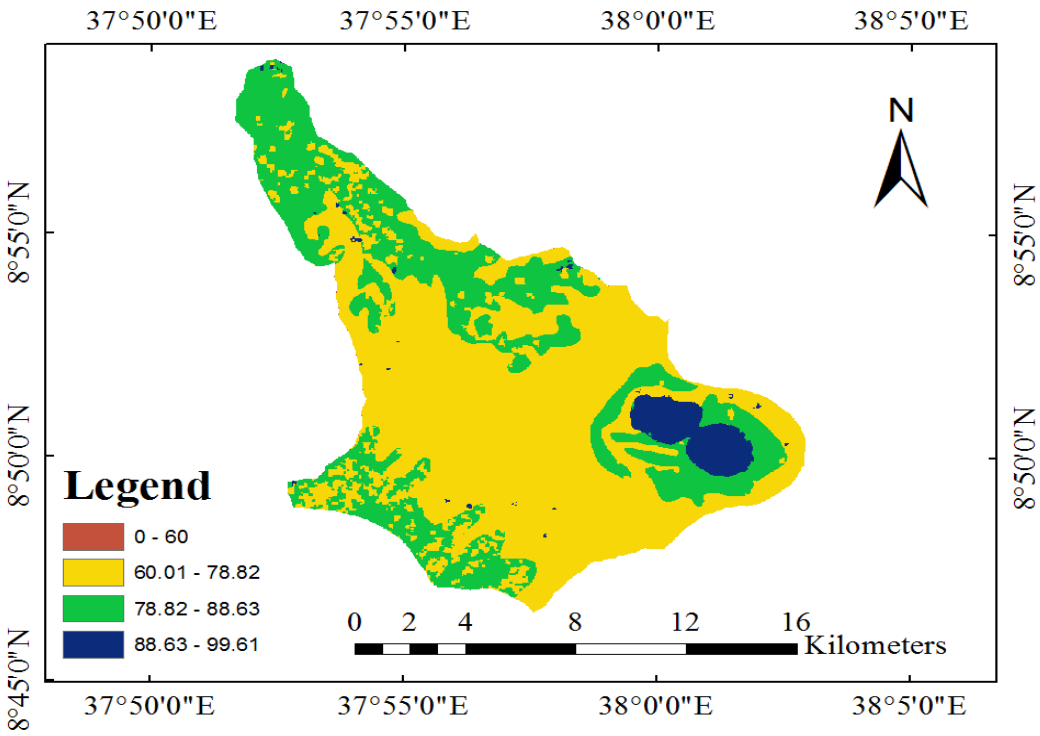

Figure 3.12 Generated Curve number of Huluka river watershed for 2011

3.8.7 Areal Precipitation

For analyses involving areas larger than a few square miles, it may be necessary to make estimates of average rainfall depths over watershed areas since a rain gauge records rainfall at a geographical point (Fetter, 2018). There are many methods available to determine the areal rainfall over the watershed from the rain gauge measurement: Arithmetic Mean, Thiessen Polygon, Isohyetal, Grid Point, Percent Normal and Hypsometric are available for estimating average precipitation over a drainage basin (Tegine, 2018).

Choice of methods requires judgment in consideration of quality and nature of the data, and the importance, use, and required precision of the result. A Thiessen polygon method is most widely used method compared to other (Aasa, 2019).

In HEC-HMS meteorological modeling can be under taken using the frequency storm, gridded precipitation, specified hyetograph method, inverse distance method and Gage weight method. In this study Gage weight method for meteorological modeling was selected as this method considered all the areal contributions of the stations under consideration. In this method, weights are given to all the measuring gauges on the basis of their areal coverage of

the watershed, thus eliminating the discrepancies in their spacing over the basins on table (3.8). In this procedure, areas and lines between adjacent stations were generated on a map of the study area by using Arc GIS 10.2 software with Arc tool box extension by selecting analysis tools under proximity create theissen polygons. The perpendicular bisector of these lines forms a pattern of polygons with one station in each polygon (figure 3.13). The area with each station is taken represents the area of its polygon, and this area is used as a factor for weighting the station precipitation. The contribution of the rainfall from each gauging station is limited by its weighing factor. According to Thiessen, the average rainfall, R_{areal} over the area can be computed (equation 3.1) (Nharo, 2019).

$$R_{areal}=\sum_{i=1}^{n}\frac{RiAi}{At} \quad \text{---------- 3.1}$$

Where, Ri is the rainfall at station i, Ai is the polygon area of station i, At is total watershed area, and n is the number of stations. The area functions Ai/At are known as the Thiessen coefficients and once they are determined for a given stable station network, the areal rainfall can be computed for the set of rainfall measurements.

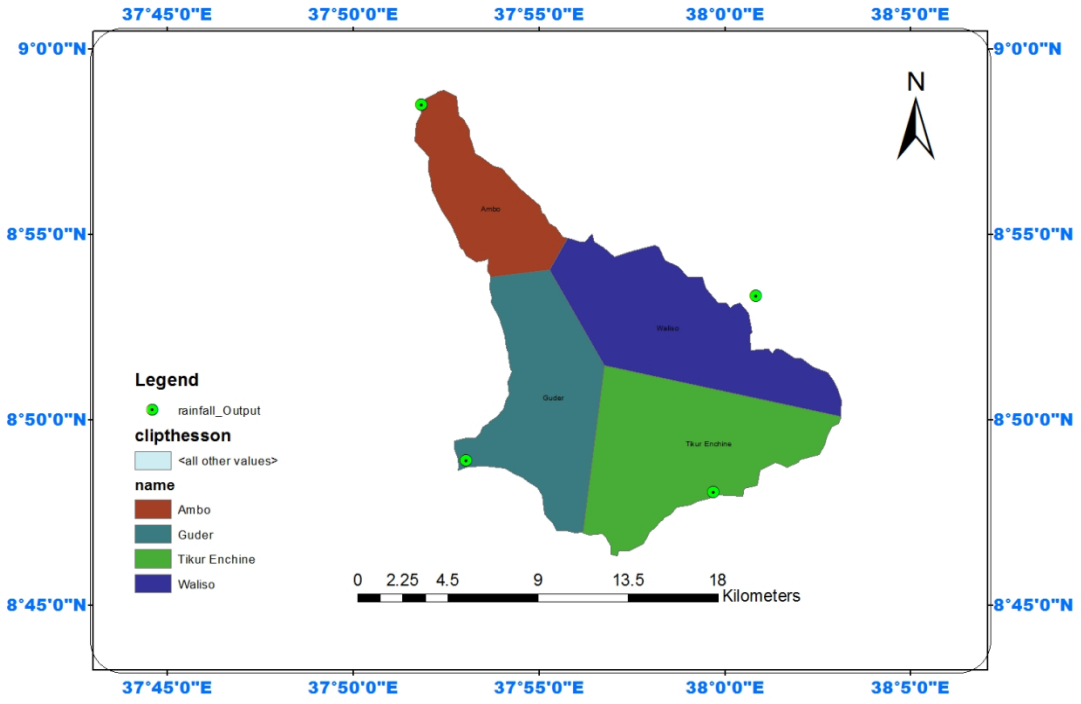

Figure 3.13 Theissen polygon for areal precipitation

Table 3.8 Stations areal weight of theissen polygon

S.no	Name of station	Area of polygon	Areal weight(ai/at)
1	Ambo	26.763	0.13
2	Guder	45.8	0.222
3	Dire Enchine	77.02	0.374
4	Waliso	57.5	0.279
Total		206.05	1.00

3.8.8 Creating Impervious Grid of study Area

Knowing percentage of impervious cover is very important in land use planning and management. It is a key factor for hydrological modeling especially in small urban watersheds. Percentage of impervious grid needed to map as a continuous variable and its value ranges from 0 to 100 percent. 0 indicates the entire area is pervious almost all of the rain fall in the area infiltrates in to subsurface of the area and 100 means all the available rainfall gives runoff and infiltration is almost 0 (Labbas, 2013).

Based on the land use classification of this study; there are 4 classifications namely, Water body, Urban area, Forest and Agriculture lands. Accordingly, percentage of impervious value for it assigned for each category and table. The assigned values are based on SCS TR55 (1986) and user's guide for the California impervious surface coefficients (Beck, 2017). Land uses may vary from watershed to watershed, but can be defined on a given range. The first step in impervious grid generation using HEC-GeoHMS is converting land use map (grid) into a polygon feature class and add percentage of impervious as on the attribute table of land use polygon feature class. Percent land use impervious is prepared in excel format and opened in Arc GIS. By using join function of Arc GIS the land use polygon feature class and the excel table are joined. Previously created impervious field on the land use polygon feature class was calculated based on the assigned impervious percent values of excel by using field calculator function.

The second step is generating impervious grid using HEC-GeoHMS feature to raster function use (Input features: land use polygon, field: land use impervious percentage area). This generated percentage of impervious grid is basic input for HEC-HMS project generation.

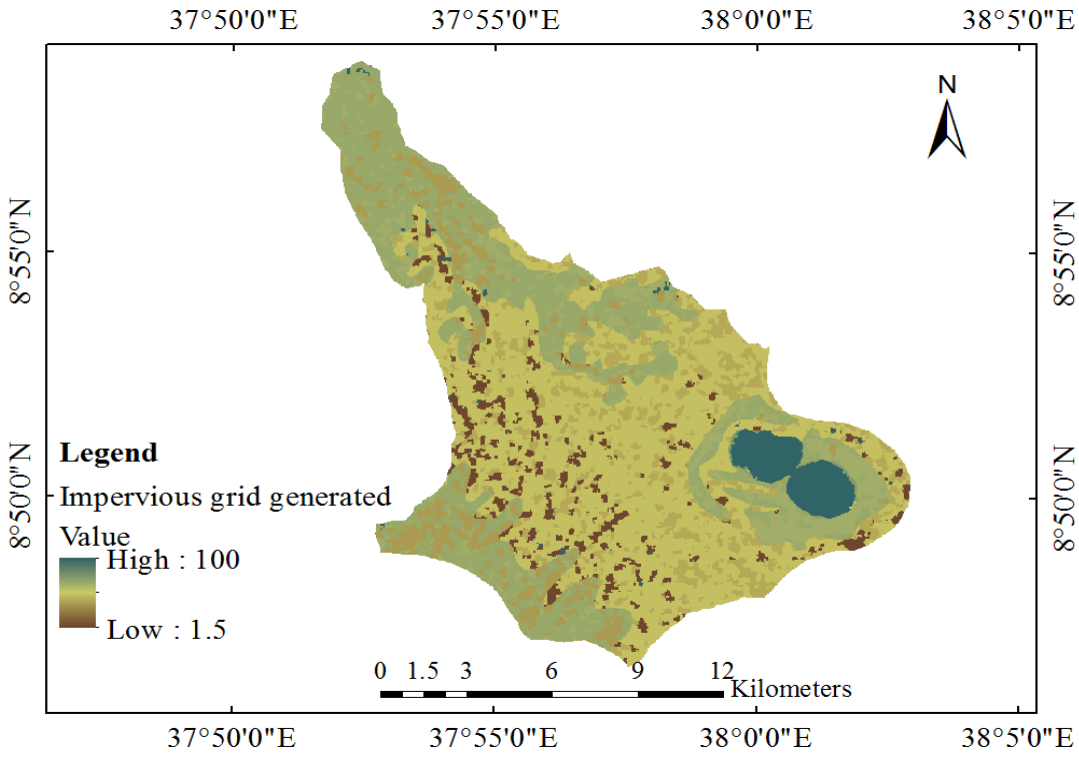

Figure 3.14 Generated impervious grid

To create an HMS project different tools of HEC- GeoHMS are used which are found on four main views namely; HMS model set up, basin characteristics, HMS input parameters and HMS menus.

HMS model setup

Data management window: The necessary data sets used for HMS project generation are added these are; row DEM, Sink filled DEM, flow direction grid, flow accumulation grid, stream network grid, stream link grid, catchment grid, adjoint catchment and drainage line. These data's are checked on the data management window of HEC- GeoHMS and assigned based on the corresponding map layers used to generate the project. Creating new HMS project: start new project; assign Huluka Watershed on project area and on the project point. Then project point and project area feature classes are created. Main outlet of the watershed assigned: the main outlet of the watershed is at Ambo town assigned by using add project

point tool of HEC- GeoHMS. Generate HMS project: before generating a project the data management window of HEC-GeoHMS is checked and HMS project is generated by creating a mesh (by delineating watershed created main outlet of the Huluka river watershed).

Extracting watershed characteristics

Extracting physical characteristics of sub-basins and streams into attribute tables is accomplished by using the basin characteristics menu of HEC- GeoHMS these are: River length: the length of each river segments is computed and stored by using the Huluka River name as input. River slope: this tool computes the slope of the river segments and stores by using raw DEM and created river. Basin slope: average slope of each the 4 sub-basins is computed using the slope grid and sub basin polygons.

Longest flow path: the longest flow path for each sub-basins of Huluka river watershed is created by using raw DEM, flow direction grid and sub basins as input. Basin centroid: a point feature class is created and stored for the centroid of each sub-basin. Basin centroid elevation: the elevation for each centroid point is created by using raw DEM and basin centroid as inputs. Centroidal longest flow path: a polyline feature class is created by using this tool. The creation of this polyline shows the flow path for each centroid point along longest flow path of each sub basin.

HMS Inputs/Parameters

The hydrologic parameters menu of HEC - GeoHMS has tools to estimate and assign watershed and stream parameters. With this menu HMS processes selected, river auto name, basin auto name, sub-basin parameters and CN lag method are computed.

HMS project creation

By using tools found in the HMS menu input files for HEC-HMS are created. Activities accomplished using those HEC- GeoHMS menu are: HMS units assigned, data checking, HMS schematic, HMS toggling and legend, add coordinates, prepare data for model export, background shape file, basin model, meteorological model created and finally HMS project is created know the project is ready for HMS Process (figure 3.15).

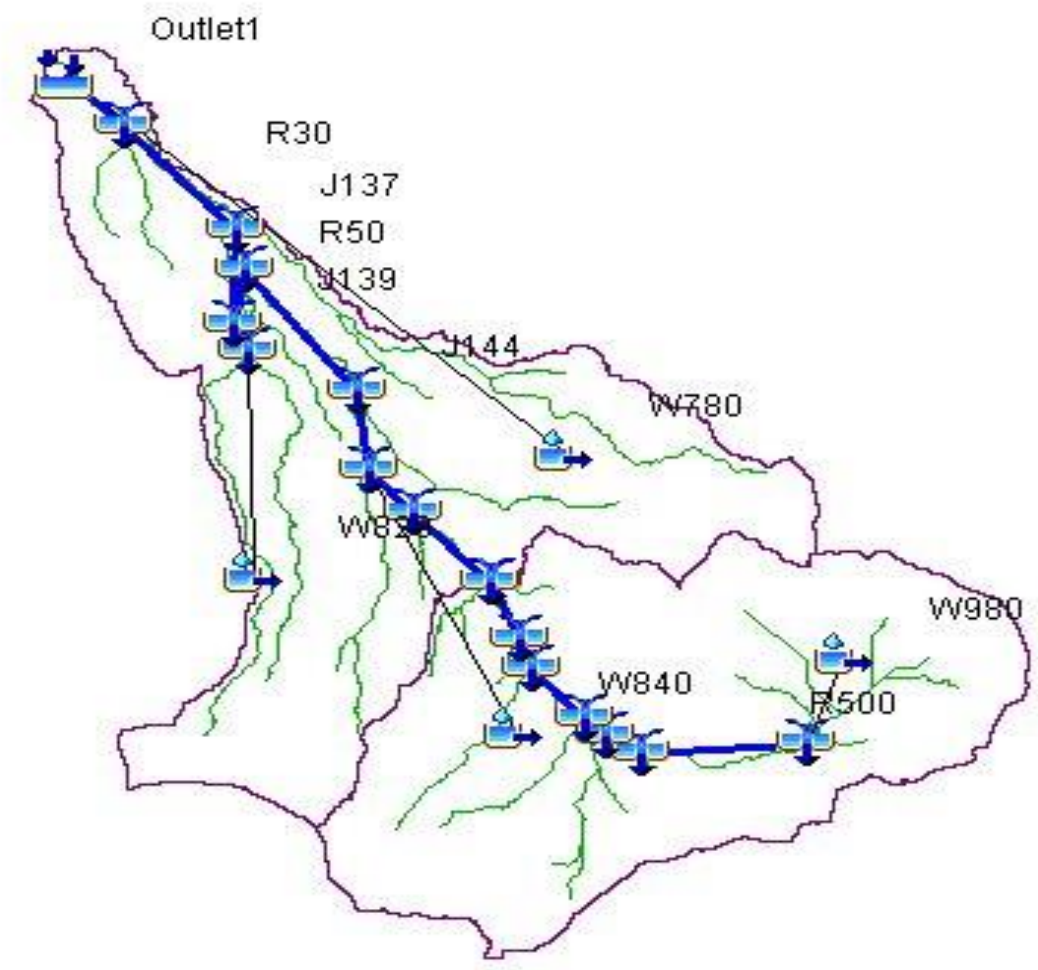

Figure 3.15 Created HEC-HMS setup

3.9 HEC-HMS Model Analysis

For simulating rainfall-runoff processes the HEC-HMS model has four major components. These are; basin model, meteorological model, control specification and time series. Totally the Huluka river watershed has 4 sub basins, 16 reaches and 16 junctions with upstream to downstream sequence. The control specification contains time related information (year, starting date and time, end date and time) for the simulation.

3.9.1 Rainfall (precipitation) loss modeling

SCS-CN was selected as a method for excess precipitation modeling. The method requires only three inputs. These are: Curve number, Initial abstraction and Percentage of impervious. As the curve number was already generated and embedded into the basin model file, the software automatically extracts and assigns the curve number value for each sub-basin (Pathan, 2019).

$$Pe = \frac{(P-Ia)2}{(P-Ia)+S} \text{----------3.1}$$

Where: Pe = Accumulated precipitation excess at time t; P = Accumulated rainfall depth at time t; Ia = Initial abstraction and S = Potential maximum retention.

Ia and S are calculated (equations 3.2). The initial abstraction comprises all the losses that occur before surface runoff begins. According to the NRCS (1986), it includes water retained in surface depressions as well as water intercepted by vegetation, evaporation and infiltration. In the CN model, Ia is assumed to be correlated to maximum retention potential S.

$$Ia = 0.2S \text{----------3.2}$$

The maximum retention S is further related to the soil and cover conditions of the analyzed watershed through the CN. Computing maximum retention potential (equation 3.3), the initial abstraction throughout each sub-basin was computed and manually assigned.

$$S = \frac{25400}{CN} - 254 \text{----------3.3}$$

Impervious surface area coverage of the study were analyzed depending up the the curve number value that can be generated from the land use land cover and hydrologic soil group types merged in well format (Dan-Jumbo, 2019). Several factors, such as the percentage of impervious area and the means of conveying runoff from impervious areas to the drainage

system, should be considered in computing CN for urban areas. Among them Connected impervious areas and Unconnected impervious areas are the main considered.

3.9.2 Transform Method

SCS-UH was chosen for transform method. The SCS-UH requires only basin lag time. As the HEC-Geo HMS can automatically extract the basin lag time from the inserted curve number grid, it is so easy to proceed with this method.

3.9.3 Flood routing method

The HEC-HMS contains different flood routing methods of which the Muskingum flood routing method was selected for Huluka river watershed. The Muskingum method is one of the most popular flood routing methods. Muskingum flood routing requires two parameters, namely: flood wave travel time (k) ranges from (0-100 hrs) and weighted coefficient of discharge (x) ranges from (0-0.5). The initial of Muskingum-K value lies between the specified ranges was calculated using (equation 3.6) and manually assigned for sub-basin and later calibrated. According to Haktanir and Ozmen (1997) the Muskingum flood routing method uses the following popular hydrologic flood routing equation.

$$\frac{ds}{dt} = I - Q \quad \text{----------3.4}$$

$$S = k[xI + (1 - x)Q] \quad \text{----------3.5}$$

Where; ds/dt is rate of change of storage per unit time, I is inflow, Q is outflow, S is Storage, x is weighted coefficient of discharge, k is wave travel length.

Wave travel time (k parameter) for each reach was calculated from equation (3.6) as the initial value. Running the model with this initial value, later the parameters were optimized.

$$K = \frac{V}{L} \quad \text{----------3.6}$$

$$V = \frac{Q}{A} \quad \text{----------3.7}$$

Where; k is flood wave travel length, v is permissible velocity, l is reach length, Q is flood discharge (m^3/s), A is cross sectional area.

Here the permissible velocity value should be in the range that neither causes erosion of the channel nor letting deposition of sediment. According to (ERA drainage manual, 2013), this

permissible velocity is classified into numerous categories depending on the channel geometry. On the basis of this assumption, 1.5m/s permissible velocity was used (3.6) in order to calculate the initial value of k. Based on this huluka river watershed has a total of 16 reaches and the correct values for Muskingum K and Muskingum X is assigned.

3.9.4 Sensitivity Analysis

Sensitivity analysis is a method to determine which parameters of the model have the greatest impact on the model results. There are three parameters (curve number, initial abstraction and lag-time) of the event model that were subject to the sensitivity analysis (Ahmadisharaf, 2019). The SCS curve number method, which is used to handle the infiltration loss in the sub-basins has three parameters such as curve number, initial abstraction and percent impervious area in the basin (Igulu, 2020). Percent impervious area is taken as 30% since there is urban settlements inside the sub-basin. Therefore, the parameters (curve number, initial abstraction and lag-time) of SCS curve number method were used for Calibration. The SCS unit hydrograph method which is used to model the transformation of precipitation excess into direct surface runoff, has lag time parameter. This parameter was also used for calibrated.

3.9.5 Model Performance Evaluation

Nash–Sutcliffe model efficiency coefficient (NSE):is used to assess the predictive power of hydrological models or used to analysis the correlation between simulated and observed hydrological data (Adla, 2019).It can be expressed as:

$$\mathrm{NSE} = 1 - \frac{\sum\left(Q_{o(t)} - Q_{m(t)}\right)^2}{\sum\left(Q_{ob(t)} - \overline{Q_{ob}}\right)^2} \quad \text{---------- 3.8}$$

Where; Q_m= modeled flow, Q_o= observed flow, $\bar{Q}$ = mean of observed flow

It can range from $-\infty$ to 1. An efficiency of 1 (NSE = 1) corresponds to a perfect match of modeled discharge to the observed data. An efficiency of 0 (NSE = 0) indicates that the model predictions are as accurate as the mean of the observed data, where as an efficiency less than zero (NSE < 0) occurs when the observed mean is a better predictor than the model or, in other words, when the residual variance (described by the numerator in the expression above), is larger than the data variance (described by the denominator). Essentially, the closer the model efficiency is to 1, the model is more accurate (Cakir, 2020).

Coefficient of Determination (R^2): The coefficient of determination (R^2) is a measure of the proportion of variance of a predicted outcome. With a value of 0 to 1, the coefficient of determination is calculated as the square of the correlation coefficient (R^2) between the sample and predicted data. The coefficient of determination shows how well a regression model fits the data. Its value represents the percentage of variation that can be explained by the regression equation (Piepho, 2019). It can be expressed as:

$$R^2 = \frac{\sum(Q_{obs(t)} - \overline{Q}_{obs}) \sum(Q_{sim(t)} - \overline{Q}_{sim(t)})^2}{\sum(Q_{obs(t)} - \overline{Q}_{obs})^2 \sum(Q_{sim(t)} - \overline{Q}_{sim(t)})^2} \quad \text{---------- 3.9}$$

Where; R^2 is coefficient of determination, Q_{obs} is observed value at the i^{th} time interval, $Q_{sim(t)}$ is simulated value at the i^{th} time interval, $\overline{Q}_{obs}$ is mean of observed discharges

$\overline{Q}_{sim(t)}$ is mean of simulated discharges value at i^{th} time interval.

A value of 1 means every point on the regression line fits the data; a value of 0.5 means only half of the variation is explained by the regression. A coefficient of determination (R^2) zero means that the dependent variable cannot be predicted from the independent variable. The coefficient of determination is also commonly used to show how accurately a regression model can predict future outcomes (Myers, 2019).

Root Mean Squared Error (RMSE) of observations given by equation 3.10.

$$RMSE = \sum_{i=1}^{n} \left(\frac{(Q_i - S_i)^2}{Q_i - \bar{Q}} \right) \quad \text{----------3.10}$$

Where, Qi is observed stream flow data, $\overline{Q}$ is average observed stream flow data, Si is simulated stream flow data.

3.10 Flood Frequency Analysis

Flood frequency analysis is the most important statistical technique in understanding the nature and magnitude of peak discharge in a river or flood plain. Flood frequency analysis gives the probability model curve to the annual flood peaks which are recorded by the period observation and data of flood occurred in 15 years (1997-2011). This method is useful to predict recurrence interval and helps to cause no damage to the public and government properties. There are different types of methods for the estimation of Flood Frequency Analysis (FFA). Before the demarcation of flood inundation area of the flood plain, peak discharge analyzing is important to obtain Probability distribution. The terms return period and recurrence interval are used to denote the reciprocal of the annual probability of exceedance. Ethiopian Roads Authority (ERA) divided the country into eight Meteorological regions based on their rainfall pattern similarity (figure3.16) and develops intensity-duration frequency curves (IDF curve) for 24hr rainfall depth for each Meteorological region as a function of the 2, 5, 10, 25, 50 , 100, 200 and 500 years return period of the storm events.

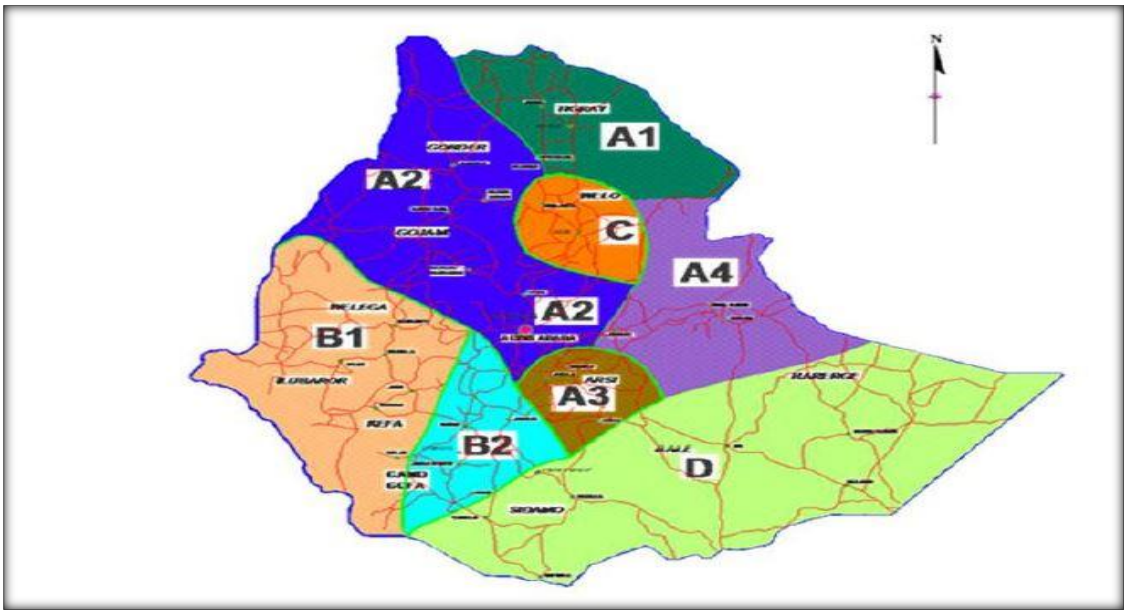

Figure 3.16 Ethiopian Rainfall regions *(ERA, 2013)*

According to ERA classification, Huluka river watershed was found in rainfall region B1(RR-B1) and the 24 hour rainfall depth for each return period was taken (table 3.9) and (Figure 3.17) shows the intensity duration frequency curve (IDF curve) of Huluka river watershed adopted from Ethiopian IDF curve developed by Ethiopian road authority.

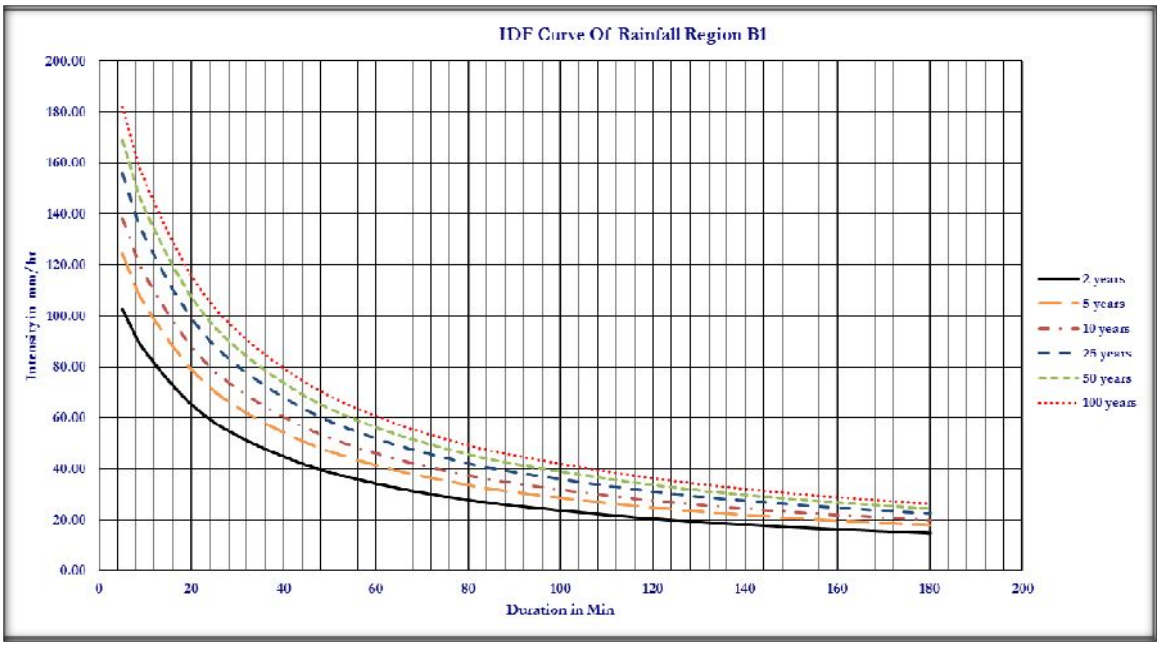

Figure 3.17 IDF curve for rainfall region B1

ERA has developed 24 hour rainfall depth for different rainfall regions of Ethiopia for corresponding return periods. Using 24 hour rainfall depth of RR B1 provided on (table 3.9) that was specified for Huluka river watershed the rainfall depth of 1, 2, 3, 6 and 12 hour were developed using (equation 3.11) and used in HEC-HMS for flood inundation area estimation.

Table 3.9 24hr Rainfall Depth (mm) Vs Frequency (yr)

24 hr Rainfall Depth (mm) vs Frequency (yr)								
Return Period Years	**2**	**5**	**10**	**25**	**50**	**100**	**200**	**500**
RR-A1	50.30	66.02	76.28	89.13	98.63	108.06	117.48	130.00
RR-A2	51.92	65.52	74.45	85.70	94.07	102.45	110.91	122.27
RR-A3	47.54	59.61	67.66	77.92	85.62	93.34	101.13	111.58
RR-A4	50.39	63.83	72.28	82.55	89.97	97.20	104.32	113.63
RR-B1	58.87	71.26	79.29	89.35	96.84	104.37	112.02	122.41
RR-B2	55.26	69.95	79.68	92.03	101.29	110.61	120.07	132.87
RR-C	56.52	71.04	80.54	92.52	101.48	110.50	119.66	132.06
RR-D	56.23	76.84	90.37	107.46	120.23	133.05	146.00	163.44

Note: RR- Rainfall Region

For drainage areas in Ethiopia, to compute the rainfall intensity at any required time using the 24hr rainfall depth, which is known as a rainfall intensity-duration-frequency (IDF) relationship.

$$\frac{R_t}{R_{24}} = \frac{t(b+24)^n}{24(b+t)^n} \quad \text{---------- 11}$$

Where: R_{Rt}= Rainfall depth ratio R_t:R_{24}, R_t = Rainfall depth in a given duration't' R_{24}= 24hr Rainfall depth, b and n are constant coefficient in which b = 0.3 and n = (0.78 – 1.09) and t = Rainfall duration.

3.11 Simulation of Hydraulic Modelling: HEC-RAS

Data required for simulation of Hydraulic modelling (HEC-RAS) are:

Triangulated Irregular Network (TIN): Digital Terrain Model in the form of Triangulated Irregular Network (TIN) is required for the hydraulic analysis of river system. TIN must be of high-resolution with continuous surface and should represent bottom of the river and adjacent flood plains as all the cross-sectional data was extracted from it. TIN of huluka river watershed were derived from respective DEM which is identified under (Appendex B). Flow data obtained from HEC-HMS software and LULC was required for the simulation of flood inundation assessement.

3.11.1 Hydraulic Model Development

A numerical model which is used to represent the hydraulic behavior of a water body is called a hydraulic model. Hydraulic models may be broadly categorized into one dimensional(1-D), two-dimensional (2-D) and three-dimensional (3-D)schemes. 1-D mathematical models are the most commonly used for flood inundation mapping and use the Saint Venant equations, and therefore rely on many high resolution morphological parameters (cross sections). Hydraulic analysis of the river system was performed with the help of HEC-RAS along with HEC-GeoRAS, an extension in ArcGIS (Jaber, 2018).

The methodology used for performing simulation of hydraulic analysis can be dividing into three parts which are as follows:

Pre-processing: Developing geometry of river in ArcGIS

Processing: Performing hydraulic computation in HEC-RAS

Post-processing: Processing RAS results in ArcGIS.

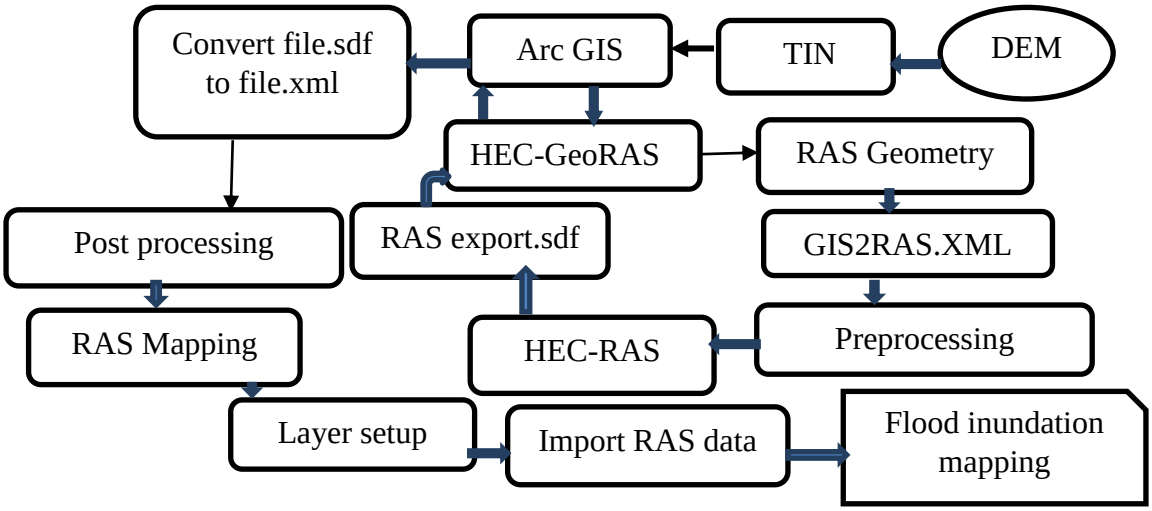

Figure 3.18 General work flow between HEC-Geo RAS and HEC-RAS for floodplain

3.11.2 RAS pre- processing

The RAS pre-processing is the task one's done in River Analysis system (RAS). River geometry was done by HEC-Geo RAS software. The HEC-Geo RAS is a GIS extension with a set of procedures, tools and utilities for the preparation of river geometry (GURMU, 2018). HEC–Geo RAS software uses Digital Terrain Model (DTM) to create river geometry. Triangular irregular Network (TIN) for Huluka watershed was developed from DEM of the huluka watershed using the 3D spatial analysis extension. A TIN is a set of adjacent, nonoverlapping triangles, computed from irregularly spaced points with x, y coordinates and z- values (Zenner, 2000).

The TIN data structure is based on irregularly spaced point, line and polygon data interpreted as mass points and break lines. Thus, TIN allows efficient generation of surface models for the analysis and display of terrain and other types of surfaces while preserving the continuous structure of features such as stream banks that are critical for hydrologic and hydraulic analyses (Burrough, 2015). Further, the river center line, River bank, flow path; XS cross-section, 3d river centerline, 3d river cross -section developed by HEC-Geo RAS. The river stream center line, bank lines, flow path center lines, and cross section lines has to be digitized from a previous river file and topographical datasets using HEC-Geo RAS interface.

The river reach (river segment between junctions), cross- section and other related data is store in the geo-database file of HEC- Geo RAS.

Creating River Centre line: The River center line layer is very important, because it represents the river network for HEC-RAS. The digitizing of stream centerline start with selecting the sketch tool from the Editor Toolbar and digitization proceed in the direction of a river flow (Akbari, 2014). The process begins from upstream end to the downstream end of the Huluka River watershed. After digitizing all of reaches, the user assigns the name of the river. This was accomplished by the selection of Assign River code / Reach Code menu item and assigning appropriate names.

Creating River bank: The interface extracts the geometric data in export RAS data in GIS2RAS.RASImport.sdf format. The bank lines layer is used to define river channel from overbank areas. The bank lines are created in similar way as the river centerline. The digitizing of bank lines starts from the upstream end, with the left bank (looking in downstream direction) being digitizing first.

Creating Flow paths:The flow path layer is a set of lines that follows the center of mass of the water flowing down the river, during the flood event (Julien, 2018). For Flood plains, the flow path center lines are digitized to represent created water flow within the flood plain. Flow path center lines are created in the upstream to downstream flow direction.

Creating cross-sections: Cross-sections are one of the most important inputs to HEC-RAS. Cross-section cut lines are used to extract the elevation data from the terrain and to create a ground profile across the flow (Patel, 2016). The intersection of cut line's with other RAS layers such as center line and flow path lines are used to compute HEC-RAS attributes such as bank stations (locations that separate main channel from floods plain) and downstream reach length (distance between cross-section). The following important basic rules were followed during the process of drawing cross section cut lines (Michotte, 2017)

Cut lines are drawn perpendicular to a direction of flow, Cut lines are drawn directionally from left to right bank, looking downstream direction and Cut line's do not intersect each other. For Huluka watershed, there are about 99 cut line's was created. Thus, for each cut line's, the 2D feature class XS Cut lines are intersected with the TIN to create a feature class with 3D cross-section. Finally, Creating GIS import file for HEC-RAS so that it could import

the GIS data to create the geometry file. First, choosing layer set up window and under required surface choose TIN, under required layers select river layer, XS-Cut line's layer and XS-Cut line's 3D layer, under optional layers. choose banks, flow path, River 3D and optional tables are not used in this study, show all null value.

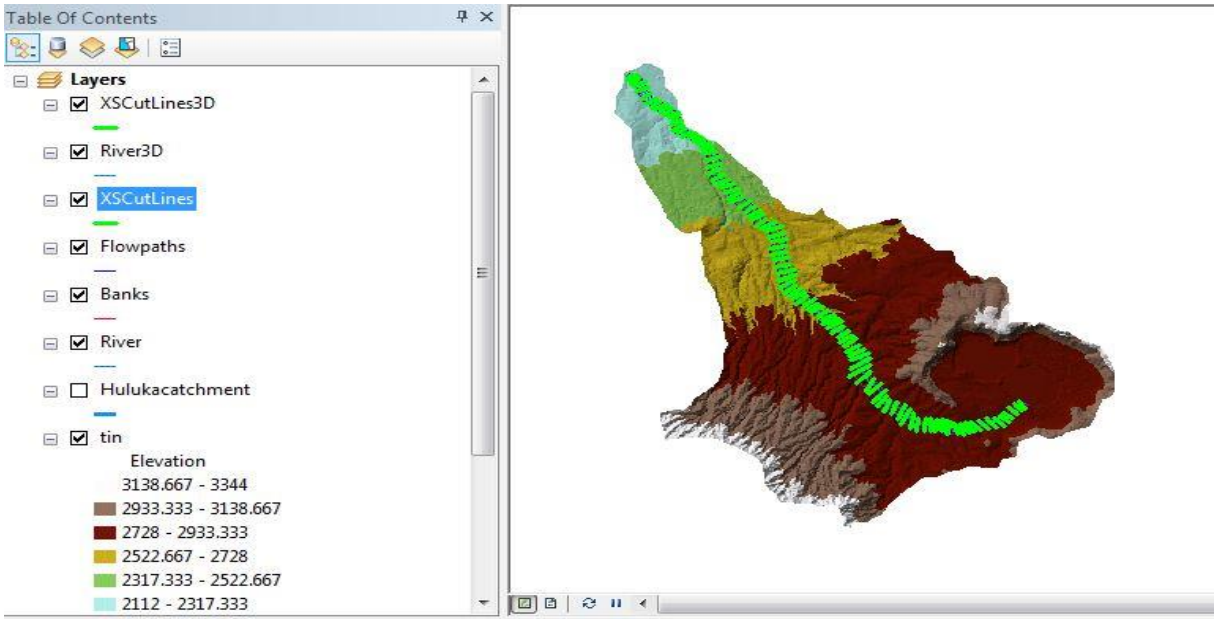

Figure 3.19 River cross section extracted from TIN for Huluka river watershed

After creating of river cross section (figure 3.19), stream center line attributes (like topology, length/stations and elevation) and XS cut line attributes were added in order to compute river station at each cross-section. The channel length, left and right over bank length were shown in (Appendex-H). Executing river geometry cross-section using Arc GIS in conjunction with HEC Geo RAS, the constructed river geometry cross-section was exported to HEC-RAS in Arc GIS format (i.e.as 'GIS2RAS.sdf'). Exporting the river geometry cross-section to HEC-RAS it was displayed as a geometric data with all the river cross-section (figure 3.20).

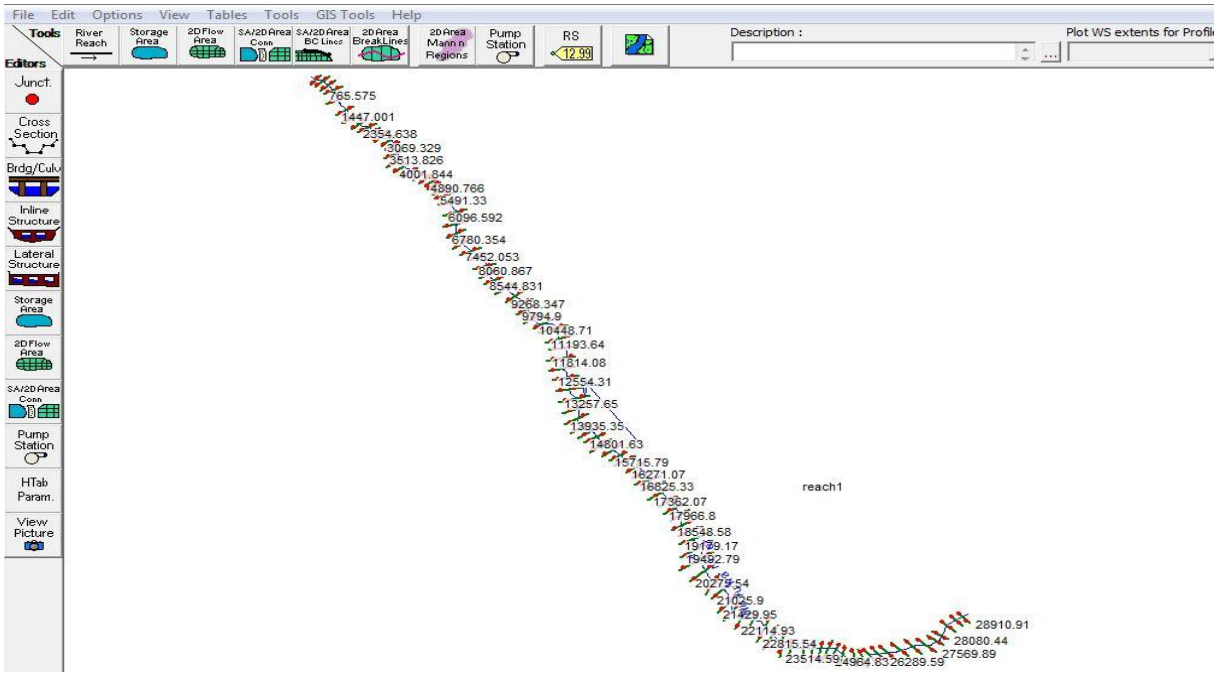

Figure 3.20 River station and river geometric cross-section exported

Having exporting the entire river cross-section from HEC-Geo RAS to HEC-RAS, it is possible to see river stations, channel, left and right over bank length in table form tabulated under (Appendex-C). Also the HEC-RAS can provide different outputs like total discharge of the channel, channel elevation, water surface elevation, critical water surface elevation, energy gradient elevation, energy gradient slope, channel velocity, flow area, top width and channel Froude number for each river station are identified. Then after exporting the river cross-section from Arc GIS through HEC-Geo RAS, geometric data like manning's roughness coefficient, flow data generally known as profile and boundary condition were added.

The manning's roughness coefficient n used for Huluka river watershed was taken from HEC-RAS reference manual considering the flood plain as the urban area and cultivated area as it was recommended in the manual in which n = 0.035 both for left and right over bank and n = 0.04 for channel. Flow data (profiles) was obtained from peak flood frequency analysis simulated in HEC-HMS for 10, 25, 50 and 100 year return period. Upstream critical depth and downstream critical depth was selected as a boundary condition. A steady flow analysis with mixed flow regime was selected and the model was run. Having running the model, the 3D view of the multiple river cross section plots were presented as on (Appendex-D).

After running the HEC-RAS successfully, the GIS data such as water surface and water surface extent, velocity, river center lines and the entire river cross-section for all profiles were exported to GIS as 'RASexport.sdf' format were presented on (Appendex-E).

3.11.3 RAS post-processing

The delineation of floodplains was accomplished by integrating the RAS-GIS output file (RASexport.sdf) and the TIN layer on GIS. The next step was overlaying the terrain TIN with water surface TIN. From this, inundation depths and floodplain boundaries are extracted.

RAS GIS output conversion: HEC- Geo RAS cannot recognize the direct output of RAS GIS file format and must be converted in to HEC-Geo RAS file format. By using *'Import RAS SDF File'* toolbar of HEC-Geo RAS, the RASexport.sdf file format was converted in to XML file format so that the Arc GIS can recognize it.

Layer setup: by using the layer setup window of HEC- Geo RAS, the type of analysis (in this case steady flow analysis), input (RAS GIS file, terrain TIN) and output data directory were identified.

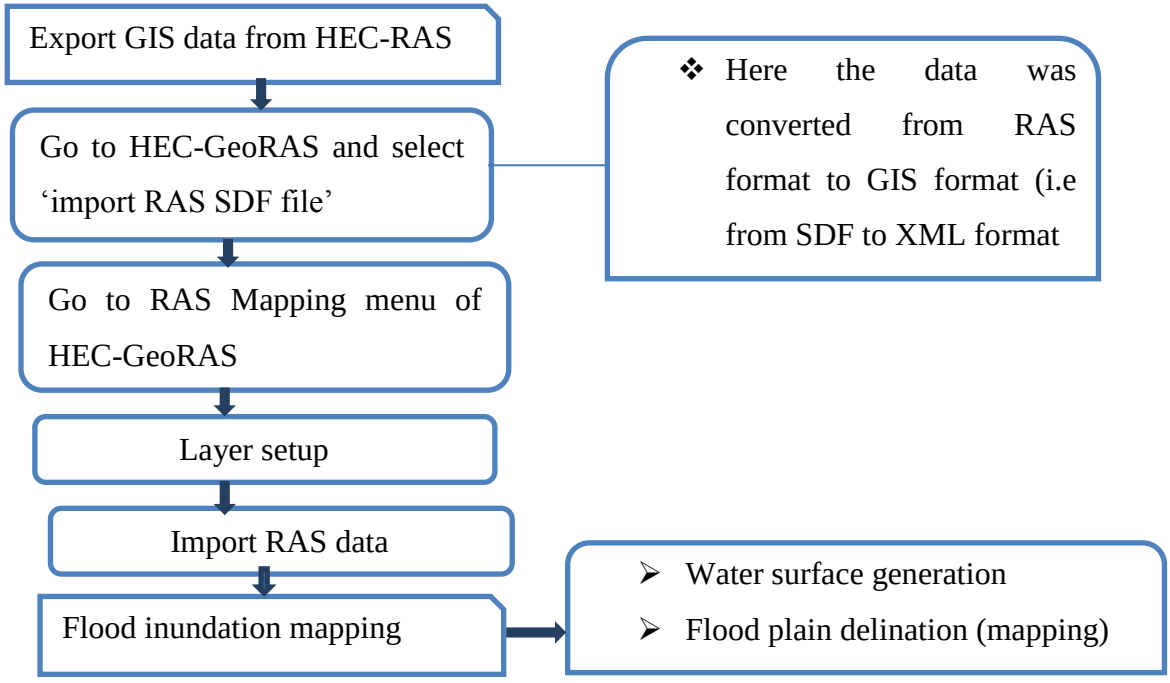

Figure 3.21 Flood inundation mapping work flow diagram

3.11.4 Generation of water surface TIN

The first step was to create a water surface TIN from the cross section water surface elevations using HEC-Geo RAS. All Six water surface profiles like, bank points, velocities, river 2D, XS cutlines, bounding polygon and TIN were selected from the window then for each selected water surface profile, a water surface TIN is created without consideration of the terrain model. The TIN was created using the Arc GIS triangulation method. This allowed for the creation of a surface using cut lines as hard break lines with constant elevation. The water surface TIN was generated using Arc GIS for flow profile used in HEC-RAS, indicated water surface TIN for 100 year return period of peak flood as in the (figure 3.22) and the water surface TIN for 10, 25 and 50 year return period were presented on (Appendex-F).

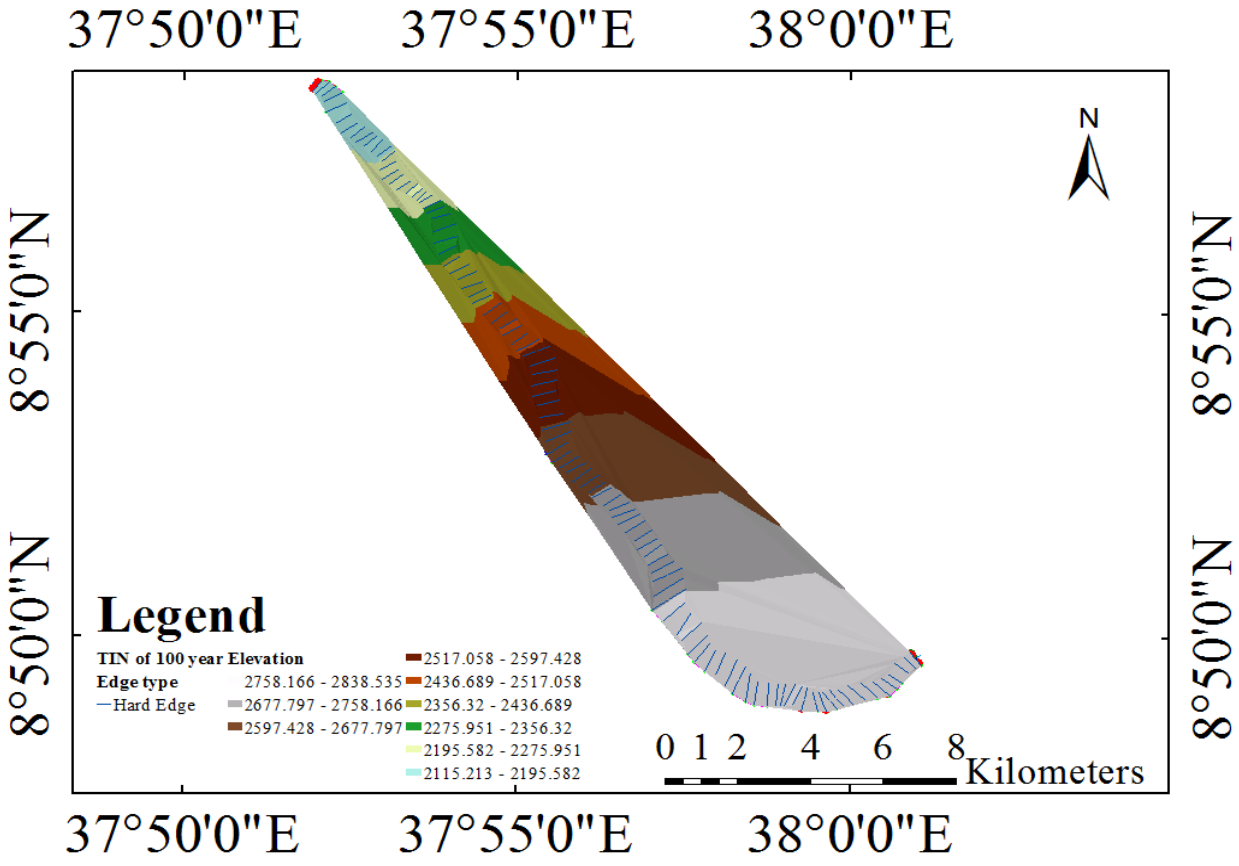

Figure 3.22 Water surface TIN for 100 year return period of peak flood

4. RESULTS AND DISCUSSION

4.1 Model performancy check

4.1.1 Sensitivity Analysis

The Value of each parameter found in HEC-HMS must be specified to use the model for estimating run-off volume and routing hydrographs. Some of the model parameters cannot be estimated by observation or measurement of the watershed characteristics. Among the parameters used in HEC-HMS for rainfall runoff modeling of this study, flood wave travel time (Muskingum-K) and weighted coefficient of discharge (Muskingum-X) were the most sensitive parameters and the calibration was carried out considering these parameters. The objective function measures the goodness of fit between computed and observed flow at the selected elements. (Table 4.1) were indicates the initial and optimized value of the parameters and objective function sensitivity value.

Table 4.1 HEC-HMS optimized parameters for Huluka river watershed

Elements	Parameters	Initial value	Optimized value	Objective function sensitivity
R10	Muskingum-K	0.6	1.303	-0.26
	Muskingum-X	0.2	0.19208	0.02
R120	Muskingum-K	0.6	0.60600	-0.01
	Muskingum-X	0.2	0.19208	0.00
R150	Muskingum-K	0.6	1.3500	0.00
	Muskingum-X	0.2	0.19208	0.00
W780	CN	80.034	52.289	0.00
W820	CN	77.122	77.122	0.00
W840	CN	77.228	46.337	0.02
W980	CN	85.747	86.55	0.00

A total of 15 years historical data from 1997 to 2011 was used. Out of this for calibration (1997- 2006) and validation (2007-2011) of HEC-HMS model.

4.1.2 Model Calibration

HEC-HMS calibration was performed for Huluka river watershed using rainfall and flow discharge at outlet on daily basis. The simulated flow from HEC-HMS was calibrated using the observed flow and optimization of the model parameters values were carried out within the recommended ranges. Nash-Sutcliffe efficiency (NSE) and coefficient of determination (R^2) result has a value of 0.744 and 0.8556 respectively, shows that there was a good agreement between simulated and observed stream flow. These results are in the acceptable range. Among the different objective functions available in HEC-HMS, Mean absolute error and RMS error were used. Mean absolute error and RMS error during calibration on (Figure 4.2) were 1.6 m^3/s and 2.6 m^3/s respectively.

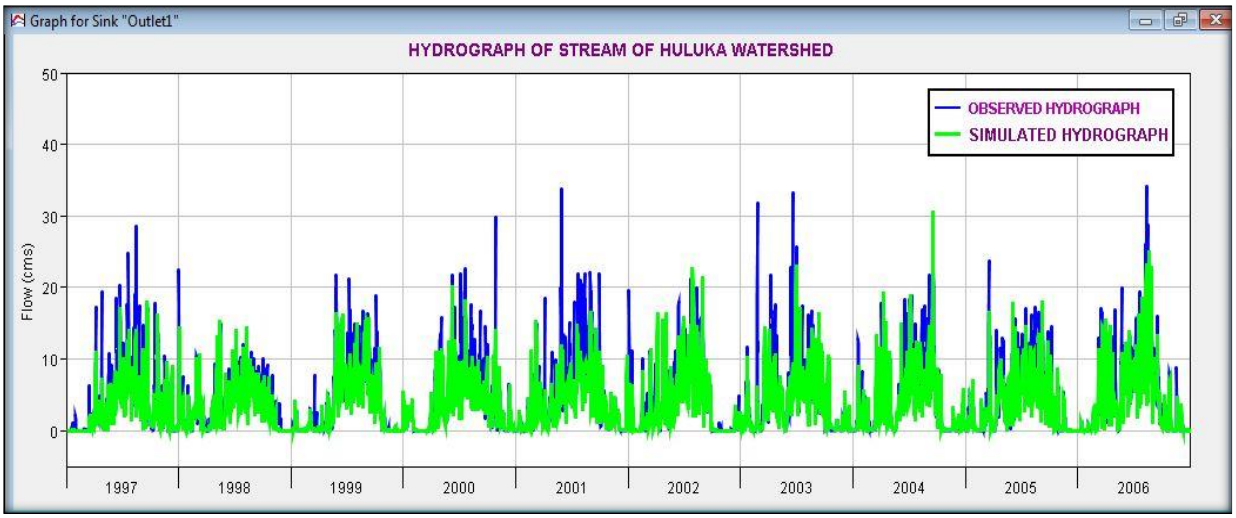

Figure 4.1 Daily hydrograph comparison between Simulated and Observed flow during calibration

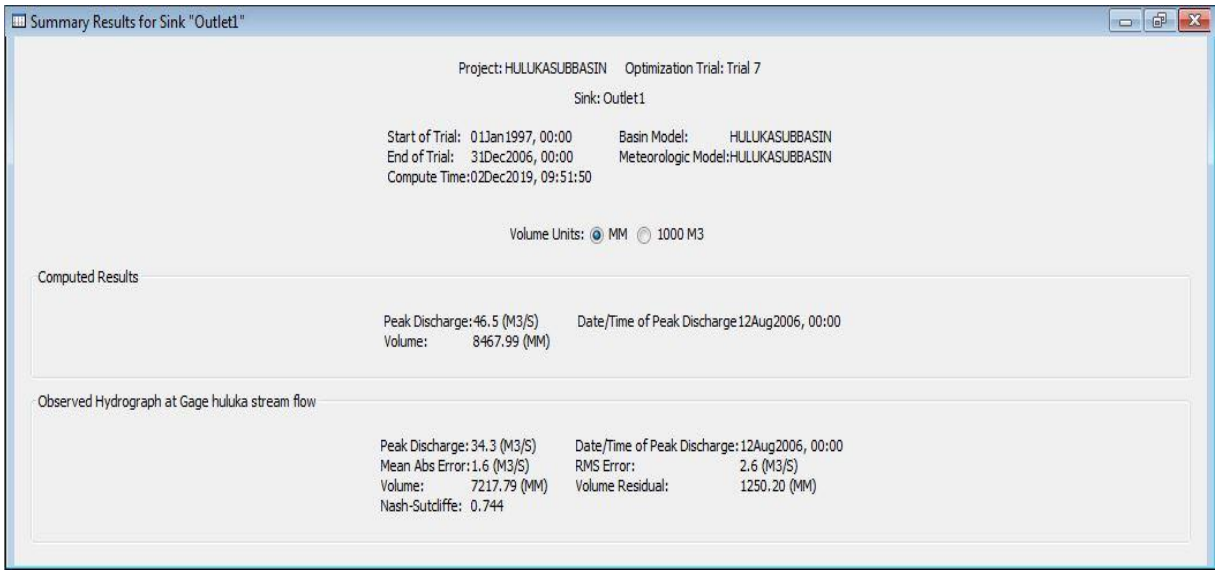

Figure 4.2 HEC-HMS Model calibration

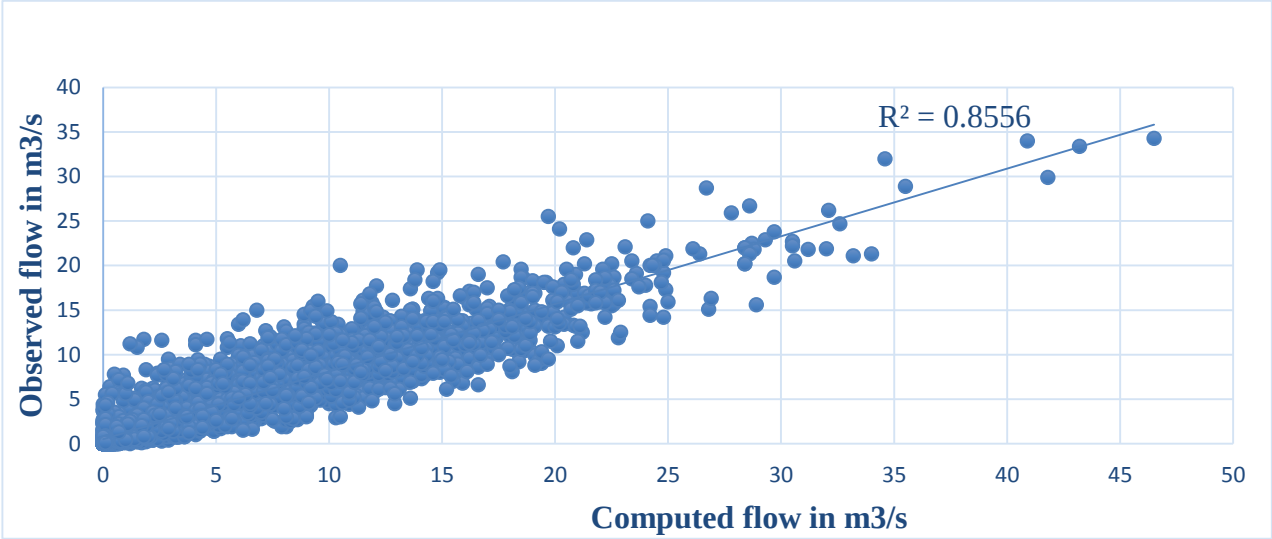

Figure 4.3 Scattering plot (R^2) of computed and observed flow during calibration results

4.1.3 Model Validation

After the calibration was completed and all model parameters were adjusted, a 5 years hydro-meteorological data (i.e. precipitation and observed flow) were entered and model validation was carried out to check whether the model with adjusted parameter was valid or not.

After processing the input data the model was generated good results without any adjustment; especially, the sensitive parameters. The Nash Sutcliff efficiency and coefficient of

determination during the model validation were 0.720 and 0.8122 respectively and graphically, Coefficient of determination during model validation were presented as figure 4.5 and 4.6. Among the different objective functions available in HEC-HMS, Mean absolute error and RMS error were used. Mean absolute error and RMS error during validation on (Figure 4.5) were 1.7 m^3/s and 3.4 m^3/s respectively.

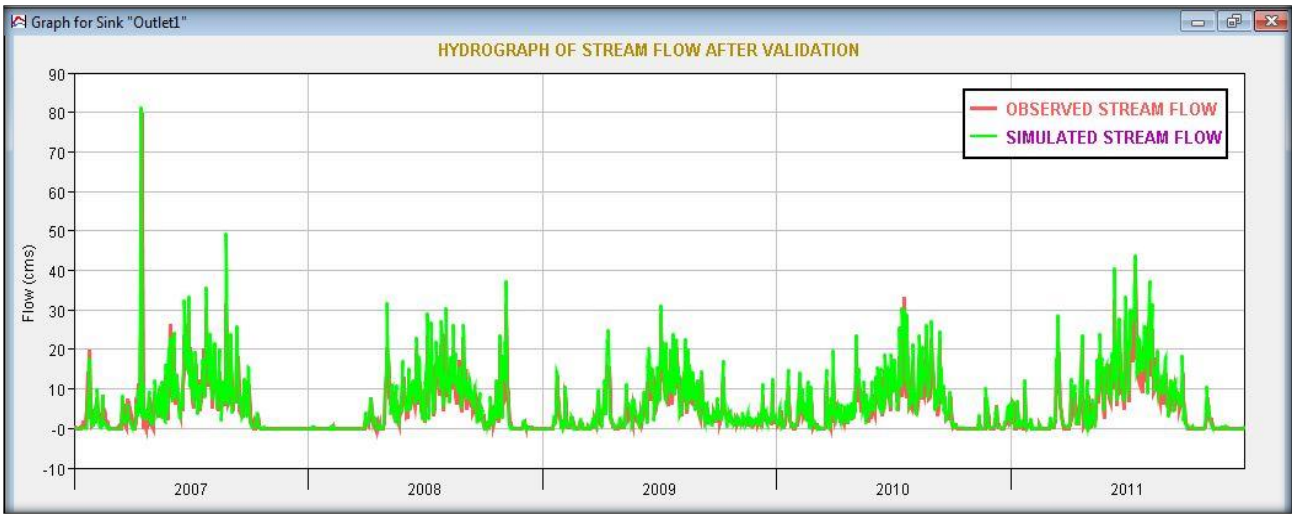

Figure 4.4 Daily hydrograph comparison between Simulated and Observed flowduring validation

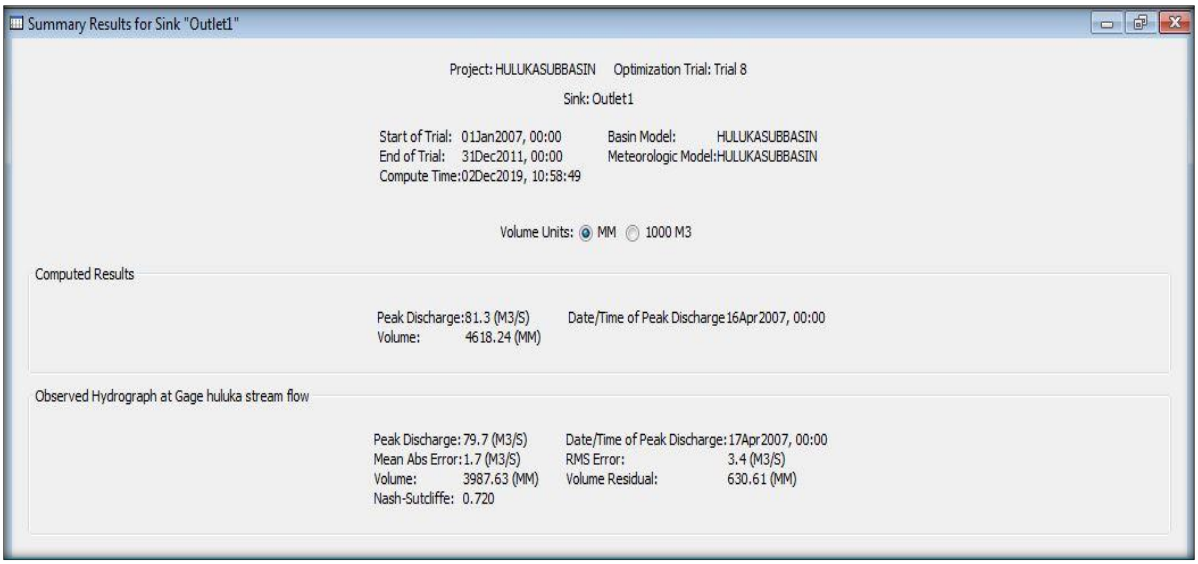

Figure 4.5 HEC-HMS Model efficiency results for validation

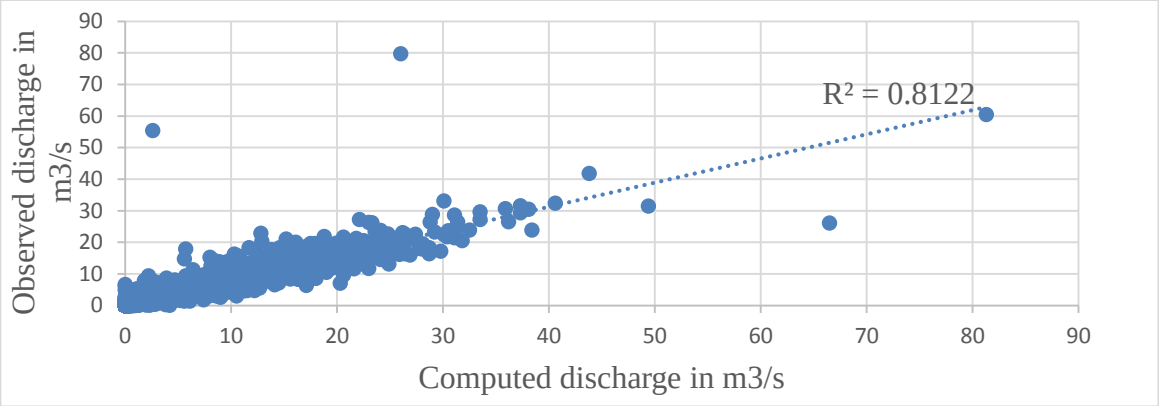

Figure 4.6 Scattering plot (R^2) of computed and observed flow of validation results

4.2 Rainfall-runoff modeling

4.2.1 Basin parameters

According to the soil classification and LULC of Huluka river watershed computed in Arc GIS 10.2 the basin parameters used were extracted and calculated in (table 4.2). The CN grid and the impervious grid incorporating LULC, soil type and hydro fill were analyzed on (figure 3.12 and 3.14 respectively).

Table 4.2 Basin parameters of Huluka river watershed

Sub-basin	Curve Numbers(CN)	Basin lag time(min)	Maximum retention potential (mm)	Intial abstractions (mm)
W780	80.034	378.174	63.365	12.673
W820	77.122	319.62	75.35	15.07
W840	77.228	416.37	74.9	14.98
W980	85.747	128.868	42.22	8.444

4.3 Land Use Change Effect on Hydrological Modeling Result

The land use of the study area is changing from time to time. Ambo town is found at the center of the watershed some portion of the agriculture land was converted in to Urban area due to current migrant of residents. Especially in recent years the change is dynamic. As shown on (Table 4.3) the percentage of Urban area increases from 5.2% in 1997 to 10.15% in 2011 where as, agricultural land decreases from 58.58% to 56.31% within these years.

Table 4.3 Percentage of land use for 1997, 2005 and 2011

S no.	Land use /land cover type	Percentage of land use		
		1997	2005	2011
1	Water body	0.73	0.68	0.56
2	Agricultural area	58.58	57.51	56.31
3	Forest area	35.49	33.31	32.98
4	Residential (Urbanization area)	5.2	8.5	10.15
	Totals	100	100	100

To evaluate the effect of the land use on surface runoff, equal amount of daily rainfall is selected. This helps to avoid the effect of rainfall variation on the generated peak discharge for all selected years. Accordingly, the generated peak discharge difference was found due to the land use change on the watershed.

The CN value is the cumulative effect of different soil types and LULC of the study area. The Curve Number value of the study area is increased from 1997 to 2011 as shown on (table 4.4). This result shows hydrological characteristics of the watershed are the major factors which alter the peak discharge of the study area using equal rain fall distribution. When the Curve Number (CN) increase the amount of peak discharge generated from Huluka River watershed also increases on (table 4.5).

Table 4.4 CN and impervious area for study area results by SCS TR55 table

Year	Composite Curve Number (CN)	Composite of Impervious area(%)	Peak discharges(m^3/s)
1997	70	20	36.5
2005	80	25	47.56
2011	85	30	61.04

The peak discharges found from HEC-HMS model at the main outlet of the study area for 1997, 2005 and 2011 are shown on (table 4.5).

Table 4.5 Huluka River watershed HEC- HMS model simulation result for different years of land use changes on surface runoff

Year	Peak discharges(m^3/s)
1997	36.5
2005	47.56
2011	61.04

4.4 Frequency Storm Method Analysis

The 1hr, 2hr, 3hr, 6hr, 12hr and 24hr duration rainfall depth for the corresponding return period was computed using (equation 3.11 and table 4.6). As it can be seen from the table, every return period under consideration has maximum rainfall depth during the 24hr.

Table 4.6 Rainfall depth (mm) vs Return period (yr) for Huluka watershed

Rainfall intensity duration	Rainfall depth vs Return periods (mm)			
	10	25	50	100
1	51.05	57.53	62.35	67.20
2	59.89	67.49	73.15	78.84
3	64.10	72.23	78.29	84.38
6	70.04	78.92	85.54	92.19
12	74.93	84.44	91.52	98.63
24	79.29	89.35	96.84	104.37

The computed rainfall depth for each rainfall duration with corresponding to return period was used in HEC-HMS to generate peak discharge for each return period. Then the peak discharge simulated from HEC-HMS was compared with the result computed by different flood frequency distribution like General Extreme Value (GEV), Log normal and Log Pearson Type 3. Those were selected based on the rank given for each statistical distribution method by statistical software known as EASYFIT 5.6. After model setup was adjusted using different parameters and model validation was carried out using daily time series data a 1hr, 2hr, 3hr, 6hr, 12hr and 24hr rainfall depth provided on (table 4.7) was inserted into HEC-HMS for the computation of 10, 25, 50 and 100 year return period peak flood

Table 4.7 24 hr Rainfall depth and its peak flood for different return period simulated by HEC-HMS.

S/no	Return period (yr)	24 Rainfall depth (mm)	Peak flow (m^3/s)
1	10	79.29	38.2
2	25	89.35	47.2
3	50	96.84	54.2
4	100	104.37	61.4

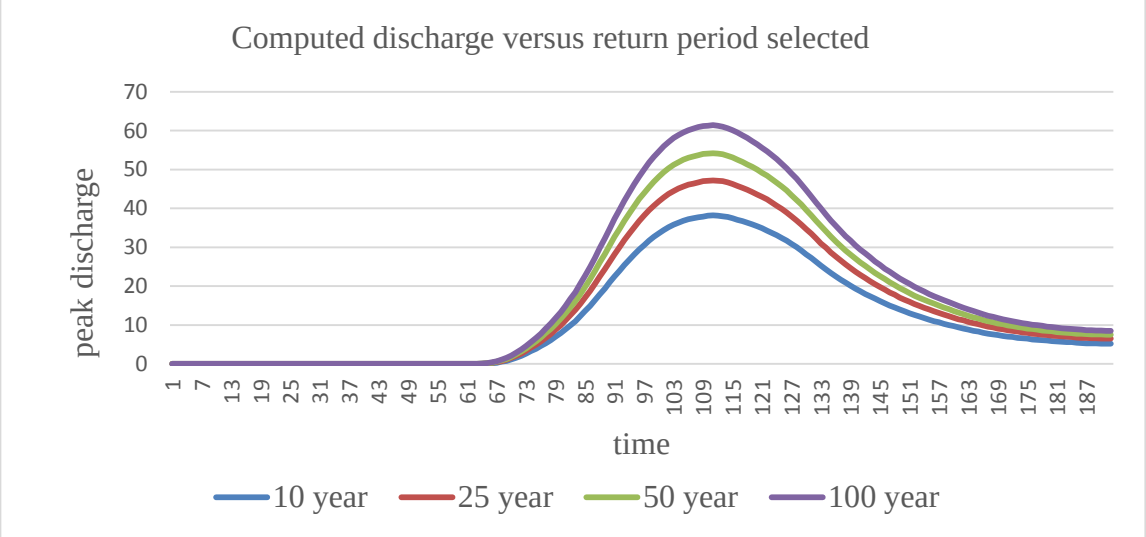

Figure 4.7 Peak discharge versus time for selected return period

The HEC-HMS result found is compared with different techniques of frequency analysis like General Extreme Value, Log normal and Log Pearson Type 3. These frequency analysis techniques are worldwide accepted methods and simple to use. For this purpose annual peak discharge record of Huluka river watershed from 1997-2011 is taken and the result is shown on (table 4.8).

Table 4.8 Flood frequency analysis and HEC-HMS results comparison

Return period(yr)	HEC-HMS(m^3/s)	GEV(m^3/s)	LOGNORMAL(3P)	LOG PEARSON III
10	38.2	37.7	46.37	47.119
25	47.2	47.7	53.732	58.059
50	54.2	56.6	59.084	66.059
100	61.4	65	68	76.541

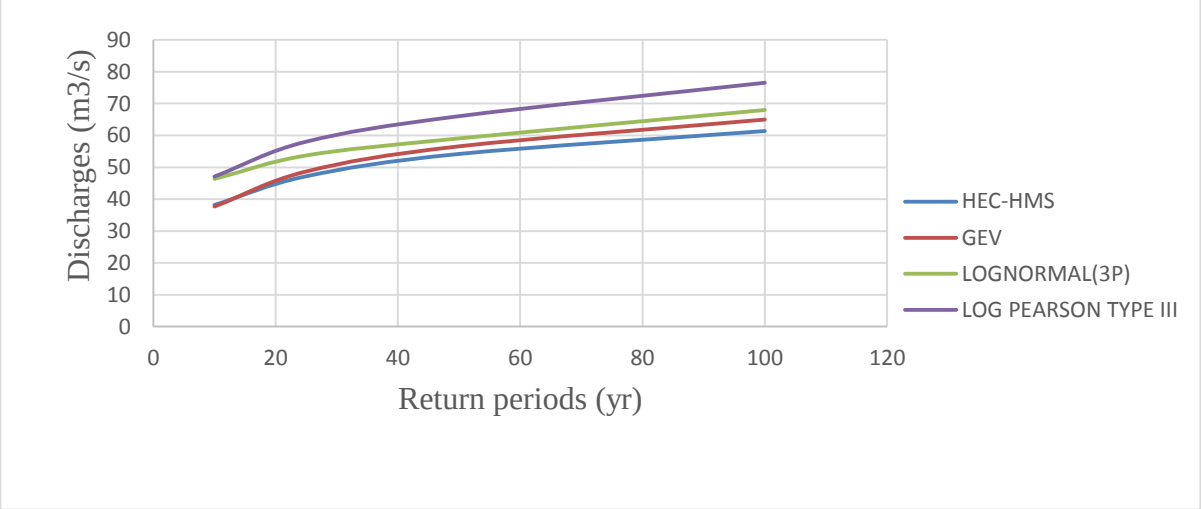

Figure 4.8 Frequency analysis and HEC-HMS results comparison

Both (table 4.8 and figure 4.8) shows the GEV and Log Normal (3p) frequency analysis type values have a closer value than Log Pearson Type III to HEC-HMS. Based on physical observation and different studies the Ambo town is poor sewerage system creates high accumulation of plastics and other materials on the river channel. This has high effect on the result found from the automatic recorder and creates less reliability on the historical river discharge data. Due to this, the result found from HEC-HMS assumed as a good representative.

4.5 Flood inundation mapping assessement

4.5.1 River geometry

River cross-section represents the river geometry like river center line, bank line, flow path line and XS Cut line along the flood plain. For Huluka river watershed 99 XS Cutlines were

digitized in Arc GIS and HEC-Geo RAS with the help of Arc GIS assigns the river stations for every XS Cut lines on (Appendex-I) and also calculated the channel length, left and right over bank length. On Appendex-I, the blue line indicated the river center line along the flood plain; the red points shown bank line points and yellow line represented the river XS Cut lines across the river center line. Having a peak flood for different return periods from HEC-HMS, river geometry and river cross-section data extracted from digital terrain model as in the (Appendex-I), manning's roughness coefficient (n = 0.035 for right and left bank and n = 0.04 for channel bed) taken from HEC-RAS manual in accordance with flood plain property and boundary condition (critical depth flow regime), the hydraulic modeling was developed for steady state 1-Dimensional flow condition. Having entering all the necessary data and running the RAS model for mixed flow regime, the river profile elevation along the flood plain was shown as on the figure 4.9.

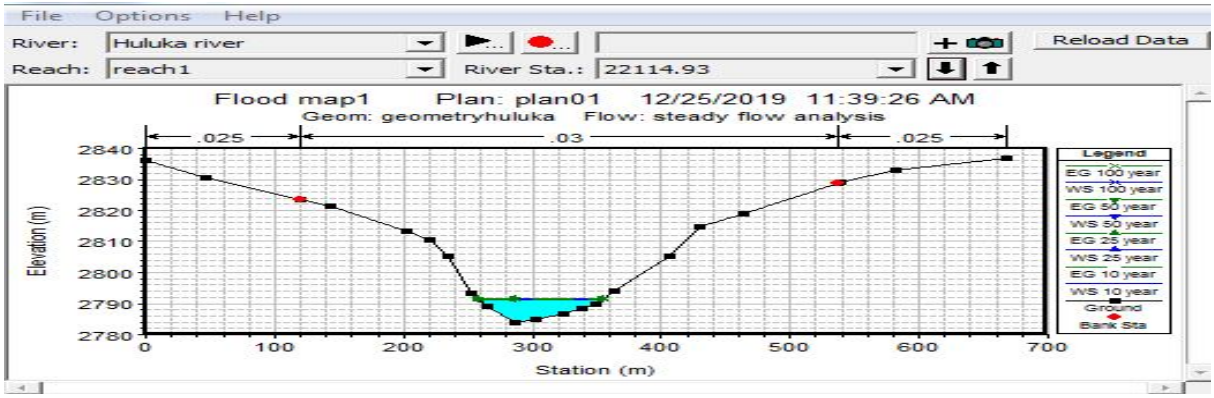

Figure 4.9 River profile and water surface elevation along Huluka river flood plain

The main river channel profile for steady one dimensional flow modeled for mixed flow regime was given as in the figure 4.10.

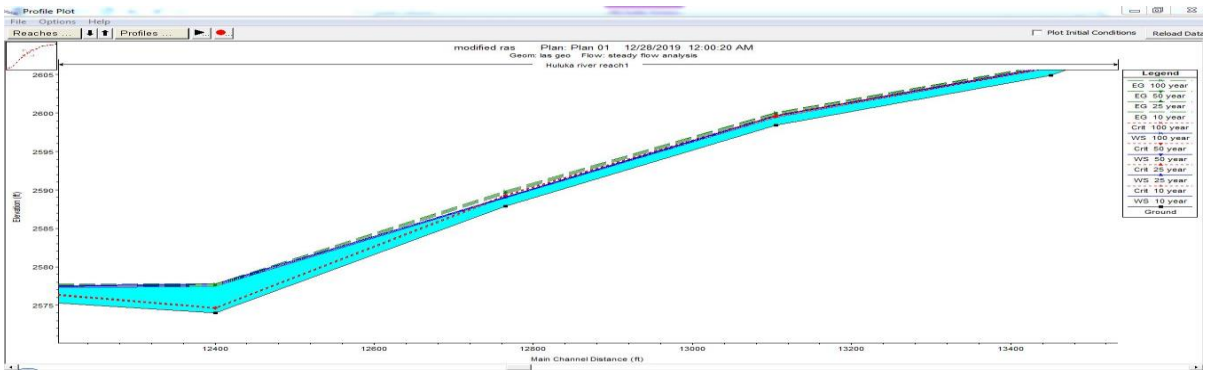

Figure 4.10 View of main channel profile

4.5.2 Flood inundation area

The GIS data exported from HEC-RAS in the RASexport.sdf file format was converted to xml file. so that it was easy to process in Arc GIS for the final flood inundation mapping. After converting the file to Arc GIS compatible using '*Import RAS SDF File'* which is one of the HEC-GeoRAS menus, HEC-Geo RAS layer setup was adjusted and the RAS data was imported and then flood inundation mapping was take place. The result indicated that a 10, 25, 50 and 100 year return period frequency storm inundates 97.58, 100.56, 103.34 and 105.54 ha respectively of the proposed flood plain with the minimum and maximum water depth of 0.002441- 17.7632, 0.00926 - 17.8779, 0.000488 - 17.95 and 0.000241-18.037 in meters respectively.

Maximum flood coverage resulted at 100 years return period frequency storm and it inundates about 105.54 ha with a minimum and maximum water depth of 0.000241 and 18.037 m respectively. The inundation area profile was illustrated in the table 4.9 and Figure 4.11 indicates the flood inundation area of Huluka river flood plain for 10 and 25 years return period and Appendex-K shown the flood inundation mapping of the whole profiles.

Table 4.9 flood inundated area with respect to expected peak flood

S/No	Return period	24 Rainfall depth(mm)	Peak flow(m3/s)	Area (ha)
1	10	79.29	38.2	97.58
2	25	89.35	47.2	100.56
3	50	96.84	54.2	103.34
4	100	104.37	61.4	105.54

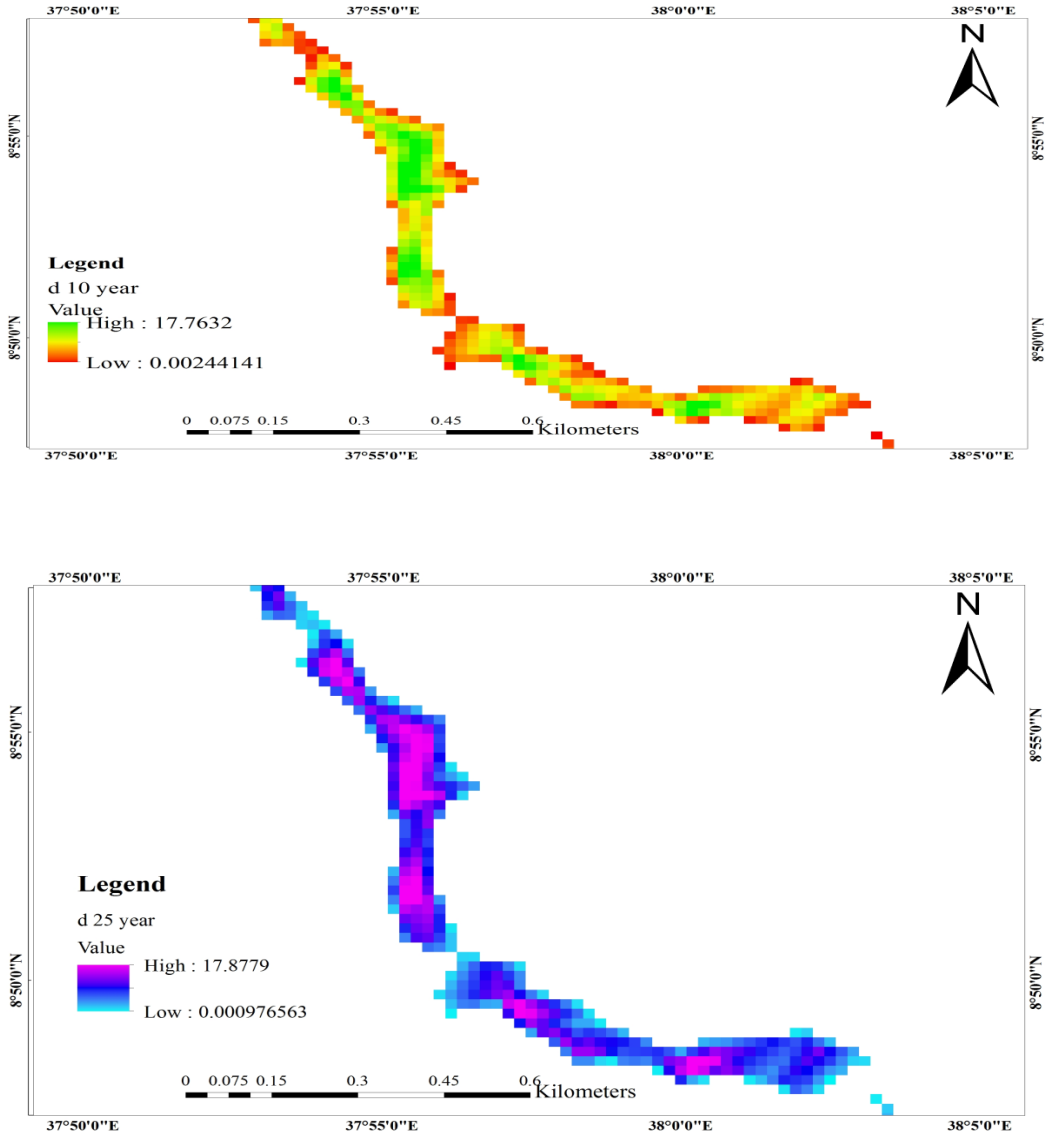

Figure 4.11 Huluka river floodplain for 10 and 25 year return period peak flow

5. CONCULUSION AND RECCOMENDATION

5.1 Conculusion

The main objective of this study was to show the effect of urban growth of the Ambo town on the amount of runoff generated at Huluka River watershed for 1997, 2005 and 2011. These years were selected based on the available cloud free satellite image. After data collected from different resiponsible originations and from well known websites hydrological and hydraulic analysis area completed and good result is founded from the analysis.

To develop hydrological modeling first development of basin model using ArcGIS and GIS extension tools was completed. The main input data's used for pre-hydrological modeling was conducted. After the pre-hydrological modeling have finished, HEC-HMS project was created and opened. The rainfall – runoff analysis was successfully performed in two ways: the first simulation shows the effect of urbanization growth on Huluka river watershed. The peak discharge from the Huluka river watershed for 1997, 2005 and 2011 is 36.5, 47.56 and 61.04m^3/s respectively. This result shows the generated peak run off difference was due to the land use change on the watershed within these years.

The second simulation result used for flood mapping. To complete this hydrological modeling frequency storm method of HEC-HMS used for 1, 2, 3, 6, 12 and 24 hour intensity duration rainfall depths. The rainfall depth for the above intensity durations found from ERA rainfall intensity-durationcurve of the study area for 10, 25, 50 and 100 return periods. After the rainfall data entered and the method of hydrological modeling determined the simulation run executed.

Accordingly, peak discharge of38.2, 47.2, 54.2 and 61.4 m3/s for 10, 25, 50 and 100 return periodis calculated. This result found from HEC-HMS frequency storm method used for hydraulic analysis and flood map generation.

By using the result from HEC-HMS frequency storm method, the hydraulic model development accomplished using HEC-RAS. Flood inundation maps produced using ArcGIS and HEC-GeoRAS extension to visualize flood depth and extent for each return period. The maximum channel flood depths found around the reach 22114.93is 17.7632, 17.8779, 17.95 and 18.0347m for 10, 25, 50 and 100 year design frequency storms respectively with flood extent of 97.58, 100.56, 103.34 and 105.54 ha for 10, 25, 50 and 100 year return periods

5.2 Recommendation

General the population of the Ambo town increases dynamically from year to year. As thepopulation of the town continues like this the demand of housing and conversion of agriculture, forest land and open spaces will increase. Also the result of this study proofs this one. Especially the recent developing town around pan Africa, addiskatama,awaro, stadium and center of the town high rate growth urbanization development of active parts.

- The weather and hydrological data used for this study was collected with some missing values. These missing values were filled using different data gap filling techniques and these techniques were based on some assumption. As the assumption was based on personal judgment, there may be some bias in data values and this on its turn affects the expected outcome. Therefore, it is better if someone uses a data no gap if possible or a data with minimum missing value or actual measurement is taken from the study area.
- Factors like LULC, topography, Soil Moisture Condition (SMC) and soil types can greatly affect Curve Number (CN) value which mainly determine the amount of flood generated. So, further researcher should take great attention to this factors while determining CN.
- For hydraulic model development, HEC-RAS needs river geometry and river cross-section, manning's roughness coefficient for precise computations of water surface elevation, water depth in the river, velocity of flow and flood inundation area. For this study, river geometry was extracted from TIN of the specified flood plain and manning's roughness coefficient wassorted from the previous study on the river basin. But the river geometry was fluctuating from time to time due to different land use management. Therefore, it is more profitable if some conducted proper field survey in order to collect river geometry and carried out someexperiment so as to investigate the actual manning's roughness coefficient. For accurate extraction of river geometry and flood inundation mapping, HEC-RAS requires high precision digital terrain model. So it is more preferable if someone uses high precision digital terrain model during hydraulic model development and flood inundation mapping using HEC-RAS

6. REFERENCES

Aasa, A. S. E. K. P. R. J. Š. J. a. P. T., 2019. Spatial interpolation of mobile positioning data for population statistics. *In 15th International Conference on Location-Based Services*, p. p. 171.

Adla, S. T. S. a. D. M., 2019. Can We Calibrate a Daily Time-Step Hydrological Model Using Monthly Time-Step Discharge Data?. *Water*, pp. 11(9), p.1750.

Ahmadisharaf, E. C. R. Z. H. H. M. a. M. Y., 2019. Calibration and validation of watershed models and advances in uncertainty analysis in TMDL studies. *Journal of Hydrologic Engineering*, pp. 24(7), p.03119001.

Akbari, A. M. G. F. M. a. H., 2014. M.S. Impact of Landuse Change on River Floodplain Using Public Domain Hydraulic Model. *Modern Applied Science*, pp. 8(5), p.80.

Anon., 1998. *Agriculture Organization for the United Nations, and Agriculture Organization. World reference base for soil resources. Vol. 3. ., ,* s.l.: Food & Agriculture Org.

Arsiso, B. K., 2017. Trends in climate and urbanization and their impacts on surface water supply in the city of Addis Ababa, Ethiopia. *Doctoral dissertation.*

Barbero-Sierra, C. M. M. a. R.-P. M., 2013. The case of urban sprawl in Spain as an active and irreversible driving force for desertification. *Journal of Arid Environments*, *90*, pp. pp.95-102.

Beck, N. C. G. K. L. a. M. M., 2017. An urban runoff model designed to inform stormwater management decisions. *Journal of environmental management*, pp. pp.257-269.

Benchimol, E. S. L. G. A. H. K. M. D. P. I. S. H. v. E. E. L. S. a. R. W. C., 2015. The REporting of studies Conducted using Observational Routinely-collected health Data. *RECORD Working Committee.*

Berhanu, B., M. & Yilma, S., 2012. GIS-based Hydrological. *Department of Earth and Environment.*

Berner, E. K. & Robert, B. A., 2012. Global environment: water, air, and geochemical cycles.. *Princeton University Press.*

Beven, K. a. G. P., 2013. Macropores and water flow in soils revisited. *Water Resources Research*, pp. 49(6), pp.3071-3092.

BEYENE, M. N., 2016. Urbanization and Its Effect on Surface Runoff. p. 6 .

Bilotta , G., Brazier , R. & Haygarth , P., 2007 . The impacts of grazing animals on the quality of soils, vegetation, and surface waters in intensively managed grasslands.. *Advances in agronomy. ,* 1(94), pp. 237-80.

Boorman, . D. B., John , M. . H. & Lilly, A., 1995. Hydrology of soil types: a hydrologically-based classification of the soils of United Kingdom.. *Institute of Hydrology, .*

Burrough, P. M. R. M. R. a. L. C., 2015. Principles of geographical information systems. *Oxford university press.*

Buytaert, W. a. D. B. B., 2012. Water for cities: The impact of climate change and demographic growth in the tropical Andes. *Water Resources Research*, p. 48(8).

Cakir, R. R. M. S. S. P.-A. J. G. Y. R. L. M. M. N. E. S.-C. M. L.-C. J. a. G. P. J., 2020. Hydrological Alteration Index as an Indicator of the Calibration Complexity of Water Quantity and Quality Modeling in the Context of Global Change. *Water*, pp. 12(1), p.115.

Cosby , B., Hornberger , G., Clapp , R. & Ginn, . T., 1984 . A statistical exploration of the relationships of soil moisture characteristics to the physical properties of soils.. *Water resources research. ,* Volume 20(6), pp. 682-90.

Dan-Jumbo, N. a. M. M., 2019. Relative Effect of Location Alternatives on Urban Hydrology. The Case of Greater Port-Harcourt Watershed, Niger Delta. *Hydrology,* pp. ,6(3), p.82.

Datoo, A., 2019. *Legal Data for Banking: Business Optimisation and Regulatory Compliance.* s.l.:s.n.

Davis, A. a. M. R., 2005. Stormwater Hydrology. *Stormwater Management for Smart Growth,* pp. pp.63-104.

Di Baldassarre, G. a. C. P., 2011. A hydraulic study on the applicability of flood rating curves. *Hydrology Research,* pp. 42(1), pp.10-19.

Fetter, C., 2018. Applied hydrogeology. *Waveland Press.*

Gant, . R. L., Guy , M. R. & Shahab , F., 2011. "Land-use change in the ‘edgelands’: Policies and pressures in London's rural–urban fringe.". *Land use policy 28.1* .

Gary W., B. C.-H., 2016. Hydraulic analysis system user's manual. *manual.*

Gashaw, W. & Dagnachew , L., 2011. Flood hazard and risk assessment using GIS and remote sensing in Fogera Woreda, Northwest Ethiopia.". *Nile River Basin. Springer, Dordrecht ,* pp. 179-206.

Good, S. N. D. a. B. G., 2015. Hydrologic connectivity constrains partitioning of global terrestrial water fluxes. *Science, 349(6244),* pp. pp.175-177.

Guarino, . L., Jarvis , A., Hijmans , R. & Maxted, . N., 2002. 36 Geographic Information Systems (GIS) and the Conservation and Use of Plant Genetic Resources. Managing plant genetic diversity..

Gulliver, J. S., 2015. Determination of Effective Impervious Area in Urban Watersheds,Department of Civil. *Environmental and Geo- Engineering University of Minnesota.*

Gumindoga, W. R. D. N. I. a. D. T., 2017. Ungauged runoff simulation in Upper Manyame Catchment, Zimbabwe: Application of the HEC-HMS model. *Physics and Chemistry of the Earth, Parts A/B/C,* pp. 100, pp.371-382.

Guohua, F., 2018. Flood control to urban agglomerations. *Internationa journals on flood control,* p. 123.

GURMU, A., 2018. FLOOD MODELING AND MAPPING OF LOWER OMO GIBE RIVER BASIN. *Doctoral dissertation, ADDIS ABABA SCIENCE AND TECHNOLOGY UNIVERSITY.*

Han, J., 2010. Stream flow Analysis Using ArcGIS and HEC-GeoHMS. Texas A&M University. *Zachry Department of Civil Engineering..*

Hasani, H., 2013. Determination of Flood Plain Zoning in Zarigol River Using the Hydraulic Model of HECRAS. *International Research Journal of Applied and Basic Sciences, 5(3),* pp. pp.399-403.

Hoornweg, ,. L. T. G. C., 2011. Cities and greenhouse gas emissions: moving forward. *Environment and Urbanization,* pp. 23(1), pp.207-227.

Hungr, O., Morgan, G. C., Van Dine, D. F. & Lister, 1987. Debris flow defenses in British Columbia. Debris Flows/Avalanches: Process, Recognition, and Mitigation.. *Geological Society of America Reviews in Engineering Geology, 7.,* pp. 201-222..

Igulu, B. a. M. E., 2020. The impact of an urbanizing tropical watershed to the surface runoff. *Global J. Environ. Sci. Manage,* pp. 6, p.2.

Jaber, A. E.-N. a. M., 2018. Floodplain Analysis using ArcGIS, HEC-GeoRAS and HEC-RAS in Attarat Um Al-Ghudran Oil Shale Concession Area, Jordan. *Journal of Civil & Environmental.*

James H., D., 2013. Geospatial hydrologic model extension. *manual.*

Jameson, A., 2019 . On the Importance of Statistical Homogeneity to the Scaling of Rain. *Journal of Atmospheric and Oceanic Technology,* pp. 36(6), pp.1063-1078.

Jantz, C. A., Scott, . G. J. & Mary , K. S., 2004. "Using the SLEUTH urban growth model to simulate the impacts of future policy scenarios on urban land use in the Baltimore-Washington metropolitan area.". *Environment and Planning B: Planning and Design 31* , Volume 2, pp. 251-271..

Jha, A. L. J. B. R. B. N. L. A. P. N. B. A. P. D. D. J. a. B. R., 2011. Five feet high and rising: cities and flooding in the 21st century. *The World Bank.*

Julien, P., 2018. River mechanics. *Cambridge University Press.*

Kabangure, H., 2016. Gerald Munyoro. *Doctoral dissertation, Chinhoyi University of Technology.*

Kaffas, K. a. H. V., 2014. Application of a continuous rainfall-runoff model to the basin of Kosynthos river using the hydrologic software HEC-HMS. Glob. *NEST,* pp. 16(188203), p.16.

Kim, N. W. Y. L. J. L. J. a. J. J., 2011. Hydrological impacts of urban imperviousness in White Rock Creek watershed. *Transactions of the ASABE,* pp. 54(5),pp.1759-1771.

Kirkby, . R. J., 2018. Urbanization in China: town and country in a developing economy 1949-2000 AD. *Routledge.*

Kotir, . J. H., 2011. Climate change and variability in Sub-Saharan Africa: a review of current and future trends and impacts on agriculture and food security.. *Environment, Development and Sustainability,* pp. 13(3), pp.587-605.

Labbas, M. B. F. B. I. K. S. J. C. K. S. M. K. J. T. D. C. a. V. E. 2., 2013. Multi-scale approach to assess the impacts of land use evolution and rainwater management practices on the hydrology of periurban catchments.. *Application to the Yzeron catchment (150 km 2).*

Lastoria, B., 2008. Hydrological processes on the land surface: A survey of modelling approaches.Università di Trento. Dipartimento di ingegneria civile e ambientale,.

Ligtenberg, J., 2017. Runoff changes due to urbanization. p. 3 .

Li, Y., 2009. "Impacts of urbanization on surface runoff of the Dardenne Creek watershed, St. Charles County, Missouri.". *Physical Geography 30.6,* pp. 556-573.

Lloyd, E., 2019. Spatial Decision Support Systems Use in Peacekeeping and Stability Operations Analysis: Spatial Analysis for US Army Civil Affairs Civil Information Management (Doctoral dissertation).

Maguire, D., 2008. ArcGIS: general purpose GIS software system. *Encyclopedia of GIS,* pp. pp.25-31.

Mark, O. et al., 2004. "Potential and limitations of 1D modelling of urban flooding.". *Journal of hydrology 299,* Volume 3-4 , pp. 284-299..

Mathew J., F. J., 2012. Hydrologic Engineering Center's Geospatial River Analysis System. *Manual.*

McColl, K. et al., 2017. The global distribution and dynamics of surface soil moisture. *Nature Geoscience,* p. 100.

McDonald, W., 2010. Applications of GIS Using ArcGIS, HEC - GeoHMS and HEC-HMS. *Model Ticky Creek Watershed, Texas A&M University, Zachry Department of Civil.*

Michotte, A., 2017. The perception of causality. *Routledge.*

Mihiretie, Y., 2017. Assessment of Environmental Impact of Quarrying Activities in Eastern Addis Ababa. *Implications on Urbanization (Doctoral dissertation, Addis Ababa University).*

Monteith, J. a. U. M., 2013. Principles of environmental physics: plants, animals, and the atmosphere. *Academic Press.*

Myers, J., 2019. Modeling continuous variables. *Multiple regression.*

Nega, M., 2016. Urbanization and Its Effect on Surface Runoff (A Case Study on Great Akaki River, Addis Ababa, Ethiopia). *Doctoral dissertation, Addis Ababa University.*

Nharo, T. M. H. a. G. W., 2019. Mapping floods in the middle Zambezi Basin using earth observation and hydrological modeling techniques. *Physics and Chemistry of the Earth, Parts A/B/C,* pp. 114,p.102787.

Olson, G., 2012. Soils and the environment: A guide to soil surveys and their applications.. *Springer Science & Business Media.*

Panigrahya., P. K. G. a. S., 2008. Agriculture, Forest and Environment Group, Space Applications Centre, ISRO, Geo-spatial Modeling of Runoff of Large Land Mass, Analysis,.

Patel, C. a. G. P., 2016. Floodplain Delineation Using HECRAS Model—A Case Study of Surat City. *Open Journal of Modern Hydrology,* pp. 6(01), p.34.

Pathan, H. a. J. G., 2019 . Estimation of Runoff Using SCS-CN Method and Arcgis for Karjan Reservoir Basin. *International Journal of Applied Engineering Research,* pp. 14(12), pp.2945-2951.

Pawan, 2016. Urbanization and Its Causes and Effects.. *IJRSI International Journal of Research and Scientific Innovation Volume III,* p. 110.

Peters, N. E., 1994. Biogeochemistry of Small Catchments. *A tool for Environmental.*

Piepho, H., 2019. A coefficient of determination (R2) for generalized linear mixed models. *Biometrical Journal,* pp. 61(4), pp.860-872.

Prakash, C. S. B., 2017. Land-Use Land-Cover Change and Its Impact on Surface Runoff. *International Journal of Advanced Remote Sensing and GIS ,* p. 2104 .

Raes, D. W. P. a. G. F., 2006. RAINBOW - a software package for analyzing data and testing the homogeneity of historical data sets. *Proceedings of the 4th International Workshop on 'Sustainable management of marginal drylands'.*

Ramakrishnan, D., Bandyopadhyay, A. & Kusuma, , . K., 2009. SCS-CN and GIS-based approach for identifying potential water harvesting sites in the Kali Watershed, Mahi River Basin, India.. *Journal of Earth System Science, 118(4), ,* pp. 355-368.

Ramirez, J. A., 2000. Prediction and Modeling of Flood Hydrology and Hydraulics, Inland FloodHazards: Human, Riparian and Aquatic Communities: Cambridge University Press..

Schaeffer, R. et al., 2012. "Energy sector vulnerability to climate change: a review.". *Energy 38*, Volume 1, pp. 1-12.

Shabir, O., 2013. *A summary case report on the health impacts and response to the Pakistan floods of 2010*, s.l.: PLoS currents 5.

ShahiriParsa, A. N. M. H. M. a. R. M., 2016. Floodplain zoning simulation by using HEC-RAS and CCHE2D models in the Sungai Maka river. *Air, Soil and Water Research, 9*, pp. pp.ASWR-S36089.

Sharffenberg, W., 2016. Hydrologic Engineering Center Hydrologic Modeling System. *User's Manual.*

Taube, N., 2019 . Understanding and linking anthropogenic and natural riverine disturbances to in-stream nutrient dynamics in an urbanized river reach.

Tausch , A., 2019. Migration from the Muslim World to the West. *Jewish Political Studies Review*, pp. 30(1/2), pp.65-225.

Tegine, E., 2018. FLOODPLAIN MAPPING AND MODELING FOR GERAY RIVER. *Doctoral dissertation, ADDIS ABABA SCIENCE AND TECHNOLOGY UNIVERSITY.*

Tshewang, J., 2017. Rainfall-runoff simulation model based on water balance concept for basinwide water resource assessment. *water resource assessment.*

UNDESA, 2015 Revision. Population Division World Urbanization Prospects.

UNEP, U., U. -H. & E., 2003. *Scientific Report on the GroundwaterVulnerability Mapping of, the Addis Ababa Water Supply Aquifers, 2003, Addis Ababa, Ethiopia.*, s.l.: s.n.

Wang, X. Z. J. S. S. G. E. W. Y. G. J. a. H. R., 2016. Adaptation to climate change impacts on water demand. *Mitigation and Adaptation Strategies for Global Change*, pp. 21(1), pp.81-99.

Weng, Q., 2001. Modeling Urban Growth Effects on Surface Runoff. *Department of Geography, Geology, and Anthropology, Indiana State ,USA.*

Zellou, B. a. R. H., 2017. Assessment of reduced-complexity landscape evolution model suitability to adequately simulate flood events in complex flow conditions. *Natural hazards*, pp. 86(1), pp.1-29.

Zenner, ,. H. D., 2000. A new method for modeling the heterogeneity of forest structure.. *Forest ecology and management*, pp. 129(1-3), pp.75-87.

Zhang, X. Q., 2016. The trends, promises and challenges of urbanisation in the world. *Habitat International*, pp. 54, pp.241-252.

Zhou, F., Youpeng Xu, Y. C.-Y. X., Gao, Y. & Du, J., 2013. Hydrological response to urbanization at different spatio-temporal scales simulated by coupling of CLUE-S and the SWAT model in the Yangtze River Delta region.". *Journal of Hydrology 485*, pp. 113-125.

APPENDEX

APPENDEX A: STUDY AREA DELINATION BY HEC-GeoHMS

Appendex A: Figures of study area delination by using HEC GeoHMS

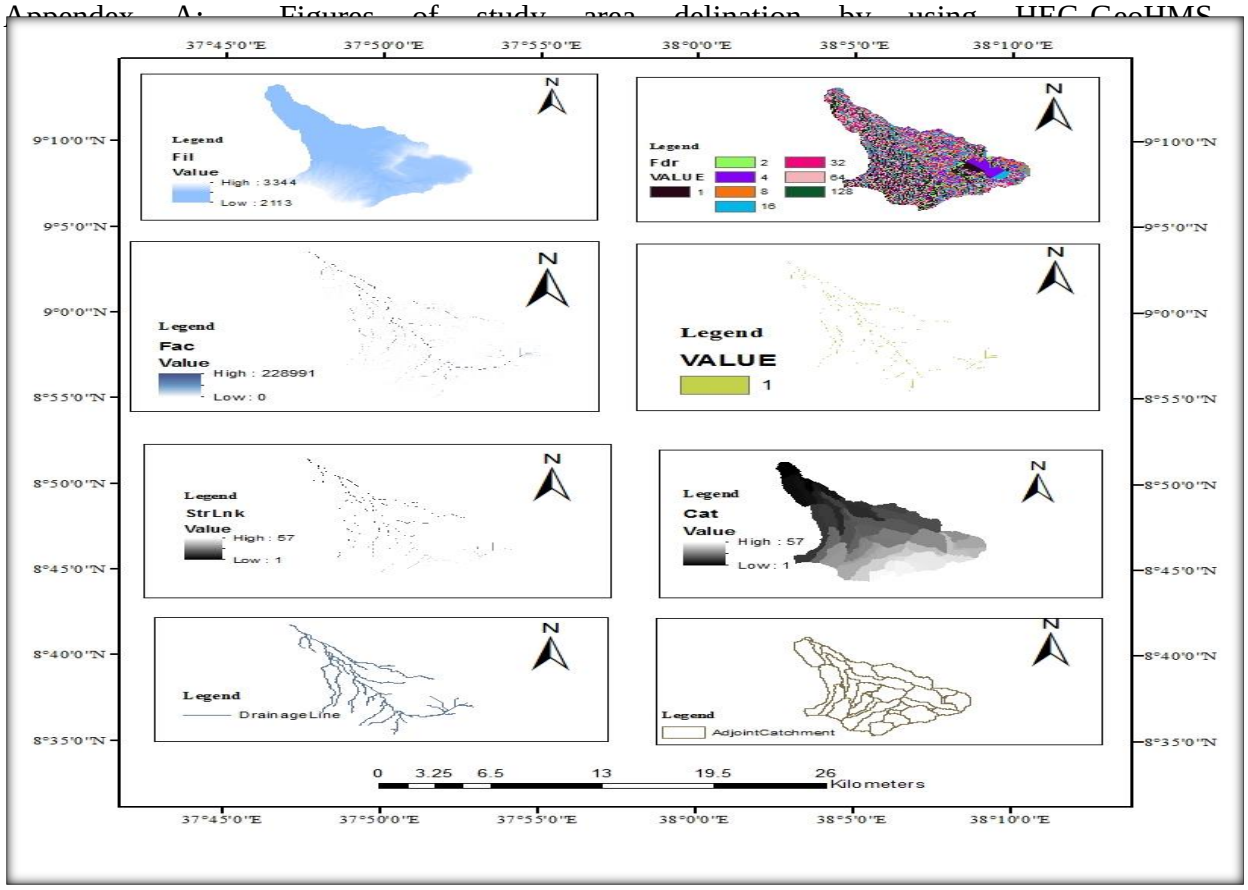

APPENDEX B: DEM from raster to TIN for geometric data prepared

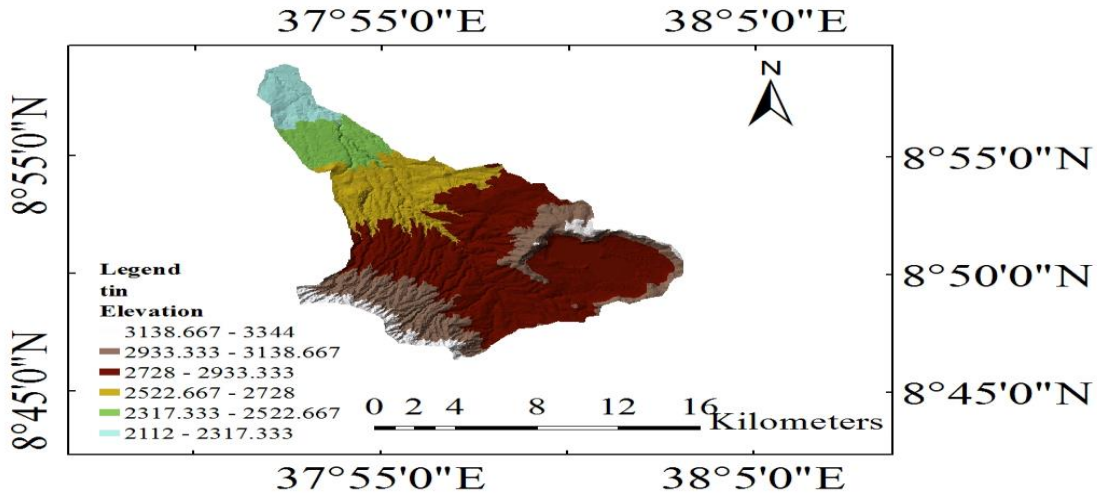

APPENDEX: C HEC-RAS Hydraulic computations

Profile Output Table - Standard Table 1

File Options Std. Tables Locations Help

HEC-RAS Plan: plan01 River: Huluka river Reach: reach1

Reach	River Sta	Profile	Q Total	Min Ch El	W.S. Elev	Crit W.S.	E.G. Elev	E.G. Slope	Vel Chnl	Flow Area	Top Width	roude # Ch
			(m3/s)	(m)	(m)	(m)	(m)	(m/m)	(m/s)	(m2)	(m)	
reach1	28910.91	10 year	38.20	2833.00	2838.33	2833.18	2838.33	0.000000	0.04	939.43	190.52	0.01
reach1	28910.91	25 year	47.20	2833.00	2838.41	2833.21	2838.41	0.000000	0.04	956.12	190.98	0.01
reach1	28910.91	50 year	54.20	2833.00	2838.47	2833.23	2838.47	0.000000	0.05	967.84	191.30	0.01
reach1	28910.91	100 year	61.40	2833.00	2838.54	2833.25	2838.54	0.000000	0.06	979.53	191.62	0.01
reach1	28709.64	10 year	38.20	2837.18	2838.11	2838.11	2838.31	0.012412	1.96	19.45	50.39	1.01
reach1	28709.64	25 year	47.20	2837.18	2838.18	2838.18	2838.39	0.012150	2.05	22.99	54.85	1.01
reach1	28709.64	50 year	54.20	2837.18	2838.22	2838.22	2838.45	0.011758	2.12	25.58	56.79	1.01
reach1	28709.64	100 year	61.40	2837.18	2838.26	2838.26	2838.51	0.011723	2.22	27.70	57.36	1.02
reach1	28429.28	10 year	38.20	2829.76	2830.72	2831.07	2831.86	0.053660	4.72	8.09	16.81	2.17
reach1	28429.28	25 year	47.20	2829.76	2830.81	2831.19	2832.06	0.052932	4.95	9.53	18.24	2.19
reach1	28429.28	50 year	54.20	2829.76	2830.86	2831.27	2832.21	0.053688	5.15	10.52	19.16	2.22
reach1	28429.28	100 year	61.40	2829.76	2830.91	2831.35	2832.34	0.053066	5.29	11.60	20.13	2.23
reach1	28080.44	10 year	38.20	2824.06	2824.64	2824.64	2824.87	0.011615	2.15	17.78	38.41	1.01
reach1	28080.44	25 year	47.20	2824.06	2824.71	2824.72	2824.98	0.011197	2.27	20.79	40.21	1.01
reach1	28080.44	50 year	54.20	2824.06	2824.77	2824.77	2825.05	0.010833	2.34	23.11	41.54	1.00
reach1	28080.44	100 year	61.40	2824.06	2824.83	2824.83	2825.12	0.010556	2.42	25.41	42.82	1.00
reach1	27863.15	10 year	38.20	2821.00	2822.14	2821.49	2822.15	0.000364	0.52	73.26	98.71	0.19
reach1	27863.15	25 year	47.20	2821.00	2822.26	2821.55	2822.27	0.000361	0.55	85.51	105.07	0.20
reach1	27863.15	50 year	54.20	2821.00	2822.34	2821.59	2822.36	0.000359	0.57	94.65	109.57	0.20
reach1	27863.15	100 year	61.40	2821.00	2822.42	2821.63	2822.44	0.000359	0.59	103.56	113.85	0.20
reach1	27569.89	10 year	38.20	2820.50	2821.53	2821.53	2821.82	0.011014	2.36	16.19	29.16	1.01
reach1	27569.89	25 year	47.20	2820.50	2821.63	2821.63	2821.94	0.010646	2.46	19.17	31.54	1.01
reach1	27569.89	50 year	54.20	2820.50	2821.70	2821.70	2822.03	0.010400	2.53	21.41	33.23	1.01
reach1	27569.89	100 year	61.40	2820.50	2821.76	2821.76	2822.11	0.010237	2.60	23.62	34.80	1.01
reach1	27209.93	10 year	38.20	2818.47	2819.37	2819.13	2819.42	0.002465	0.99	38.60	83.44	0.46
reach1	27209.93	25 year	47.20	2818.47	2819.44	2819.19	2819.50	0.002507	1.06	44.61	88.30	0.48
reach1	27209.93	50 year	54.20	2818.47	2819.49	2819.23	2819.56	0.002502	1.10	49.27	91.91	0.48
reach1	27209.93	100 year	61.40	2818.47	2819.54	2819.27	2819.61	0.002526	1.14	53.70	95.20	0.49
reach1	26891.98	10 year	38.20	2817.00	2817.73	2817.73	2817.90	0.012808	1.82	20.94	62.19	1.00
reach1	26891.98	25 year	47.20	2817.00	2817.79	2817.79	2817.97	0.012396	1.90	24.84	67.76	1.00
reach1	26891.98	50 year	54.20	2817.00	2817.83	2817.83	2818.02	0.012478	1.97	27.49	71.29	1.01
reach1	26891.98	100 year	61.40	2817.00	2817.87	2817.87	2818.07	0.012264	2.02	30.39	74.96	1.01
reach1	26539.13	10 year	38.20	2812.00	2813.72	2813.13	2813.80	0.001531	1.25	30.65	32.57	0.41
reach1	26539.13	25 year	47.20	2812.00	2813.90	2813.25	2813.99	0.001521	1.27	37.10	38.08	0.41
reach1	26539.13	50 year	54.20	2812.00	2814.03	2813.33	2814.11	0.001493	1.29	42.09	41.84	0.41
reach1	26539.13	100 year	61.40	2812.00	2814.14	2813.41	2814.23	0.001457	1.30	47.19	45.37	0.41
reach1	26289.59	10 year	38.20	2811.11	2813.35		2813.44	0.001334	1.34	28.57	24.37	0.39
reach1	26289.59	25 year	47.20	2811.11	2813.50		2813.61	0.001453	1.46	32.41	25.92	0.42
reach1	26289.59	50 year	54.20	2811.11	2813.61		2813.73	0.001534	1.54	35.22	27.00	0.43
reach1	26289.59	100 year	61.40	2811.11	2813.71		2813.84	0.001605	1.62	38.01	28.03	0.44
reach1	26084.62	10 year	38.20	2811.51	2812.52	2812.52	2812.83	0.010708	2.45	15.62	26.01	1.01
reach1	26084.62	25 year	47.20	2811.51	2812.62	2812.62	2812.96	0.010350	2.59	18.20	27.02	1.01
reach1	26084.62	50 year	54.20	2811.51	2812.69	2812.69	2813.06	0.010079	2.69	20.16	27.77	1.01
reach1	26084.62	100 year	61.40	2811.51	2812.76	2812.76	2813.15	0.009925	2.78	22.05	28.47	1.01
reach1	25848.27	10 year	38.20	2808.36	2809.21	2809.28	2809.54	0.018694	2.56	14.90	35.26	1.26
reach1	25848.27	25 year	47.20	2808.36	2809.26	2809.36	2809.66	0.019859	2.77	17.05	37.64	1.31
reach1	25848.27	50 year	54.20	2808.36	2809.30	2809.41	2809.74	0.020704	2.94	18.44	38.39	1.35
reach1	25848.27	100 year	61.40	2808.36	2809.34	2809.47	2809.83	0.021300	3.09	19.86	39.15	1.39
reach1	25592.74	10 year	38.20	2802.35	2809.08	2803.83	2809.08	0.000003	0.15	260.24	69.67	0.02
reach1	25592.74	25 year	47.20	2802.35	2809.24	2803.97	2809.24	0.000005	0.17	271.50	70.39	0.03
reach1	25592.74	50 year	54.20	2802.35	2809.35	2804.06	2809.35	0.000006	0.19	279.40	70.89	0.03
reach1	25592.74	100 year	61.40	2802.35	2809.46	2804.15	2809.46	0.000007	0.21	286.98	71.36	0.03
reach1	25188.59	10 year	38.20	2806.72	2808.97		2809.06	0.001488	1.37	27.80	24.73	0.41
reach1	25188.59	25 year	47.20	2806.72	2809.11		2809.22	0.001654	1.51	31.32	26.25	0.44
reach1	25188.59	50 year	54.20	2806.72	2809.20		2809.33	0.001775	1.60	33.83	27.28	0.46
reach1	25188.59	100 year	61.40	2806.72	2809.29		2809.44	0.001882	1.69	36.33	28.25	0.48

Reach	River Sta	Profile	Q Total	Min Ch El	W.S. Elev	Crit W.S.	E.G. Elev	E.G. Slope	Vel Chnl	Flow Area	Top Width	roude # Ch
			(m3/s)	(m)	(m)	(m)	(m)	(m/m)	(m/s)	(m2)	(m)	
reach1	16271.07	50 year	54.20	2677.51	2681.31	2679.10	2681.34	0.000192	0.78	69.93	31.10	0.17
reach1	16271.07	100 year	61.40	2677.51	2681.44	2679.20	2681.47	0.000212	0.83	74.03	31.95	0.17
reach1	15930.37	10 year	38.20	2679.14	2680.42	2680.42	2680.81	0.009873	2.74	13.96	18.36	1.00
reach1	15930.37	25 year	47.20	2679.14	2680.55	2680.55	2680.98	0.009644	2.88	16.38	19.55	1.01
reach1	15930.37	50 year	54.20	2679.14	2680.64	2680.64	2681.10	0.009437	2.97	18.23	20.42	1.01
reach1	15930.37	100 year	61.40	2679.14	2680.73	2680.73	2681.21	0.009384	3.07	19.98	21.22	1.01
reach1	15715.79	10 year	38.20	2671.39	2671.76	2672.18	2674.47	0.351548	7.29	5.24	23.37	4.91
reach1	15715.79	25 year	47.20	2671.39	2671.80	2672.26	2674.82	0.334668	7.69	6.14	24.31	4.89
reach1	15715.79	50 year	54.20	2671.39	2671.83	2672.32	2674.95	0.307181	7.82	6.93	25.11	4.75
reach1	15715.79	100 year	61.40	2671.39	2671.87	2672.38	2675.04	0.279915	7.89	7.78	25.94	4.60
reach1	15450.97	10 year	38.20	2666.00	2667.23	2667.23	2667.54	0.010451	2.46	15.53	25.18	1.00
reach1	15450.97	25 year	47.20	2666.00	2667.34	2667.34	2667.68	0.010440	2.59	18.21	27.27	1.01
reach1	15450.97	50 year	54.20	2666.00	2667.42	2667.42	2667.77	0.010047	2.65	20.49	28.92	1.00
reach1	15450.97	100 year	61.40	2666.00	2667.49	2667.49	2667.86	0.010025	2.73	22.52	30.32	1.01
reach1	15109.41	10 year	38.20	2662.80	2663.50	2663.51	2663.76	0.011638	2.26	16.87	33.67	1.02
reach1	15109.41	25 year	47.20	2662.80	2663.57	2663.59	2663.88	0.011792	2.45	19.30	34.66	1.05
reach1	15109.41	50 year	54.20	2662.80	2663.62	2663.65	2663.96	0.012436	2.61	20.78	35.24	1.08
reach1	15109.41	100 year	61.40	2662.80	2663.67	2663.71	2664.05	0.012564	2.73	22.49	35.90	1.10
reach1	14801.63	10 year	38.20	2655.32	2656.24	2656.54	2657.23	0.048500	4.40	8.68	18.55	2.06
reach1	14801.63	25 year	47.20	2655.32	2656.32	2656.66	2657.42	0.045666	4.63	10.20	19.36	2.03
reach1	14801.63	50 year	54.20	2655.32	2656.40	2656.74	2657.51	0.041163	4.67	11.61	20.08	1.96
reach1	14801.63	100 year	61.40	2655.32	2656.45	2656.82	2657.63	0.039684	4.80	12.80	20.66	1.95
reach1	14568.96	10 year	38.20	2646.03	2647.23	2647.56	2648.23	0.031526	4.42	8.63	13.11	1.74
reach1	14568.96	25 year	47.20	2646.03	2647.33	2647.70	2648.46	0.032779	4.71	10.02	14.26	1.79
reach1	14568.96	50 year	54.20	2646.03	2647.39	2647.81	2648.66	0.035060	4.99	10.86	14.92	1.87
reach1	14568.96	100 year	61.40	2646.03	2647.45	2647.90	2648.82	0.035925	5.18	11.85	15.65	1.90
reach1	14250.23	10 year	38.20	2633.35	2634.55	2634.97	2635.91	0.048841	5.17	7.39	12.33	2.13
reach1	14250.23	25 year	47.20	2633.35	2634.66	2635.11	2636.11	0.045936	5.32	8.87	13.51	2.10
reach1	14250.23	50 year	54.20	2633.35	2634.75	2635.22	2636.24	0.043772	5.41	10.01	14.35	2.07
reach1	14250.23	100 year	61.40	2633.35	2634.82	2635.31	2636.37	0.042213	5.51	11.15	15.14	2.05
reach1	13935.35	10 year	38.20	2617.18	2617.72	2618.11	2619.18	0.057042	3.31	7.50	18.97	2.02
reach1	13935.35	25 year	47.20	2617.18	2617.78	2618.21	2619.49	0.062456	3.68	8.53	20.24	2.15
reach1	13935.35	50 year	54.20	2617.18	2617.81	2618.29	2619.75	0.067347	3.96	9.21	21.04	2.25
reach1	13935.35	100 year	61.40	2617.18	2617.86	2618.35	2619.88	0.066326	4.12	10.20	22.14	2.26
reach1	13600.5	10 year	38.20	2604.91	2605.92	2606.09	2606.48	0.025019	3.33	11.48	22.82	1.50
reach1	13600.5	25 year	47.20	2604.91	2606.00	2606.19	2606.62	0.024592	3.49	13.54	24.78	1.51
reach1	13600.5	50 year	54.20	2604.91	2606.07	2606.27	2606.71	0.023581	3.55	15.26	26.31	1.49
reach1	13600.5	100 year	61.40	2604.91	2606.13	2606.33	2606.81	0.023509	3.66	16.78	27.58	1.50
reach1	13257.65	10 year	38.20	2598.43	2599.67	2599.77	2600.20	0.013787	3.24	11.80	15.43	1.18
reach1	13257.65	25 year	47.20	2598.43	2599.79	2599.91	2600.39	0.013788	3.43	13.74	16.42	1.20
reach1	13257.65	50 year	54.20	2598.43	2599.87	2600.01	2600.53	0.014060	3.59	15.08	17.07	1.22
reach1	13257.65	100 year	61.40	2598.43	2599.95	2600.11	2600.66	0.013975	3.71	16.54	17.76	1.23
reach1	12919.07	10 year	38.20	2587.88	2588.92	2589.42	2590.75	0.078875	5.99	6.38	12.24	2.65
reach1	12919.07	25 year	47.20	2587.88	2589.01	2589.58	2591.01	0.076816	6.25	7.55	13.32	2.65
reach1	12919.07	50 year	54.20	2587.88	2589.09	2589.68	2591.15	0.073319	6.36	8.53	14.15	2.62
reach1	12919.07	100 year	61.40	2587.88	2589.15	2589.77	2591.33	0.072754	6.54	9.39	14.85	2.63
reach1	12554.31	10 year	38.20	2574.00	2577.88	2574.75	2577.88	0.000007	0.17	225.23	83.23	0.03
reach1	12554.31	25 year	47.20	2574.00	2578.04	2574.83	2578.04	0.000009	0.20	238.88	84.45	0.04
reach1	12554.31	50 year	54.20	2574.00	2578.15	2574.88	2578.16	0.000010	0.22	248.59	85.30	0.04
reach1	12554.31	100 year	61.40	2574.00	2578.26	2574.94	2578.27	0.000012	0.24	257.95	86.12	0.04
reach1	12247.64	10 year	38.20	2576.04	2577.47	2577.47	2577.83	0.010166	2.67	14.32	20.02	1.01
reach1	12247.64	25 year	47.20	2576.04	2577.60	2577.60	2577.99	0.009877	2.78	16.97	21.79	1.01
reach1	12247.64	50 year	54.20	2576.04	2577.69	2577.69	2578.10	0.009636	2.85	19.00	23.06	1.00
reach1	12247.64	100 year	61.40	2576.04	2577.77	2577.77	2578.21	0.009592	2.94	20.90	24.19	1.01
reach1	11814.08	10 year	38.20	2556.49	2557.04	2557.68	2563.31	0.621654	11.09	3.44	12.49	6.75
reach1	11814.08	25 year	47.20	2556.49	2557.09	2557.77	2563.85	0.595710	11.51	4.10	13.63	6.70
reach1	11814.08	50 year	54.20	2556.49	2557.12	2557.83	2564.59	0.621065	12.10	4.48	14.25	6.89
reach1	11814.08	100 year	61.40	2556.49	2557.17	2557.89	2564.24	0.531138	11.77	5.22	15.38	6.46
reach1	11503.85	10 year	38.20	2552.67	2553.47	2553.47	2553.70	0.011843	2.13	17.96	39.90	1.01
reach1	11503.85	25 year	47.20	2552.67	2553.54	2553.54	2553.80	0.011132	2.25	20.95	40.74	1.00

reach1	11503.85	50 year	54.20	2552.67	2553.59	2553.59	2553.87	0.010789	2.35	23.11	41.34	1.00
reach1	11503.85	100 year	61.40	2552.67	2553.64	2553.64	2553.95	0.010628	2.44	25.15	41.89	1.01
reach1	11193.64	10 year	38.20	2538.44	2539.51	2540.29	2543.86	0.187630	9.25	4.13	7.76	4.05
reach1	11193.64	25 year	47.20	2538.44	2539.60	2540.46	2544.40	0.185662	9.71	4.86	8.42	4.08
reach1	11193.64	50 year	54.20	2538.44	2539.66	2540.57	2544.72	0.181012	9.96	5.44	8.91	4.07
reach1	11193.64	100 year	61.40	2538.44	2539.73	2540.68	2544.90	0.171369	10.06	6.10	9.43	3.99
reach1	10858.33	10 year	38.20	2532.91	2534.45	2534.45	2534.83	0.010085	2.73	14.01	18.81	1.01
reach1	10858.33	25 year	47.20	2532.91	2534.59	2534.59	2535.00	0.009668	2.82	16.73	20.68	1.00
reach1	10858.33	50 year	54.20	2532.91	2534.68	2534.68	2535.11	0.009494	2.90	18.72	21.95	1.00
reach1	10858.33	100 year	61.40	2532.91	2534.77	2534.77	2535.22	0.009417	2.97	20.64	23.11	1.00
reach1	10448.71	10 year	38.20	2504.55	2504.89	2505.51	2520.61	2.939846	17.56	2.18	12.75	13.58
reach1	10448.71	25 year	47.20	2504.55	2504.93	2505.59	2520.16	2.447481	17.28	2.73	14.29	12.63
reach1	10448.71	50 year	54.20	2504.55	2504.97	2505.65	2518.98	1.996371	16.58	3.27	15.64	11.58
reach1	10448.71	100 year	61.40	2504.55	2504.97	2505.71	2523.15	2.601257	18.89	3.25	15.59	13.21
reach1	10117.76	10 year	38.20	2495.45	2497.20	2497.37	2497.92	0.016156	3.76	10.16	11.65	1.29
reach1	10117.76	25 year	47.20	2495.45	2497.35	2497.54	2498.14	0.015874	3.94	11.99	12.65	1.29
reach1	10117.76	50 year	54.20	2495.45	2497.46	2497.67	2498.28	0.015136	4.00	13.54	13.44	1.27
reach1	10117.76	100 year	61.40	2495.45	2497.51	2497.78	2498.47	0.017082	4.32	14.21	13.77	1.36
reach1	9794.9	10 year	38.20	2489.85	2490.91	2491.09	2491.50	0.024662	3.41	11.21	21.22	1.50
reach1	9794.9	25 year	47.20	2489.85	2490.99	2491.20	2491.66	0.025756	3.65	12.93	22.78	1.55
reach1	9794.9	50 year	54.20	2489.85	2491.03	2491.28	2491.80	0.027738	3.89	13.95	23.67	1.62
reach1	9794.9	100 year	61.40	2489.85	2491.12	2491.35	2491.86	0.024388	3.82	16.07	25.41	1.53
reach1	9562.237	10 year	38.20	2462.91	2463.76	2464.78	2474.55	0.623511	14.55	2.63	6.15	7.11
reach1	9562.237	25 year	47.20	2462.91	2463.86	2464.94	2474.57	0.536483	14.50	3.26	6.85	6.72
reach1	9562.237	50 year	54.20	2462.91	2463.94	2465.06	2474.23	0.463450	14.20	3.82	7.42	6.32
reach1	9562.237	100 year	61.40	2462.91	2463.97	2465.17	2475.74	0.510071	15.19	4.04	7.63	6.67
reach1	9268.347	10 year	38.20	2458.80	2460.45	2460.51	2460.94	0.011559	3.10	12.31	14.90	1.09
reach1	9268.347	25 year	47.20	2458.80	2460.59	2460.66	2461.14	0.011641	3.28	14.39	16.11	1.11
reach1	9268.347	50 year	54.20	2458.80	2460.69	2460.76	2461.27	0.011451	3.37	16.06	17.02	1.11
reach1	9268.347	100 year	61.40	2458.80	2460.75	2460.87	2461.41	0.012524	3.60	17.05	17.54	1.17
reach1	8927.437	10 year	38.20	2453.67	2455.42	2455.63	2456.18	0.017057	3.86	9.89	11.30	1.32
reach1	8927.437	25 year	47.20	2453.67	2455.57	2455.79	2456.41	0.016678	4.04	11.69	12.28	1.32
reach1	8927.437	50 year	54.20	2453.67	2455.67	2455.92	2456.57	0.016735	4.19	12.95	12.93	1.34
reach1	8927.437	100 year	61.40	2453.67	2455.81	2456.03	2456.69	0.015236	4.17	14.73	13.79	1.29
reach1	8544.831	10 year	38.20	2423.91	2424.58	2425.46	2435.99	0.888247	14.96	2.55	7.63	8.25
reach1	8544.831	25 year	47.20	2423.91	2425.60	2425.60	2426.05	0.009756	2.95	15.98	18.36	1.01
reach1	8544.831	50 year	54.20	2423.91	2424.71	2425.71	2436.25	0.714775	15.05	3.60	9.06	7.62
reach1	8544.831	100 year	61.40	2423.91	2424.74	2425.80	2437.35	0.740391	15.73	3.90	9.43	7.81
reach1	8304.63	10 year	38.20	2414.52	2416.20	2416.49	2417.13	0.021915	4.25	8.98	10.67	1.48
reach1	8304.63	25 year	47.20	2414.52	2415.81	2416.66	2419.85	0.136325	8.90	5.30	8.20	3.54
reach1	8304.63	50 year	54.20	2414.52	2416.43	2416.78	2417.55	0.022485	4.69	11.56	12.11	1.53
reach1	8304.63	100 year	61.40	2414.52	2416.51	2416.90	2417.74	0.023411	4.91	12.50	12.59	1.57
reach1	8060.867	10 year	38.20	2411.27	2413.06	2413.07	2413.56	0.009867	3.14	12.18	12.62	1.02
reach1	8060.867	25 year	47.20	2411.27	2413.24	2413.24	2413.78	0.009225	3.23	14.60	13.75	1.00
reach1	8060.867	50 year	54.20	2411.27	2413.33	2413.36	2413.93	0.009822	3.43	15.81	14.28	1.04
reach1	8060.867	100 year	61.40	2411.27	2413.44	2413.47	2414.07	0.009652	3.52	17.46	14.97	1.04
reach1	7723.669	10 year	38.20	2400.30	2401.27	2402.09	2405.06	0.129573	8.63	4.43	6.85	3.43
reach1	7723.669	25 year	47.20	2400.30	2401.37	2402.28	2405.65	0.130261	9.16	5.16	7.31	3.48
reach1	7723.669	50 year	54.20	2400.30	2401.48	2402.45	2405.66	0.114006	9.05	5.99	7.80	3.30
reach1	7723.669	100 year	61.40	2400.30	2401.56	2402.59	2405.94	0.111029	9.27	6.63	8.15	3.28
reach1	7452.053	10 year	38.20	2384.95	2385.75	2385.94	2386.37	0.037969	3.50	10.90	27.41	1.77
reach1	7452.053	25 year	47.20	2384.95	2385.80	2386.02	2386.53	0.040191	3.77	12.51	29.36	1.85
reach1	7452.053	50 year	54.20	2384.95	2385.84	2386.09	2386.66	0.043225	4.02	13.48	30.37	1.93
reach1	7452.053	100 year	61.40	2384.95	2385.87	2386.14	2386.78	0.043536	4.21	14.58	30.82	1.95
reach1	7116.062	10 year	38.20	2357.38	2358.52	2359.32	2362.61	0.164589	8.97	4.26	7.50	3.80
reach1	7116.062	25 year	47.20	2357.38	2358.63	2359.49	2362.85	0.148400	9.09	5.19	8.28	3.67
reach1	7116.062	50 year	54.20	2357.38	2358.73	2359.61	2362.87	0.131944	9.01	6.02	8.92	3.50
reach1	7116.062	100 year	61.40	2357.38	2358.80	2359.72	2363.11	0.128250	9.19	6.68	9.39	3.48
reach1	6780.354	10 year	38.20	2350.05	2350.88	2350.90	2351.18	0.012484	2.44	15.65	29.32	1.07
reach1	6780.354	25 year	47.20	2350.05	2350.95	2350.98	2351.31	0.012997	2.67	17.66	29.71	1.11

reach1	6780.354	50 year	54.20	2350.05	2350.99	2351.05	2351.40	0.013411	2.84	19.08	29.98	1.14
reach1	6780.354	100 year	61.40	2350.05	2351.04	2351.11	2351.50	0.013736	3.00	20.49	30.25	1.16
reach1	6480.047	10 year	38.20	2323.00	2323.53	2324.36	2337.85	1.489416	16.76	2.28	8.55	10.37
reach1	6480.047	25 year	47.20	2323.00	2324.47	2324.47	2324.85	0.010038	2.71	17.42	23.65	1.01
reach1	6480.047	50 year	54.20	2323.00	2324.56	2324.56	2324.95	0.009705	2.77	19.57	25.06	1.00
reach1	6480.047	100 year	61.40	2323.00	2324.64	2324.64	2325.05	0.009544	2.84	21.62	26.34	1.00
reach1	6096.592	10 year	38.20	2302.93	2303.85	2303.98	2304.33	0.025267	3.05	12.51	28.45	1.47
reach1	6096.592	25 year	47.20	2302.93	2304.07	2304.07	2304.39	0.010403	2.49	18.96	30.03	1.00
reach1	6096.592	50 year	54.20	2302.93	2304.13	2304.13	2304.48	0.010142	2.60	20.88	30.49	1.00
reach1	6096.592	100 year	61.40	2302.93	2303.50	2304.19	2312.31	0.830785	13.14	4.67	16.36	7.85
reach1	5742.829	10 year	38.20	2293.00	2294.30	2294.59	2295.18	0.026345	4.17	9.16	13.22	1.60
reach1	5742.829	25 year	47.20	2293.00	2294.12	2294.73	2296.40	0.075050	6.68	7.07	11.04	2.66
reach1	5742.829	50 year	54.20	2293.00	2294.20	2294.83	2296.60	0.075966	6.86	7.90	11.95	2.69
reach1	5742.829	100 year	61.40	2293.00	2294.81	2294.93	2295.43	0.012926	3.47	17.70	19.78	1.17
reach1	5491.33	10 year	38.20	2280.46	2281.23	2281.65	2283.01	0.113835	5.92	6.46	16.85	3.05
reach1	5491.33	25 year	47.20	2280.46	2281.46	2281.75	2282.41	0.040751	4.32	10.93	21.16	1.92
reach1	5491.33	50 year	54.20	2280.46	2281.51	2281.83	2282.55	0.040631	4.51	12.02	21.77	1.94
reach1	5491.33	100 year	61.40	2280.46	2281.22	2281.91	2286.03	0.311432	9.72	6.32	16.67	5.04
reach1	5278.947	10 year	38.20	2274.08	2275.33	2275.42	2275.77	0.014836	2.95	12.94	20.73	1.19
reach1	5278.947	25 year	47.20	2274.08	2275.33	2275.54	2276.00	0.022493	3.64	12.98	20.75	1.47
reach1	5278.947	50 year	54.20	2274.08	2275.39	2275.62	2276.12	0.022618	3.77	14.36	21.83	1.49
reach1	5278.947	100 year	61.40	2274.08	2275.57	2275.69	2276.14	0.015023	3.34	18.39	24.70	1.24
reach1	5038.309	10 year	38.20	2267.78	2268.81	2269.13	2269.89	0.046124	4.58	8.33	16.12	2.04
reach1	5038.309	25 year	47.20	2267.78	2269.02	2269.23	2269.69	0.030894	3.62	13.04	26.69	1.65
reach1	5038.309	50 year	54.20	2267.78	2269.07	2269.30	2269.80	0.030789	3.79	14.32	27.32	1.67
reach1	5038.309	100 year	61.40	2267.78	2269.03	2269.36	2270.11	0.048496	4.59	13.37	26.85	2.08
reach1	4890.766	10 year	38.20	2258.54	2258.86	2259.12	2259.88	0.108381	4.47	8.55	32.83	2.80
reach1	4890.766	25 year	47.20	2258.54	2258.86	2259.20	2260.49	0.178532	5.66	8.35	32.75	3.58
reach1	4890.766	50 year	54.20	2258.54	2258.88	2259.25	2260.67	0.174783	5.92	9.16	33.05	3.59
reach1	4890.766	100 year	61.40	2258.54	2258.97	2259.31	2260.31	0.095531	5.13	11.97	34.04	2.76
reach1	4730.395	10 year	38.20	2249.72	2251.18	2251.49	2252.15	0.027050	4.36	8.76	12.01	1.63
reach1	4730.395	25 year	47.20	2249.72	2251.35	2251.64	2252.30	0.022950	4.32	10.92	13.41	1.53
reach1	4730.395	50 year	54.20	2249.72	2251.43	2251.76	2252.46	0.023129	4.49	12.08	14.10	1.55
reach1	4730.395	100 year	61.40	2249.72	2251.45	2251.86	2252.71	0.028021	4.97	12.35	14.25	1.71
reach1	4548.986	10 year	38.20	2222.00	2223.56	2223.56	2223.95	0.009877	2.77	13.77	17.71	1.00
reach1	4548.986	25 year	47.20	2222.00	2223.69	2223.69	2224.12	0.009675	2.90	16.27	19.24	1.01
reach1	4548.986	50 year	54.20	2222.00	2223.79	2223.79	2224.24	0.009394	2.97	18.24	20.38	1.00
reach1	4548.986	100 year	61.40	2222.00	2223.88	2223.88	2224.36	0.009198	3.04	20.19	21.44	1.00
reach1	4270.501	10 year	38.20	2218.64	2219.81	2219.94	2220.31	0.018295	3.14	12.17	20.77	1.31
reach1	4270.501	25 year	47.20	2218.64	2219.90	2220.06	2220.47	0.018974	3.36	14.06	22.33	1.35
reach1	4270.501	50 year	54.20	2218.64	2219.96	2220.14	2220.59	0.019760	3.53	15.37	23.34	1.39
reach1	4270.501	100 year	61.40	2218.64	2220.01	2220.22	2220.70	0.020401	3.68	16.70	24.41	1.42
reach1	4001.844	10 year	38.20	2207.77	2208.80	2209.33	2210.85	0.088967	6.34	6.03	11.67	2.81
reach1	4001.844	25 year	47.20	2207.77	2208.91	2209.47	2211.04	0.081496	6.46	7.30	12.84	2.74
reach1	4001.844	50 year	54.20	2207.77	2208.99	2209.56	2211.14	0.075545	6.50	8.33	13.72	2.66
reach1	4001.844	100 year	61.40	2207.77	2209.06	2209.66	2211.25	0.071133	6.56	9.36	14.54	2.61
reach1	3782.173	10 year	38.20	2207.81	2208.53	2208.53	2208.80	0.011113	2.31	16.53	30.90	1.01
reach1	3782.173	25 year	47.20	2207.81	2208.62	2208.62	2208.92	0.010735	2.45	19.30	32.28	1.01
reach1	3782.173	50 year	54.20	2207.81	2208.69	2208.69	2209.01	0.010310	2.52	21.50	33.34	1.00
reach1	3782.173	100 year	61.40	2207.81	2208.75	2208.75	2209.09	0.010178	2.61	23.52	34.28	1.01
reach1	3513.826	10 year	38.20	2199.94	2200.73	2201.12	2202.20	0.089530	5.37	7.11	17.93	2.72
reach1	3513.826	25 year	47.20	2199.94	2200.80	2201.22	2202.45	0.090886	5.69	8.29	19.35	2.78
reach1	3513.826	50 year	54.20	2199.94	2200.84	2201.30	2202.65	0.094016	5.97	9.08	20.25	2.85
reach1	3513.826	100 year	61.40	2199.94	2200.88	2201.37	2202.80	0.093183	6.14	10.00	21.26	2.86
reach1	3261.167	10 year	38.20	2196.00	2197.33	2197.33	2197.67	0.010278	2.56	14.90	22.37	1.00
reach1	3261.167	25 year	47.20	2196.00	2197.45	2197.45	2197.81	0.010170	2.69	17.53	24.27	1.01
reach1	3261.167	50 year	54.20	2196.00	2197.53	2197.53	2197.92	0.009901	2.76	19.64	25.69	1.01
reach1	3261.167	100 year	61.40	2196.00	2197.61	2197.61	2198.02	0.009779	2.83	21.66	26.98	1.01
reach1	3069.329	10 year	38.20	2189.50	2190.39	2190.93	2192.72	0.121609	6.75	5.66	12.67	3.22
reach1	3069.329	25 year	47.20	2189.50	2190.48	2191.05	2192.95	0.114950	6.96	6.78	13.86	3.18

reach1	3069.329	50 year	54.20	2189.50	2190.53	2191.14	2193.15	0.113177	7.17	7.56	14.64	3.18
reach1	3069.329	100 year	61.40	2189.50	2190.59	2191.22	2193.32	0.109869	7.31	8.40	15.43	3.16
reach1	2768.386	10 year	38.20	2185.87	2187.16	2187.16	2187.50	0.010423	2.57	14.86	22.45	1.01
reach1	2768.386	25 year	47.20	2185.87	2187.28	2187.28	2187.64	0.010151	2.68	17.64	24.63	1.01
reach1	2768.386	50 year	54.20	2185.87	2187.36	2187.36	2187.74	0.009876	2.74	19.81	26.20	1.00
reach1	2768.386	100 year	61.40	2185.87	2187.44	2187.44	2187.84	0.009813	2.81	21.84	27.58	1.01
reach1	2544.211	10 year	38.20	2178.79	2179.10	2179.41	2180.81	0.277289	5.79	6.60	34.85	4.25
reach1	2544.211	25 year	47.20	2178.79	2179.13	2179.48	2181.10	0.269526	6.21	7.60	35.30	4.28
reach1	2544.211	50 year	54.20	2178.79	2179.15	2179.53	2181.33	0.268467	6.53	8.29	35.62	4.32
reach1	2544.211	100 year	61.40	2178.79	2179.17	2179.58	2181.53	0.264333	6.81	9.01	35.94	4.34
reach1	2354.638	10 year	38.20	2175.76	2178.61	2177.29	2178.64	0.000358	0.79	48.30	33.92	0.21
reach1	2354.638	25 year	47.20	2175.76	2178.76	2177.42	2178.80	0.000413	0.88	53.66	35.76	0.23
reach1	2354.638	50 year	54.20	2175.76	2178.87	2177.52	2178.91	0.000453	0.94	57.50	37.02	0.24
reach1	2354.638	100 year	61.40	2175.76	2178.96	2177.61	2179.02	0.000494	1.00	61.13	38.17	0.25
reach1	2054.857	10 year	38.20	2176.95	2178.03	2178.03	2178.31	0.011054	2.32	16.45	30.40	1.01
reach1	2054.857	25 year	47.20	2176.95	2178.13	2178.13	2178.43	0.010878	2.43	19.39	33.01	1.01
reach1	2054.857	50 year	54.20	2176.95	2178.19	2178.19	2178.51	0.010658	2.50	21.68	34.90	1.01
reach1	2054.857	100 year	61.40	2176.95	2178.28	2178.28	2178.59	0.010456	2.45	25.05	40.96	1.00
reach1	1794.641	10 year	38.20	2170.00	2170.98	2171.38	2172.38	0.065412	5.25	7.28	14.92	2.40
reach1	1794.641	25 year	47.20	2170.00	2171.05	2171.50	2172.66	0.067978	5.62	8.40	16.04	2.48
reach1	1794.641	50 year	54.20	2170.00	2171.12	2171.59	2172.77	0.064555	5.70	9.50	17.06	2.44
reach1	1794.641	100 year	61.40	2170.00	2171.17	2171.67	2172.93	0.064363	5.88	10.45	17.88	2.45
reach1	1447.001	10 year	38.20	2162.00	2163.20	2163.25	2163.56	0.012608	2.66	14.38	23.94	1.09
reach1	1447.001	25 year	47.20	2162.00	2163.30	2163.36	2163.70	0.012575	2.80	16.87	25.93	1.11
reach1	1447.001	50 year	54.20	2162.00	2163.37	2163.43	2163.80	0.012896	2.92	18.54	27.18	1.13
reach1	1447.001	100 year	61.40	2162.00	2163.43	2163.50	2163.89	0.013004	3.03	20.30	28.43	1.14
reach1	1073.795	10 year	38.20	2143.62	2144.39	2145.12	2149.78	0.344906	10.28	3.72	9.65	5.29
reach1	1073.795	25 year	47.20	2143.62	2144.47	2145.25	2150.10	0.317834	10.51	4.49	10.61	5.16
reach1	1073.795	50 year	54.20	2143.62	2144.53	2145.35	2150.14	0.288683	10.49	5.17	11.38	4.97
reach1	1073.795	100 year	61.40	2143.62	2144.58	2145.43	2150.29	0.271333	10.58	5.81	12.06	4.87
reach1	550.3049	10 year	38.20	2132.97	2134.39	2134.39	2134.76	0.010199	2.67	14.33	20.12	1.01
reach1	550.3049	25 year	47.20	2132.97	2134.52	2134.52	2134.91	0.009971	2.79	16.93	21.87	1.01
reach1	550.3049	50 year	54.20	2132.97	2134.61	2134.61	2135.03	0.009745	2.86	18.95	23.14	1.01
reach1	550.3049	100 year	61.40	2132.97	2134.69	2134.69	2135.13	0.009628	2.94	20.90	24.30	1.01
reach1	377.8101	10 year	38.20	2124.50	2125.24	2125.87	2129.41	0.281070	9.04	4.23	11.45	4.75
reach1	377.8101	25 year	47.20	2124.50	2125.31	2125.99	2129.70	0.261369	9.27	5.09	12.57	4.65
reach1	377.8101	50 year	54.20	2124.50	2125.36	2126.08	2129.92	0.250829	9.45	5.73	13.34	4.61
reach1	377.8101	100 year	61.40	2124.50	2125.41	2126.16	2130.09	0.239333	9.58	6.41	14.10	4.54
reach1	163.0885	10 year	38.20	2113.97	2115.02	2115.21	2115.62	0.024729	3.41	11.20	21.25	1.50
reach1	163.0885	25 year	47.20	2113.97	2115.11	2115.31	2115.78	0.025517	3.64	12.98	22.87	1.54
reach1	163.0885	50 year	54.20	2113.97	2115.16	2115.39	2115.90	0.026046	3.79	14.28	23.99	1.57
reach1	163.0885	100 year	61.40	2113.97	2115.21	2115.47	2116.01	0.026567	3.94	15.57	25.05	1.60

APPENDEX D 3D view of multiple river cross sections

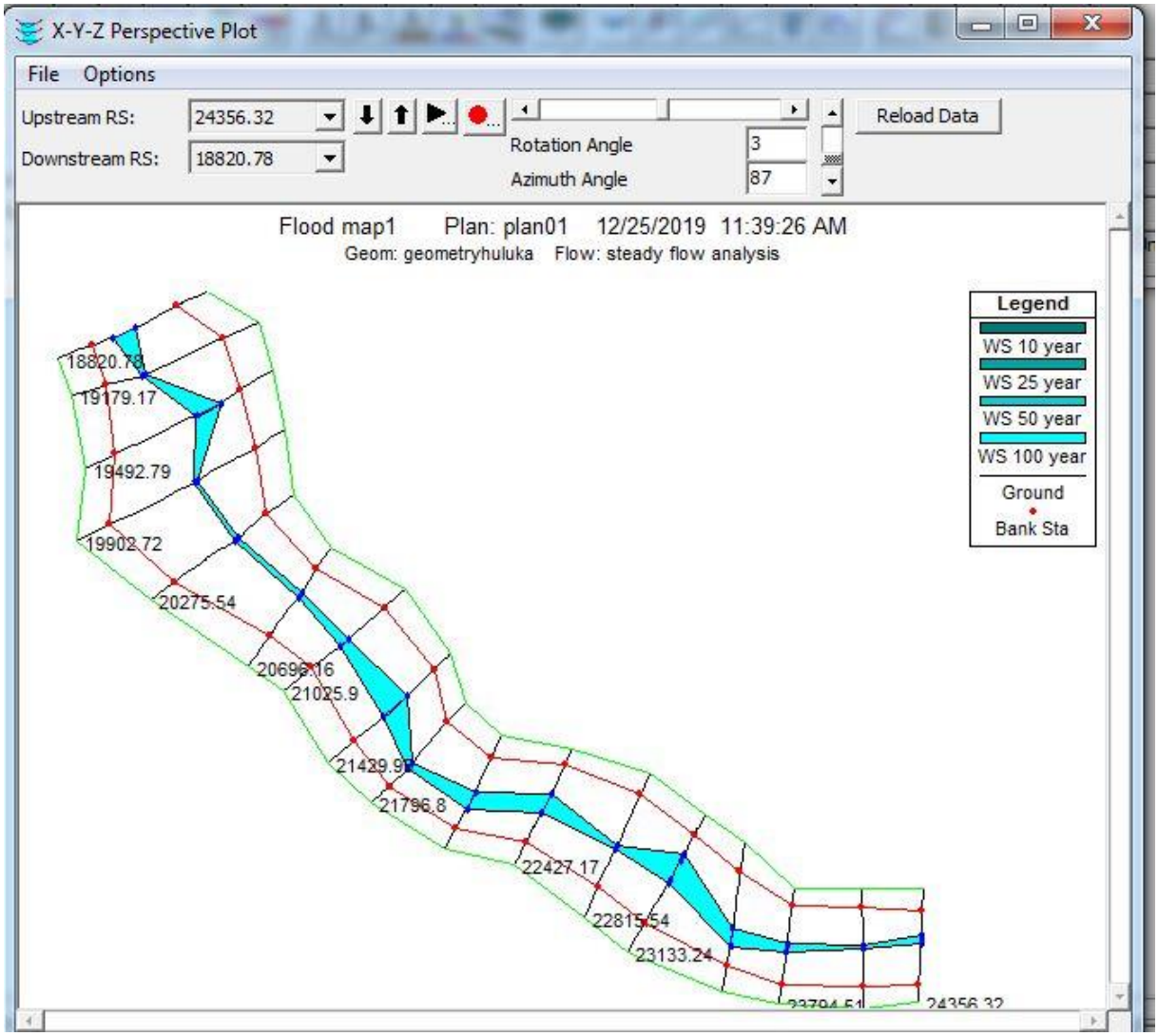

APPENDEX-E GIS data exported from HEC-RAS to Arc GIS

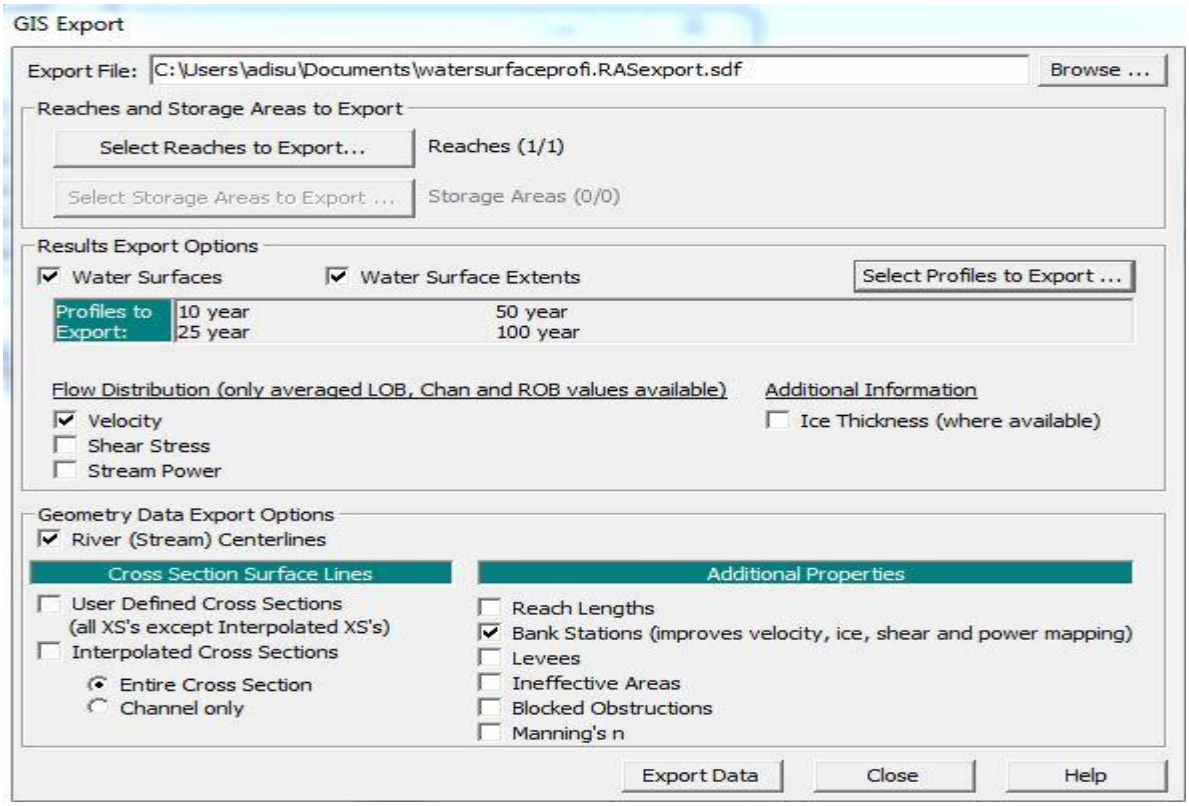

APPENDEX F Water surface TIN profiles for 10, 25 and 50

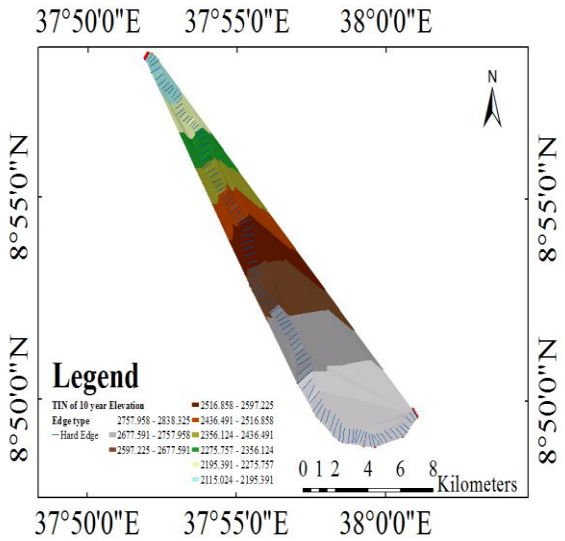

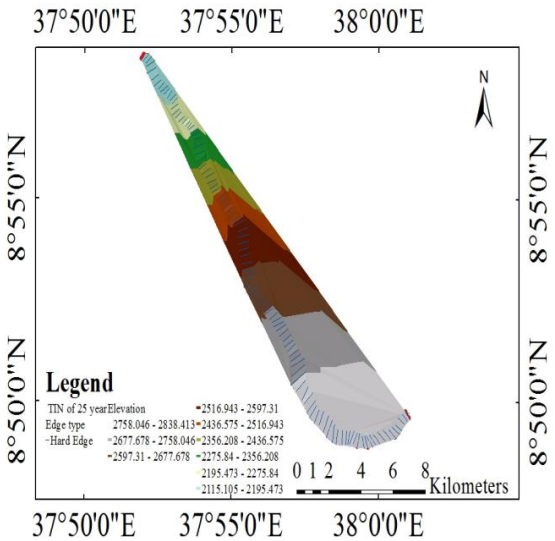

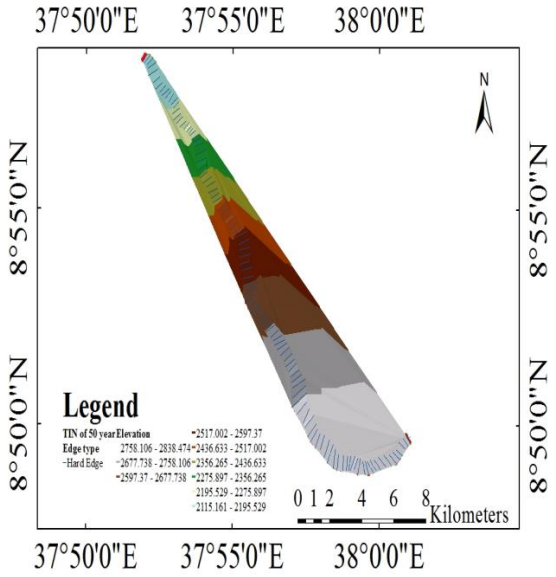

APPENDEX G: Rating curve

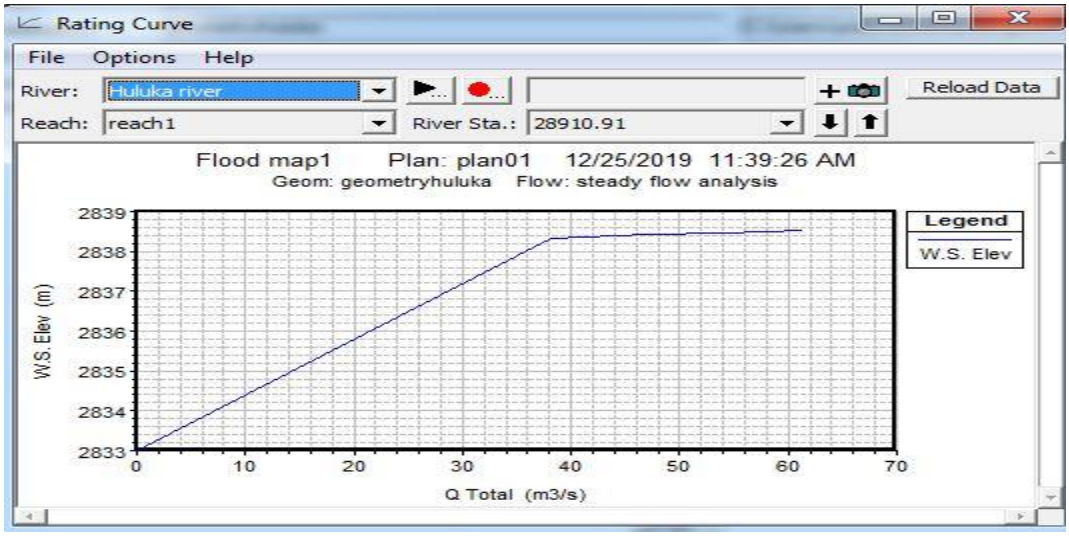

APPENDEX: H Table of River station with Left over bank, Channel and Right over bank length

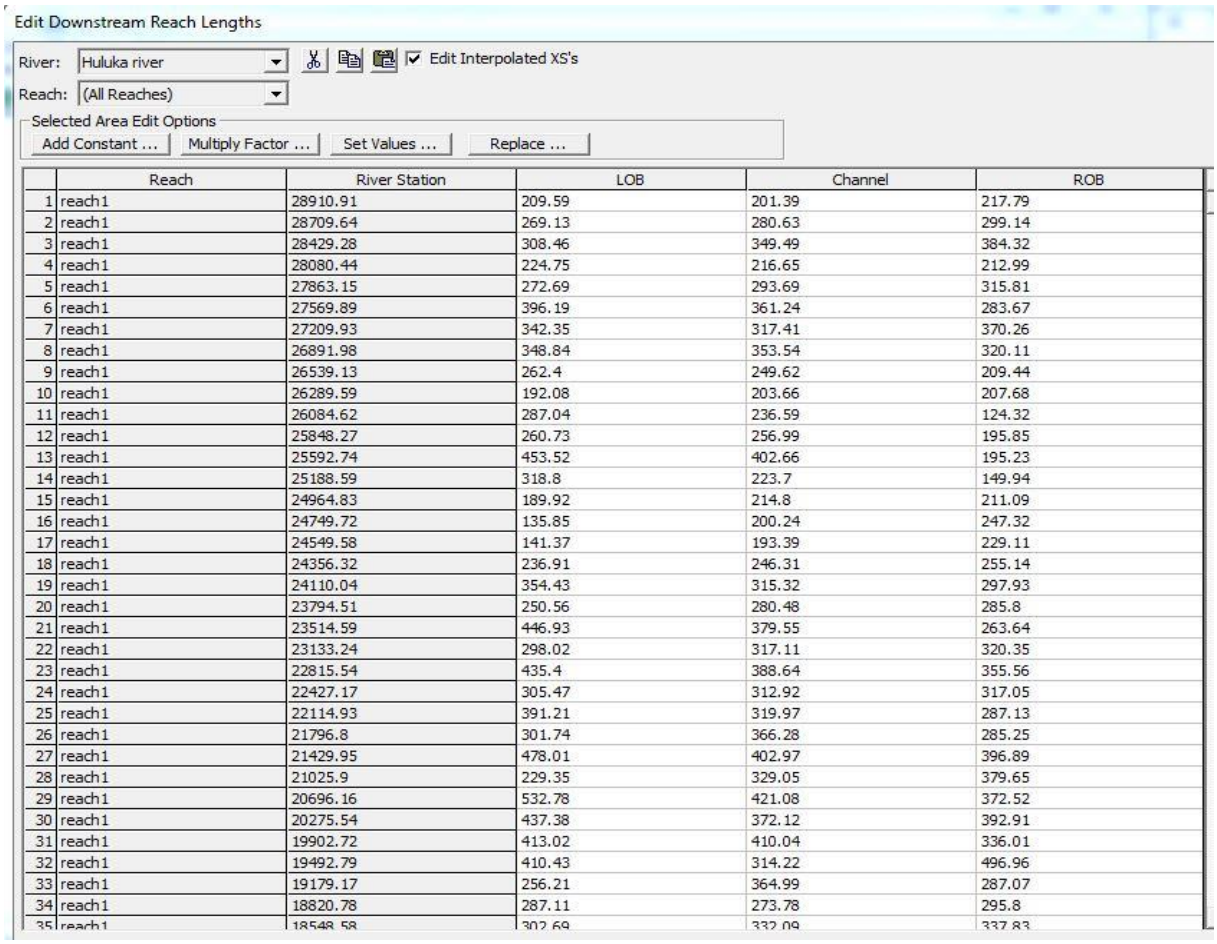

Edit Downstream Reach Lengths

River: Huluka river Edit Interpolated XS's

Reach: (All Reaches)

Selected Area Edit Options

Add Constant ... | Multiply Factor ... | Set Values ... | Replace ...

	Reach	River Station	LOB	Channel	ROB
1	reach1	28910.91	209.59	201.39	217.79
2	reach1	28709.64	269.13	280.63	299.14
3	reach1	28429.28	308.46	349.49	384.32
4	reach1	28080.44	224.75	216.65	212.99
5	reach1	27863.15	272.69	293.69	315.81
6	reach1	27569.89	396.19	361.24	283.67
7	reach1	27209.93	342.35	317.41	370.26
8	reach1	26891.98	348.84	353.54	320.11
9	reach1	26539.13	262.4	249.62	209.44
10	reach1	26289.59	192.08	203.66	207.68
11	reach1	26084.62	287.04	236.59	124.32
12	reach1	25848.27	260.73	256.99	195.85
13	reach1	25592.74	453.52	402.66	195.23
14	reach1	25188.59	318.8	223.7	149.94
15	reach1	24964.83	189.92	214.8	211.09
16	reach1	24749.72	135.85	200.24	247.32
17	reach1	24549.58	141.37	193.39	229.11
18	reach1	24356.32	236.91	246.31	255.14
19	reach1	24110.04	354.43	315.32	297.93
20	reach1	23794.51	250.56	280.48	285.8
21	reach1	23514.59	446.93	379.55	263.64
22	reach1	23133.24	298.02	317.11	320.35
23	reach1	22815.54	435.4	388.64	355.56
24	reach1	22427.17	305.47	312.92	317.05
25	reach1	22114.93	391.21	319.97	287.13
26	reach1	21796.8	301.74	366.28	285.25
27	reach1	21429.95	478.01	402.97	396.89
28	reach1	21025.9	229.35	329.05	379.65
29	reach1	20696.16	532.78	421.08	372.52
30	reach1	20275.54	437.38	372.12	392.91
31	reach1	19902.72	413.02	410.04	336.01
32	reach1	19492.79	410.43	314.22	496.96
33	reach1	19179.17	256.21	364.99	287.07
34	reach1	18820.78	287.11	273.78	295.8
35	reach1	18548.58	302.69	332.09	337.83

APPENDEX-I River station and cross section network exported from Arc GIS to HEC-RAS

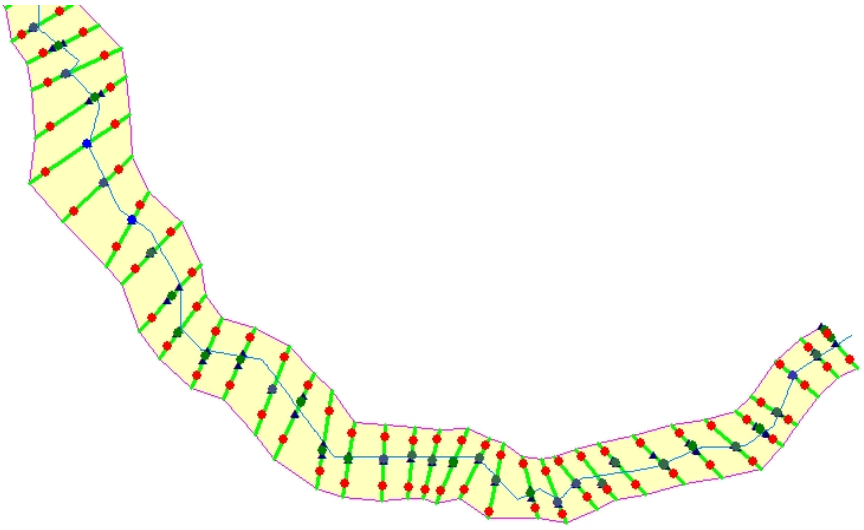

APPENDEX-J Land use /land cover classified for different selected years for 1997, 2005 and 2011

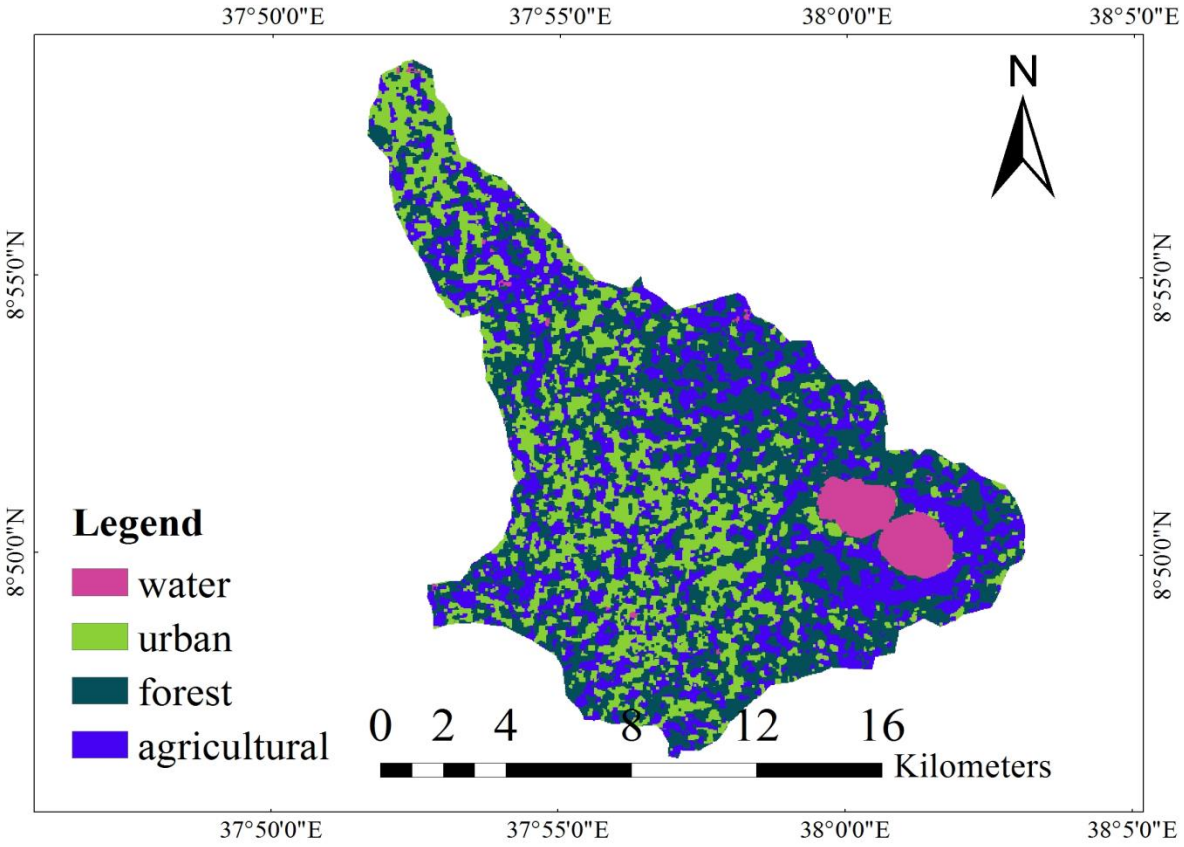

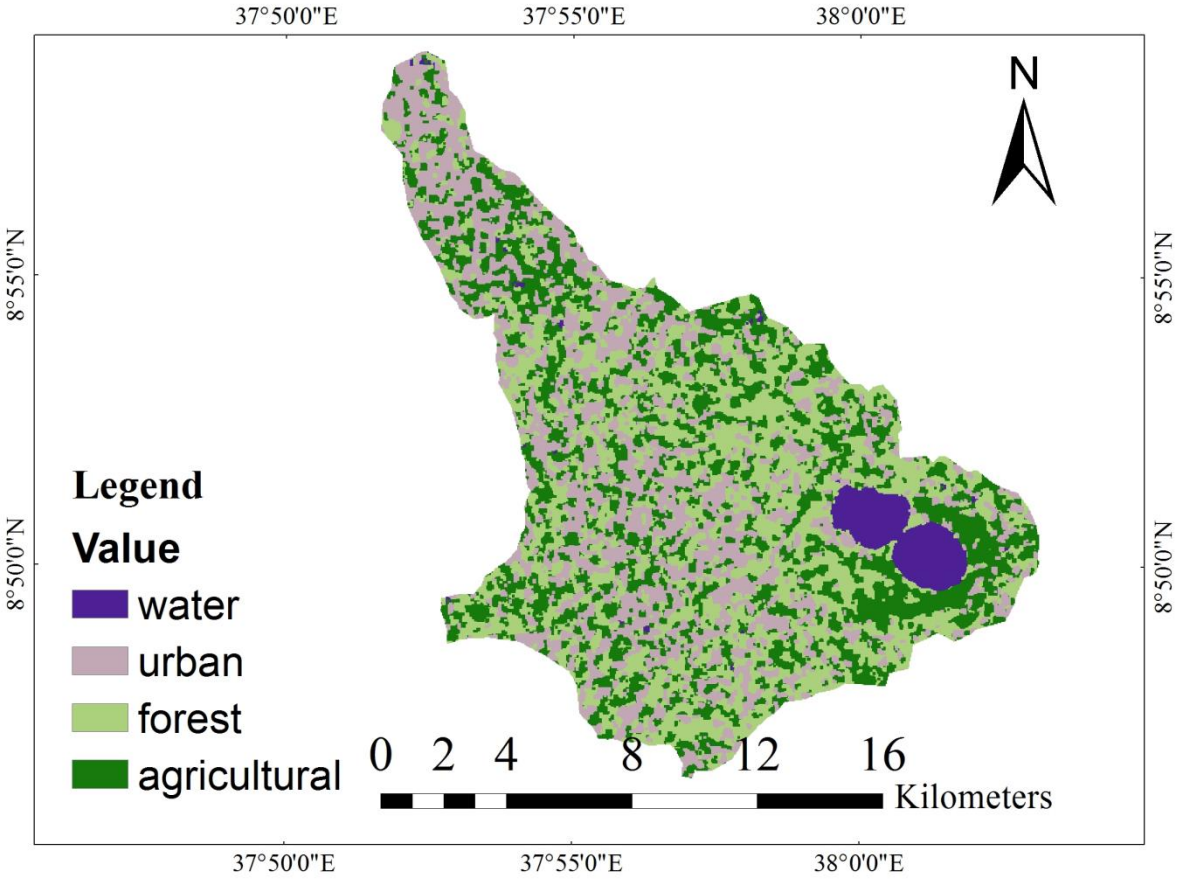
37°50'0"E
37°55'0"E
38°0'0"E
8°55'0"N
8°50'0"N
N
Legend
Value
water
urban
forest
agricultural
0 2 4 8 12 16
Kilometers

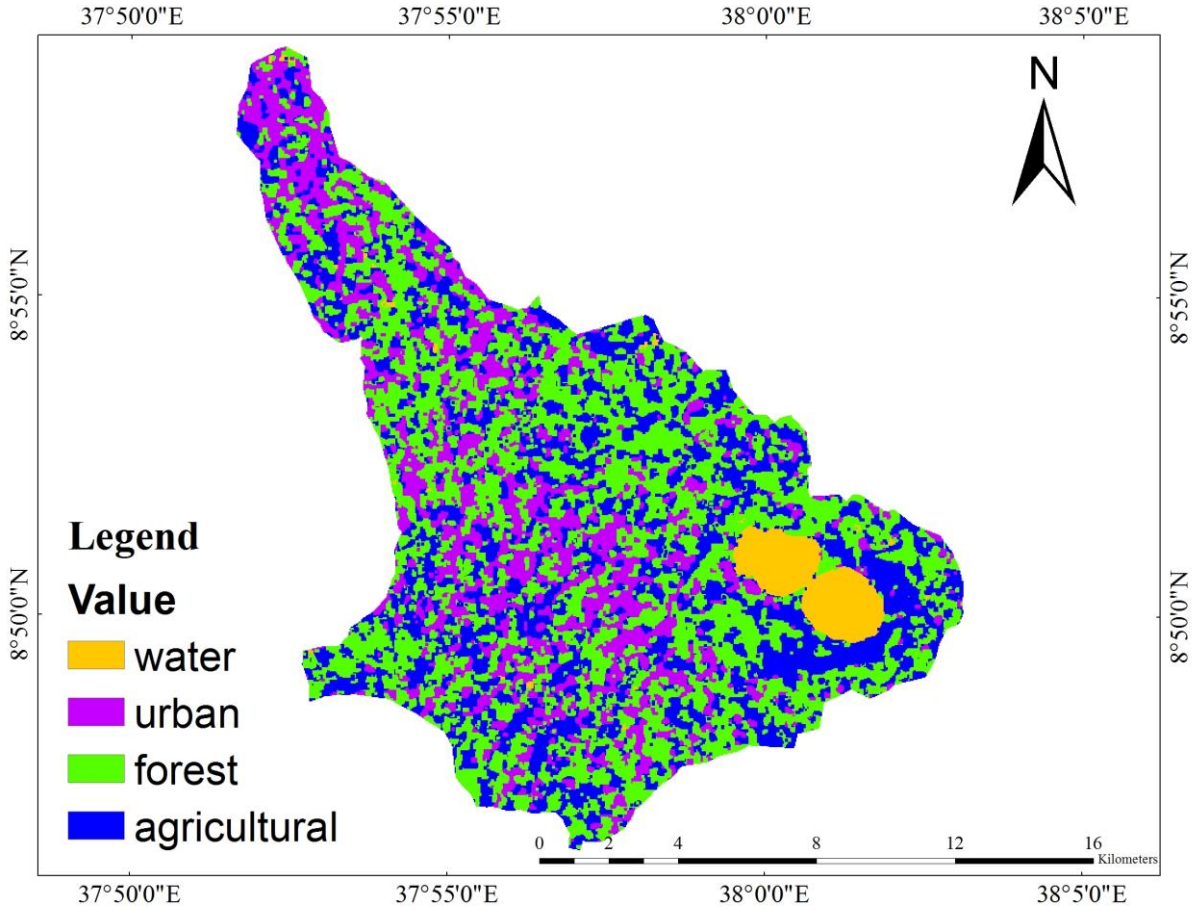
37°50'0"E
37°55'0"E
38°0'0"E
38°5'0"E
8°55'0"N
8°50'0"N
N
Legend
Value
water
urban
forest
agricultural
0
2
4
8
12
16
Kilometers

Appendex-K Floodplain area for 50 and 100 year return period of Huluka river watershed

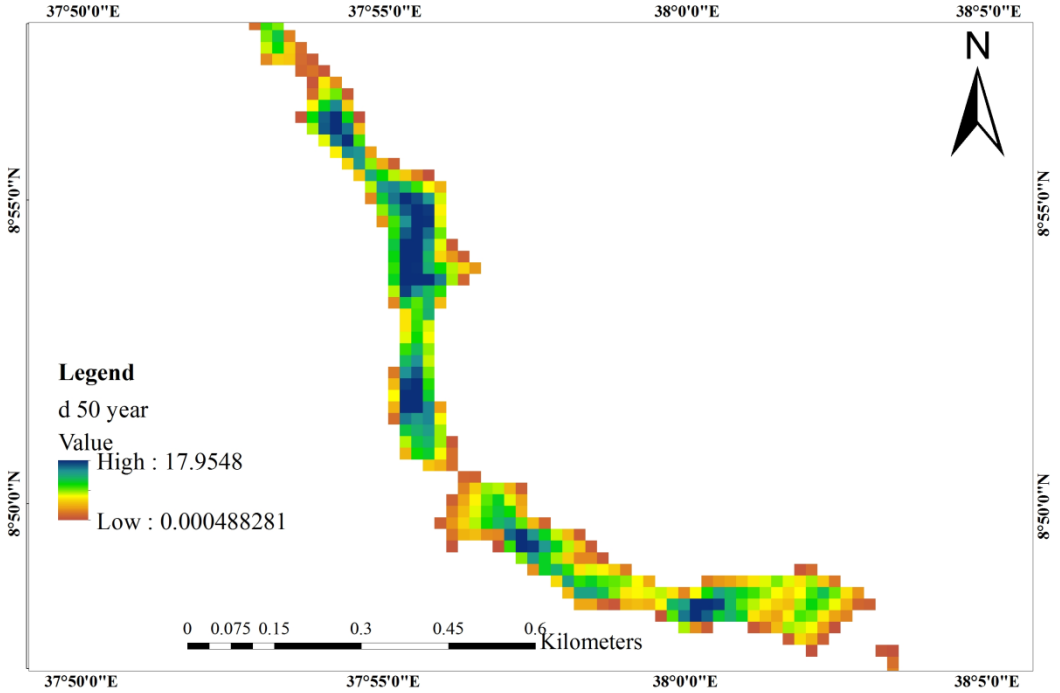

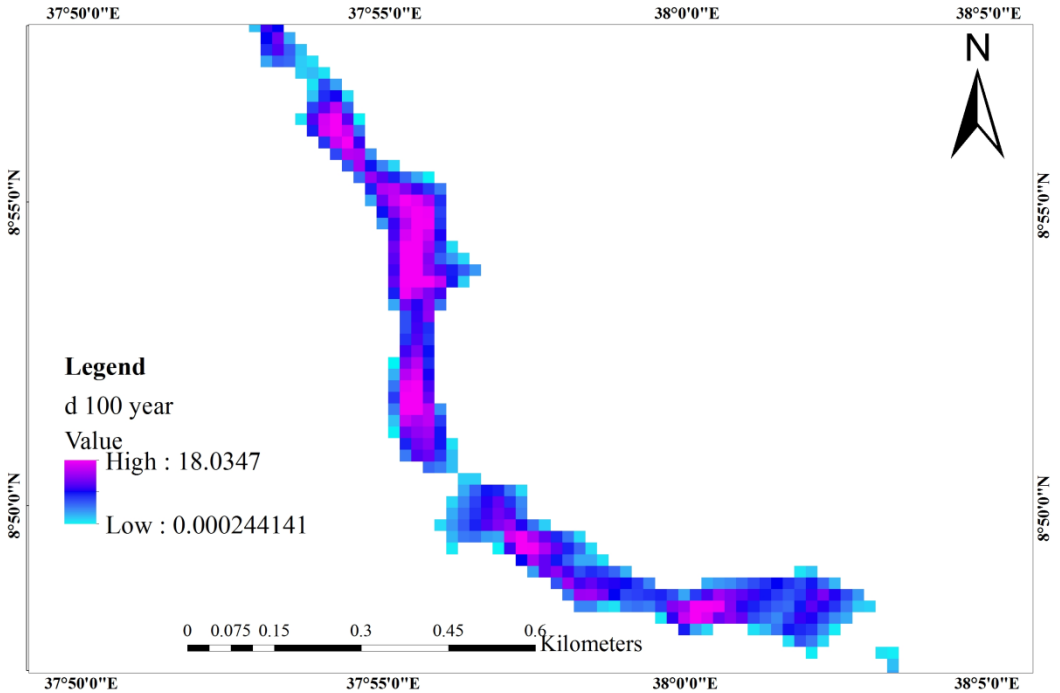

Appendex-L Soil, land use classification and percentage of impervious area determination by SCS TR55 Data's

Cover description		Curve numbers for hydrologic soil group			
Cover type and hydrologic condition	Average percent impervious area [2]	A	B	C	D
Fully developed urban areas (vegetation established)					
Open space (lawns, parks, golf courses, cemeteries, etc.) [3]:					
Poor condition (grass cover < 50%)		68	79	86	89
Fair condition (grass cover 50% to 75%)		49	69	79	84
Good condition (grass cover > 75%)		39	61	74	80
Impervious areas:					
Paved parking lots, roofs, driveways, etc. (excluding right-of-way)		98	98	98	98
Streets and roads:					
Paved; curbs and storm sewers (excluding right-of-way)		98	98	98	98
Paved; open ditches (including right-of-way)		83	89	92	93
Gravel (including right-of-way)		76	85	89	91
Dirt (including right-of-way)		72	82	87	89
Western desert urban areas:					
Natural desert landscaping (pervious areas only) [4]		63	77	85	88
Artificial desert landscaping (impervious weed barrier, desert shrub with 1- to 2-inch sand or gravel mulch and basin borders)		96	96	96	96
Urban districts:					
Commercial and business	85	89	92	94	95
Industrial	72	81	88	91	93
Residential districts by average lot size:					
1/8 acre or less (town houses)	65	77	85	90	92
1/4 acre	38	61	75	83	87
1/3 acre	30	57	72	81	86
1/2 acre	25	54	70	80	85
1 acre	20	51	68	79	84
2 acres	12	46	65	77	82
Developing urban areas					
Newly graded areas (pervious areas only, no vegetation) [5]		77	86	91	94

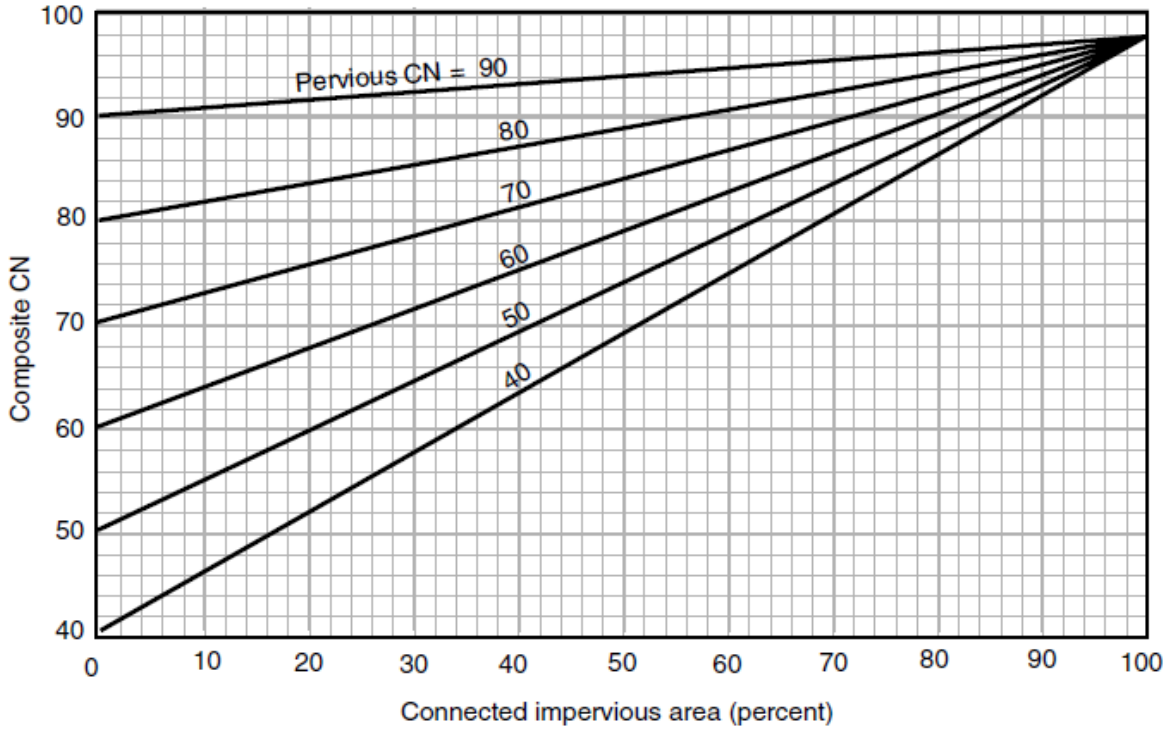
Composite CN
Connected impervious area (percent)
Pervious CN = 90
80
70
60
50
40
100
90
80
70
60
50
40
0
10
20
30
40
50
60
70
80
90
100

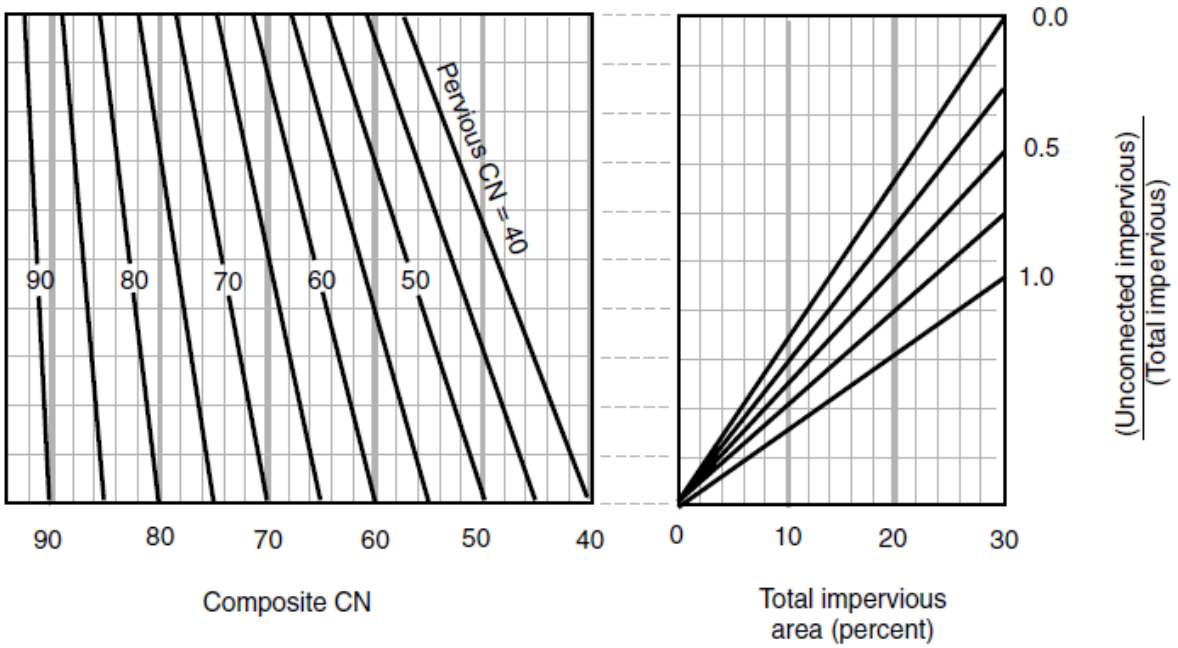
Pervious CN = 40
90
80
70
60
50
90
80
70
60
50
40
Composite CN
0
10
20
30
Total impervious area (percent)
0.0
0.5
1.0
(Unconnected impervious) / (Total impervious)